United States Forest Service Wood Innovations Grant

Study to Validate the Floor Vibration Design of a New Mass Timber Building

May 13, 2024 | Final Report

kpff
Consulting
Engineers

Study to Validate the Floor Vibration Design of a New Mass Timber Building

May 13, 2024

Prepared for:

United States Department of Agriculture

Prepared by:

Andrew W. Taylor, PhD, SE, FACI
Jacob McCann, SE
Addie Lederman
Alec Yeutter

USDA Grant Number:

19-DG-11062765-735

KPFF Project Number:

10041900047

Acknowledgements:

University of Washington, who performed testing in the Structural Research Laboratory at the College of Engineering's Department of Civil and Environmental Engineering.
Lease Crutcher Lewis, the design-build contractor who led construction of the Health Sciences Education Building and the lab test specimens.
The Miller Hull Partnership, the architect who designed the Health Sciences Education Building.

Table of Contents

List of Figures

List of Tables

Appendices

Appendix A – Structural Research Laboratory Testing Report
Appendix B – Plots of Frequency Spectra from Laboratory Impulse Testing
Appendix C – Vibration Plots for Field Testing with and without Concrete Slab
Appendix D – Vibration Plots for Field Testing with and without Building Finishes
Appendix E – Example Calculations for Orthogonal CLT Section Properties

Appendices – List of Figures

Appendices – List of Tables

1. Project Overview

GOALS AND OBJECTIVES OF GRANT

The purpose of this study is to apply the floor vibration design procedures outlined in the *U.S. Mass Timber Floor Vibration Design Guide* (WoodWorks – Wood Products Council, First Edition, March 2021, referred to here as the "Design Guide") to a mass timber construction project, and then to compare the levels of floor vibration predicted by the Design Guide with the levels of vibration measured in the completed structure. The focus of the Design Guide, and this study, is vibrations of mass timber floors created by people walking within the structure. Although this study focuses on footfall-induced vibrations, further study and calibration of the analysis principles described in this report could lead to analysis methods for other sources of mass timber floor vibrations, such as building mechanical equipment and vehicles driving on nearby roadways.

A distinguishing feature of the mass timber floor systems incorporated in this building, and tested in the structural laboratory as part of this study, was the composite action created between the structural steel floor beams, cross-laminated timber (CLT) floor panels, and cast-in-place concrete floor topping slab as shown in Figure 1. Composite action was achieved using conventional welded, headed, shear studs installed along the top flanges of the steel floor beams. Laboratory tests of two composite beams were carried out to explore the relative contributions of the beams, slabs, and CLT to the elastic stiffness of the composite section. In addition, laboratory tests were performed on isolated CLT panels to determine the orthogonal stiffness properties of the panels for use in computer models that were developed to calculate floor vibration response in accordance with the Design Guide.

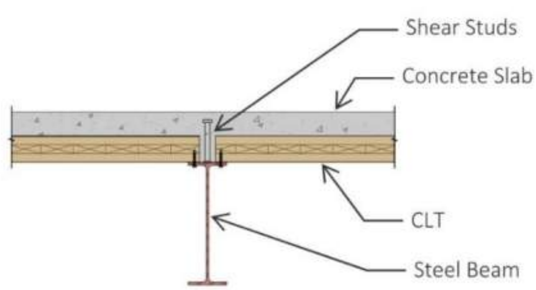

Figure 1: Typical Composite Floor Section

PROJECT DESCRIPTION

The subject of the study described in this report is the vibration analysis, vibration design, and field vibration testing of the composite mass timber floor system of the new Health Sciences and Education Building (HSEB) on the Seattle Campus of the University of Washington. Figure 2 shows the nearly completed building as viewed from the northwest. This building has four levels above grade, one level below grade, is approximately 73 feet tall, and measures about 90 feet by 210 feet in plan. Elevated Floors 2 and 3 were the main focus of this study. The structural framing of Floors 2 and 3 comprises steel beams and girders, 3-ply CLT panels spanning between beams, and a cast-in-place concrete topping slab over the top of the beams and CLT. The topping slab is made composite with the steel beams by leaving a gap between the edges of CLT panel along the tops of beams, and installing conventional welded, headed, shear studs along the center lines of the top flanges.

Figure 2: University of Washington Health Sciences Education Building

The primary structural analysis and design of the HSEB took place between July 2019 and September 2020. Construction began in September 2020, and was substantially complete by April 2022. The duration of this study ran from August 2019 to May 2022, and laboratory testing of isolated composite beams and isolated CLT panels took place from May 2020 to July 2020. Field tests of the vibration response of the composite floor system focused on Level 2 of the HSEB, which houses a variety of functions ranging from teaching labs, to classrooms, to public circulation spaces. Field tests on Level 2 were conducted at three stages of construction: when steel floor framing was complete and all CLT panels were placed, but before the concrete topping slab had been placed; after the concrete topping slab had been placed and the floor was still "bare structure," (that is, before any interior partition walls, floor finishes, casework, furniture, or building mechanical systems had been installed); and after substantial completion, with all structural and non-structural elements in place, and the building ready for occupancy.

The laboratory testing program supported the HSEB case study by providing empirical data on the stiffness and vibration frequencies of two simply-supported composite beams that were nearly identical to the composite beams incorporated in the design of the HSEB. In addition, several simply-supported CLT panels were tested to determine the effective flexural stiffness and natural frequencies of the panels. The laboratory testing and a discussion of the results are presented in a later section of this report.

Occupancy and Use

As the name of the facility implies, the Health Sciences Education Building provides classrooms, teaching laboratories, offices and meeting spaces for diverse medical education programs at the University. While the HSEB does not house academic research laboratories, it does contain functions with moderate levels of vibration sensitivity, including large, column-free classrooms, and teaching laboratories that may be used to demonstrate and practice vibration-sensitive procedures. Figure 3 is a plan of Level 2 showing the locations of primary functions.

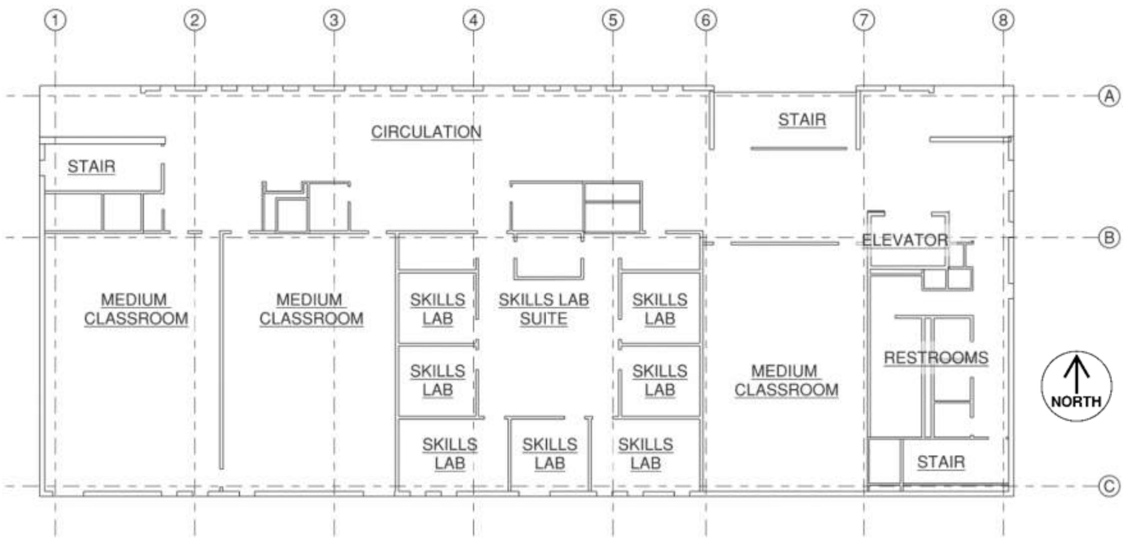

Figure 3: Level 2 Occupancy and Use

Structural System

Typical floor framing consists of three-ply cross-laminated timber (CLT) with a 3-inch concrete topping slab. The CLT is 105V Crosslam panels with grade V2M1.1 as manufactured by Structurlam. The floor deck is non-composite and spans about 10 feet between steel beams.

There are two predominant beam spans, as shown in Figure 4. The beams at the north bays are typically W16x36 and span about 30 feet. The beams at the south bays are typically W27x84 and span about 54 feet. The typical girders are W30x90 and span 30 feet between steel wide flange columns. The beams have a composite connection to the concrete topping and the girders are non-composite.

The lateral force resisting system uses buckling restrained braced frames at four locations near the perimeter of the building. The concrete topping slab is designed to resist in-plane diaphragm forces.

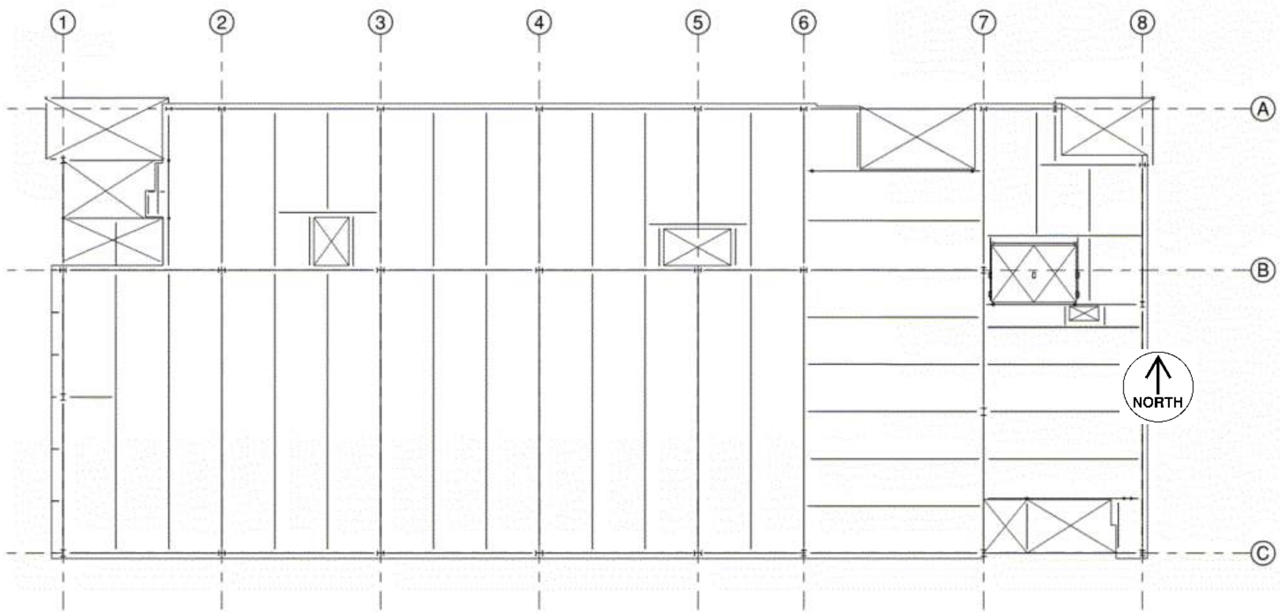

Figure 4: Level 2 Structural Framing

STRUCTURAL VIBRATION CRITERIA

To evaluate the vibration performance of a floor, through analysis, laboratory testing, or through field testing, structural vibration criteria must be defined. The two most common parameters used to assess floor vibrations are the vertical peak acceleration of the floor, and the vertical root-mean-square (RMS) velocity spectra of the floor. Peak accelerations are most often associated with evaluations for human comfort, and RMS velocity spectra are most often used to evaluate the vibration environment for sensitive equipment such as microscopes, balances, spectrometers, and MRI or CT scanning machines. Both peak accelerations and RMS velocity spectra are discussed below.

Peak Acceleration

Typically, peak accelerations are reported simply as the maximum absolute value of acceleration recorded during a laboratory test or field vibration measurement, or derived from a transient dynamic structural analysis of a floor. Peak accelerations are usually expressed in units of “g,” where “g” is the acceleration due to gravity. For example, a peak acceleration of 0.20 g is an acceleration equal to 20% of the acceleration due to gravity.

The value of the peak acceleration in a floor vibration record, a_{max}, may be governed by an extreme, momentary, outlying acceleration spike. The presence of infrequent acceleration spikes may raise the value of a_{max} far above the general level of floor accelerations that characterize the vibration record. Therefore, it is useful to examine both the peak acceleration in the vibration record, a_{max}, and a statistical measure of the dispersion of acceleration peaks in the record, namely the value of the mean measured acceleration (the mean value for a vibrating floor is usually close to zero g) plus or minus some factor times the standard deviation of all acceleration values in the vibration record, e.g. {Mean + 2σ} or {Mean + 3σ}. The value of the peak acceleration in a record, a_{max}, may be governed by an extreme, momentary, outlying acceleration spike, whereas the values of {Mean + 2σ} or {Mean + 3σ} may be more generally representative of the maximum acceleration for the entire record.

An example appears in Figure 5. The figure shows the measured accelerations recorded by two identical accelerometers located near one another on the same floor, and responding to the same floor vibration input. Under these conditions, we would expected the peak acceleration of the two records to be nearly the same. However, the absolute momentary peak acceleration, a_{max}, for Channel 2 (red trace) at 7.5 seconds is 0.0165 g, while the absolute momentary peak acceleration for Channel 3 (blue trace) at 10.8 seconds is 0.0195 g, an 18% difference from Channel 2.

On the other hand, in the same figure the {Mean + 2σ} and {Mean - 2σ} values are shown by a pair of horizontal lines, one above and one below the horizontal axis. One pair of lines is shown for Channel 2 is shown in yellow, and the other pair of lines for Channel 3 is shown in green. The {Mean + 2σ} line for Channels 2 is at 0.0101 g, and the {Mean + 2σ} line for Channels 3 is at 0.0108 g, a 7% difference from Channel 2. This is as expected, since the two identical accelerometers located a short distance apart should record approximately the same maximum acceleration.

Although Figure 5 illustrates only a single example of the difference between momentary peak acceleration values, a_{max}, and {Mean + 2σ} and {Mean - 2σ} acceleration values, the example is representative of our experience: by defining the maximum value of an acceleration record as the {Mean + 2σ} and {Mean - 2σ} of the record, the result is a more consistent and repeatable value of maximum acceleration than focusing on the absolute momentary peak acceleration, a_{max}, of the record.

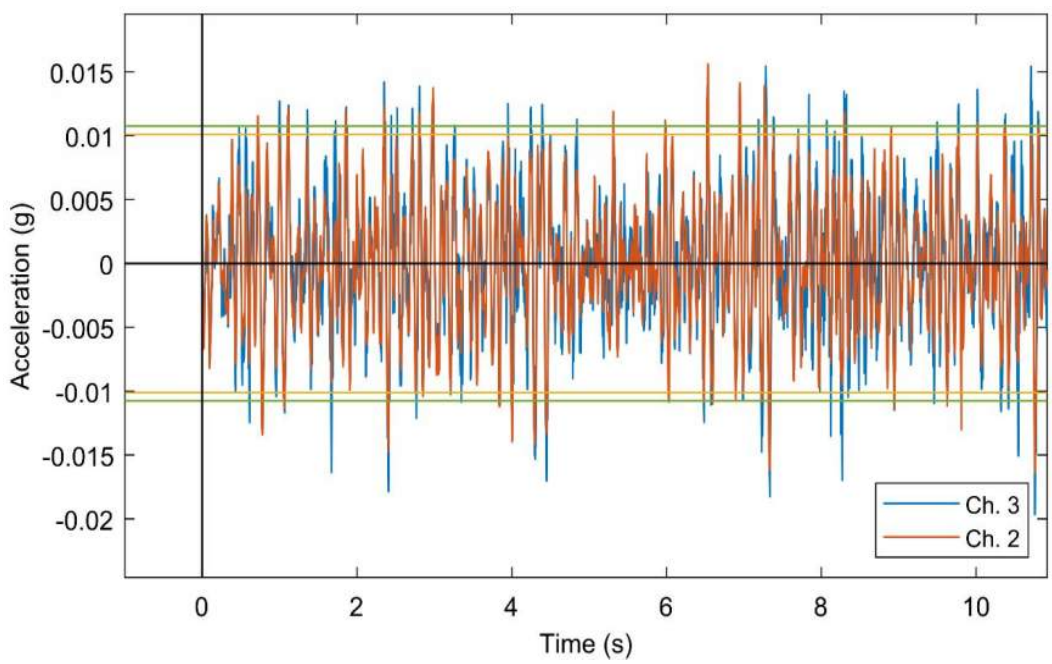

Figure 5: Example of {Mean + 2σ} of Ch. 2 (yellow lines) and Ch. 3 (green lines)

Values of “allowable” accelerations for evaluating human comfort have been proposed by many researchers and practitioners at different times, but currently the most widely accepted values in the United States are those shown in Table 1 below. The table lists peak acceleration thresholds for three human comfort ratings. It should be noted that these values are not exact thresholds, but should be treated as general guidance. For the purposes of this study, the most important acceleration limit in Table 1 is the peak acceleration of 0.005 g, which is the level at which floor vibrations begin to disturb a significant proportion of the occupants of a classroom, office, or other quiet work area. While sensitivity to floor vibrations varies widely from person to person, KPFF’s experience has confirmed that 0.005 g is a reasonable threshold for gaging the comfort of office occupants.

Table 1: Maximum Peak Acceleration for Three Human Comfort Ratings

Occupancy	Maximum Acceptable Acceleration, g’s
Quiet areas in offices	0.005
Active, open areas, like shopping malls	0.015
Outdoor pedestrian bridges	0.050

Root-mean-square (RMS) Velocity Spectra

Another common method of evaluating vibration data is to plot the data as a frequency spectrum showing root-mean-square (RMS) velocity. This data is further processed by presenting the RMS velocity spectrum in a “one-third octave band” format. The reasons for creating one-third octave band RMS velocity plots are partially related to traditional methods of presenting and interpreting data from acoustical measurements (sound pressure oscillations, typically 30 Hz and higher) and partially due to the practical observation that the vibration environment for sensitive equipment is often best assessed by plotting RMS velocity in the frequency domain, rather than peak acceleration, velocity, or displacement in either the time domain or frequency domain.

In this report, plots showing RMS velocity spectra have units of frequency in Hertz (Hz) on the horizontal axis, and units of RMS velocity in micro-inches per second on the vertical axis. The units “micro-inches per second” are sometimes referred to as “mips.” For example, 4,000 mips represents 4,000 micro-inches per second. A range of “threshold” levels of one-third octave band RMS velocity have been developed for various types of building occupancies and equipment types. These thresholds begin with “ISO-W” at the highest, least sensitive, level of vibration, and progress down to “VC-E” at the lowest, most sensitive, level. An explanation of each vibration threshold is shown in Table 2 below, and the vibration thresholds are shown graphically in Figure 7. Note that at frequencies lower than 8 Hz the vibration thresholds increase. This reflects the observation that equipment typically exhibits increased tolerance for vibrations at low frequencies.

Table 2: Vibration Criteria (1)

Criterion Curve	Max Level (2) (micro-inches/sec, RMS)	Detail Size (3) (microns)	Description of Use
Workshop (ISO)	32,000	N/A	Distinctly feelable vibration. Appropriate to workshops and nonsensitive areas.
Office (ISO)	16,000	N/A	Feelable vibrations. Appropriate to offices and nonsensitive areas.
Residential Day (ISO)	8,000	75	Barely feelable vibration. Appropriate to sleep areas in most instances. Probably adequate for computer equipment, probe test equipment, and low-power (to 20X) microscopes.
Operating Theater (ISO)	4,000	25	Vibration not feelable. Suitable for sensitive sleep areas. Suitable in most instances for microscopes to 100X and for other equipment of low sensitivity.
VC-A	2,000	8	Adequate in most instances for optical microscopes to 400X, microbalances, optical balances, proximity, and projection aligners, etc.
VC-B	1,000	3	An appropriate standard for optical microscopes to 1000X, inspection, and lithography equipment (including steppers) to 3 micron line widths.
VC-C	500	1	A good standard for most lithography and inspection equipment to 1 micron detail size.
VC-D	250	0.3	Suitable in most instances for the most demanding equipment including electron microscopes (TEMs and SEMs) and E-Beam systems, operating to the limits of their capability.
VC-E	125	0.1	A difficult criterion to achieve in most instances. Assumed to be adequate for the most demanding of sensitive systems including long path, laser-based, small target systems and other systems requiring extraordinary dynamic stability.

Notes: (1) After Gordon, Colin G., *Proceedings of the SPIE Conference on Vibration Control for Optomechanical Systems*, July 1999, Denver, CO.

(2) As measured in one-third octave bands of frequency over the frequency range 8 to 100 Hz.

(3) The detail size refers to the particle (cell) size for medical and pharmaceutical research.

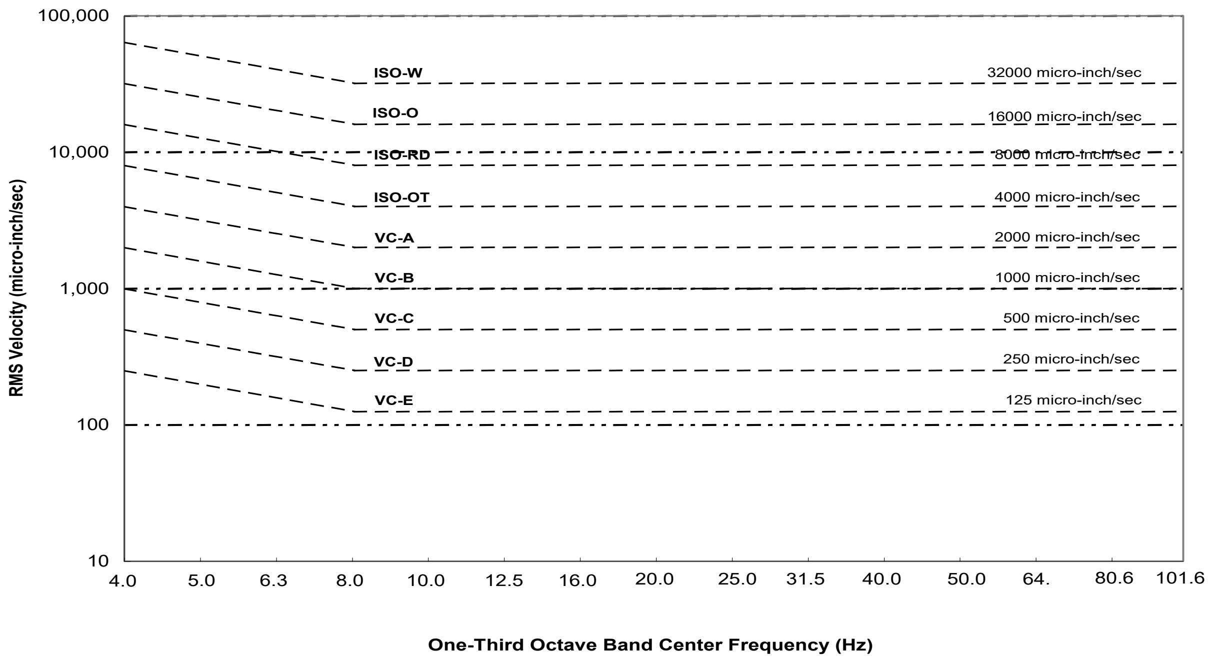

Figure 6: Generic Vibration Criteria Curves (VC and ISO) for Sensitive Equipment and Human Comfort

2. Laboratory Measurements of Dynamic Properties

Laboratory testing was performed at the Structural Research Laboratory (SRL) in the Department of Civil and Environmental Engineering at the University of Washington. This work was led by Professor Jeffrey Berman, who is the SRL Director and Vince Chaijaroen, who is the SRL Manager. The results of these experiments are summarized in the *Structural Research Laboratory Commercial Testing Report*, which is included in Appendix A.

The goal of the laboratory testing was to confirm the stiffness and frequency of the mass timber floor assembly. Table 3 summarizes the seven specimens that were tested. This included a range of bare panels with different CLT thicknesses, topped panels with different composite connections, and two composite beams that were identical. The CLT panels had a simply supported span of 11 feet and the composite beams had a simply supported span of 31 feet. Details of the test specimens and testing procedures are contained in Appendix A.

Table 3: Laboratory Investigation Test Matrix

Specimen	CLT Layup	Concrete Topping	Composite Steel Beam
3-Ply Bare CLT Panel	V2M1.1-105V	No	No
5-Ply Bare CLT Panel	V2M1.1-175V	No	No
7-Ply Bare CLT Panel	V2M1.1-245V	No	No
3-Ply Panel w/ 3” Concrete Topping	V2M1.1-105V	3” Topping	No
3-Ply Panel w/ 3” Concrete Topping over Expanded Sheet Metal Mesh	V2M1.1-105V	3” Topping	No
Composite Beam 1	V2M1.1-105V	3” Topping	W16x36 w/ ¾”Øx5 ¾” Studs
Composite Beam 2	V2M1.1-105V	3” Topping	W16x36 w/ ¾”Øx5 ¾” Studs

STIFFNESS TESTING

Flexural stiffness was tested in the laboratory by measuring deflection at mid-span while applying a vertical point load at mid-span. The point load was increased until each specimen reached its strength limit. Figures 7 and 8 show the load versus displacement curves for the CLT panels.

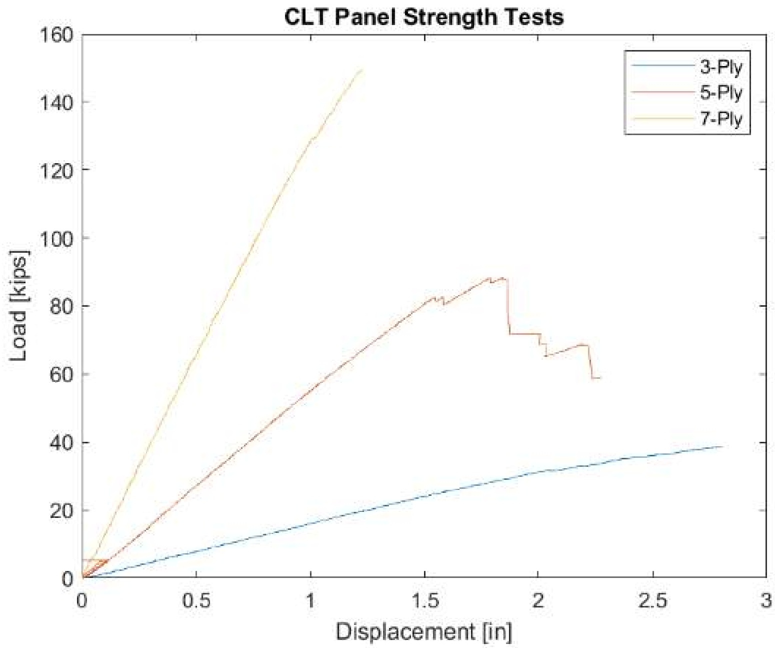

Figure 7: Bare CLT Panels Load Versus Displacement

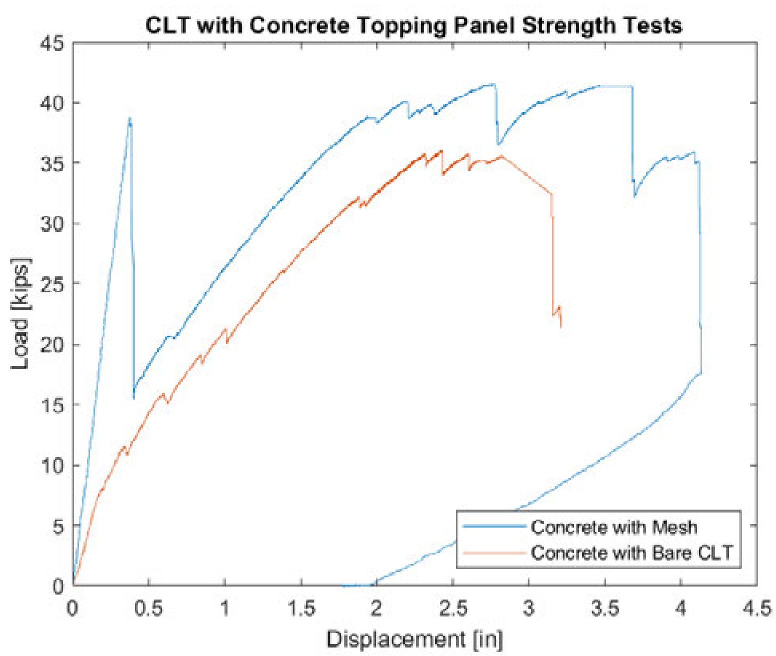

Figure 8: CLT Panel with Concrete Topping Load Versus Displacement

The stiffness of the bare panels was linear within the elastic range. The concrete-topped panels exhibited decreasing stiffness as the load increased. This was likely due to horizontal slippage between the CLT and concrete, as well as cracking of the concrete.

One of the specimens incorporated a metal mesh to increase the interaction between the concrete and the CLT. The mesh significantly increased the initial stiffness of the panel until the displacement reached about 3/8 of an inch, at which point the interlock between the CLT and concrete topping slipped suddenly (Figure 8). The mesh connection was not used in the constructed building, so this configuration was not studied further.

Table 4 compares the section stiffness, EI, from the panel experiments with the EI calculated in accordance with the 2019 *Standard for Performance-Rated Cross-Laminated Timber* (reference PRG 320). The measured EI and calculated EI of the 3-ply panel agree within about 1%. However, the measured EI is 7% less than the calculated EI for the 5-ply panel, and 14% less for the 7-ply panel. The reason the experimental stiffnesses for the 5-ply and 7-ply panels were lower than the calculated stiffnesses is that the stiffness calculation method of PRG 320 does not fully account for the contributions of shear strains to panel deflections. This effect is negligible for slender panels that exhibit flexure-dominated behavior, that is, panels with relatively high span-to-depth ratios. Typical span-to-depth ratios encountered in design practice vary over a range of roughly 24 to 30. But the effect is more pronounced for panels with span-to-depth ratios lower than this range. Thus, the measured and calculated EI values for the 3-ply panel were nearly the same because the span-to-depth ratio was high, at 31.9. However, the measured values of EI were lower than calculated values of EI for the 5-ply and 7-ply panels, because they had lower span-to-depth ratios of 19.1 and 13.7.

The 3-ply panel with a concrete topping slab had a measured stiffness that was 4% higher than the PRG 320 stiffness, assuming non-composite action. This added stiffness suggests there may have been limited composite interaction between the CLT and the concrete, even though no special effort was made to promote a bond between the two materials.

Table 4: CLT Panel Stiffness Comparison

Specimen	Linear Regression Stiffness (kip/in.)	EI – Experimental (Kip-in.^{2}/ft. width)	EI - Calculated (kip-in.^{2}/ft. width)
3-Ply	16.1	97,000	96,000
5-Ply	56.7	340,000	366,000
7-Ply	130	780,000	906,000
3-Ply w/ Concrete	47.1	282,000	270,000

VIBRATION TESTING

In the laboratory, both the panel specimens and the beam specimens were subject to dynamic load to explore the natural (free vibration) frequencies of the specimens and the response of the specimens to typical walking loads. Three types of dynamic loading were applied.

1. Ambient Vibration Conditions: This was a check to confirm under quiet environmental conditions, with no intentional dynamic loads applied, that there were no undetected sources of ambient vibrations, such as nearby machinery, or vehicular traffic. These measurement results are included in some of the results presented in this section simply to demonstrate that background vibrations did not influence the vibration response measured under intentional dynamic loading.

2. Walking Excitation: The primary focus of this study was to investigate the predication and mitigation of footfall-induced vibrations in composite CLT floors. Therefore, many of the tests on the CLT panels and composite beams were walking tests. An individual weighing approximately 190 pounds walked on top of the panel or beam at prescribed step rates of 80, 100, and 120 steps per minute (SPM). The resulting

dynamic response was measured by a vertical-axis accelerometer placed at the center of the panel or beam.

3. Impulse Loading: The objective of these tests was to determine the natural frequencies of the CLT panels and beams by applying a vertical impulse to the top of the specimen, and then allowing the specimen to vibrate freely until all motions ceased due to internal damping of the specimen. The impulse was applied by means of a “heel drop,” which is a widely accepted method for applying an impulse to a floor. A person stands on the specimen, raises up their heels several inches while balancing on the balls of their feet, and then drops their heels to strike the top of the specimen with their full body weight. The magnitude of the impact is not important; the key objective is to apply a significant impulsive load to the specimen.

Walking Test Results

When evaluating the vibration performance of floors that support sensitive equipment, the most common way of expressing data is in the form of frequency spectra of root-mean-square (RMS) velocity, presented in the form of one-third octave band plots. The basis of these plots, and their interpretation, are presented earlier in Section 1.

In Figures 9 through 12, the RMS velocity plots are presented for walking tests of the bare CLT panels, the concrete-topped CLT panels, and the two composite beam specimens.

Bare CLT Panels

Figure 9 illustrates the measured vibration responses for 3-ply, 5-ply, and 7-ply bare CLT panels (without concrete toppings). Each panel spanned 11 feet between knife-edge supports, and the width of each panel perpendicular to the span was 8 feet. The panels were tested at three different walking speeds: 80, 100, and 120 steps per minute (SPM).

The results shown Figure 9 generally follow expected trends: vibration response decreases as panels become thicker; and for a given panel thickness vibration response generally (but not universally) increases with increasing walking speed. In addition, the frequencies at which maximum responses were recorded increases with increasing panel thickness, which is expected because the first resonant frequency of a panel increases with increasing panel thickness.

With regard to the magnitudes of vibrations measured for the three panels, Figure 9 indicates very high response for the bare 3-ply panel at all three walking speeds. Even at a slow walking speed of 80 SPM, response velocity exceeds 32,000 micro-inches per second (mips), which would be unacceptable even in an industrial workshop setting. It should be recognized, though, that the panel walking tests were conducted under unusually demanding conditions: an 11-foot clear span for a bare 3-ply CLT panel approaches the maximum span that would be used in practice; the panels were simply supported on knife edges and tested as single units, so there was no moderating influence from the mass, stiffness or damping provided by interactions with adjoining panels. For the 5-ply panels, maximum response was near 16,000 mips, which would usually be considered acceptable for office occupancies. For the 7-ply panels, maximum response was in the range of 4,000 to 8,000 mips, which would be appropriate for residential applications and some quiet work areas.

Concrete-Topped CLT Panels

Three tests on 3-ply panels were conducted to evaluate the effects of adding a 3-inch-thick concrete topping layer to the CLT panel. Figure 10 shows the response of an untopped panel, a panel with a conventional concrete topping, and a concrete-topped panel that included a layer of expanded steel mesh that was stapled to the top of the CLT before placing the topping concrete.

The difference in vibration response between the topped and untopped panels is significant: while the untopped panel response exceeded 32,000 mips, the responses of both panels with toppings were in the range of 8,000 to 16,000 mips. This illustrates the effectiveness of a concrete topping in reducing footfall vibration response. It appears that the addition of the expanded steel mesh in the third specimen had little if any discernable influence on vibration response of the panel.

Composite Steel/Concrete/CLT Beams

The two composite beam specimens were nominally identical, but they were tested with slightly different load protocols. The spans of both beams were 31 feet, and they were simply supported with a single point load applied at mid-span. The point load was applied through a spreader beam that distributed the load across the width of the top concrete flange. Beam 1 was loaded to 75% of its design live load (13.6 kips), unloaded, then subjected to ambient and walking-induced vibration tests. The beam was then re-loaded up to 150% of its design live load (27.1 kips), unloaded, and the ambient and walking vibration tests were repeated. A similar protocol was followed for Beam 2, but for applied loads of 0, 50%, 100%, and 150% of the design live load (0, 8.8, 17.5, and 27.1 kips).

Figures 11 and 12 show the results of the vibration tests. Beam 2 had a lower first mode frequency than Beam 1 (see the section titled “Measured Natural Frequencies” below). It is also apparent that the background ambient vibrations during testing of Beam 2 were erratic, in one case reaching about 6,000 mips. The source of the background vibrations within the laboratory could not be identified. These factors may explain why the vibration response of Beam 2 was consistently higher than Beam 1 over the frequency band of 7 to 10 Hz.

An important observation from both beam tests was that the application and then removal of live loads in the range of 50% to 150% of the design live load did not create consistent or systematic variation in the measured walking-induced vibration response. Although there was a weak tendency for vibration response to increase with increased live load, a careful study of Figures 11 and 12 reveals several counterexamples to this trend. Further, much of the variation in vibration response shown in Figures 11 and 12 could be attributed to normal variations between independent experiments.

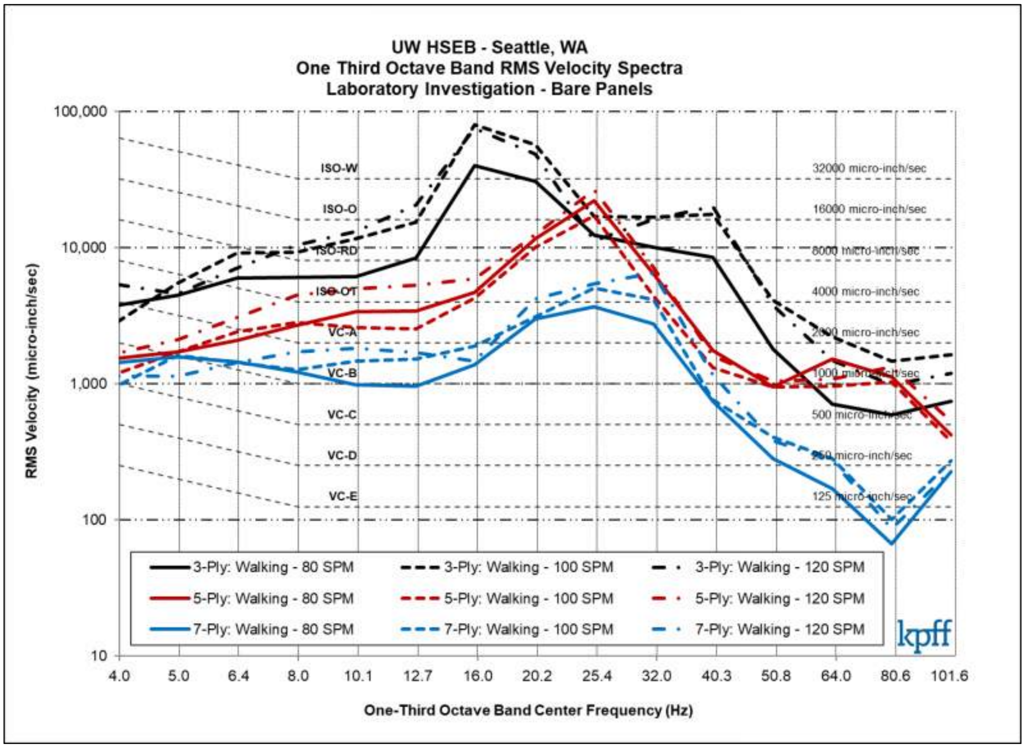

Figure 9: Bare CLT Panels Vibration Response

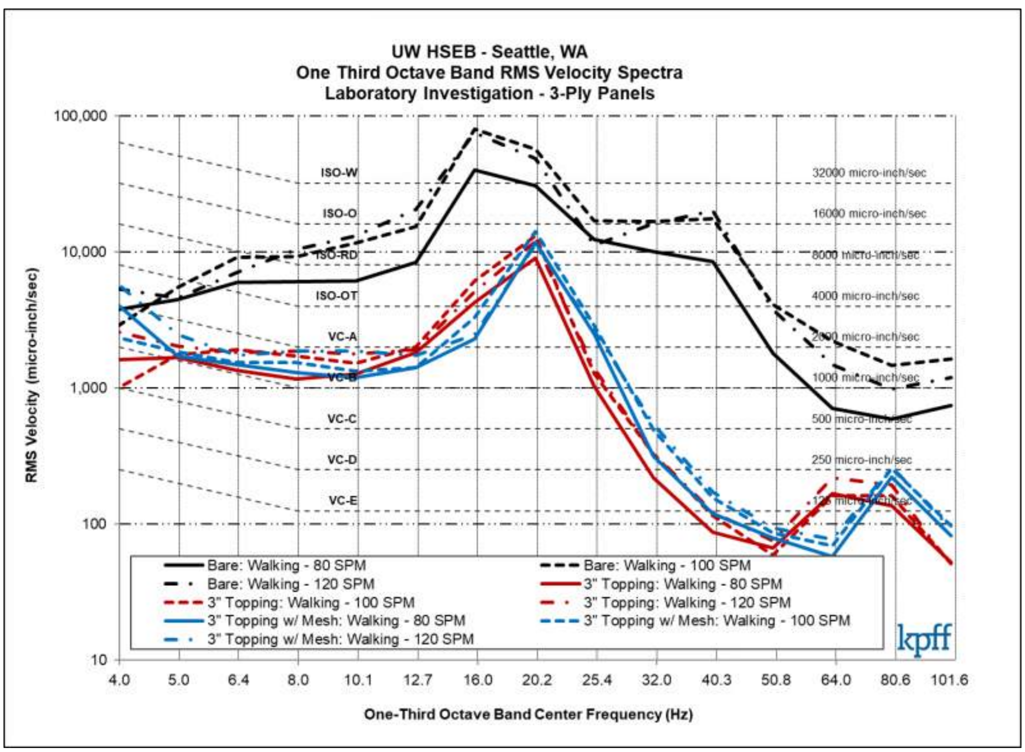

Figure 10: 3-Ply CLT Panels Vibration Response

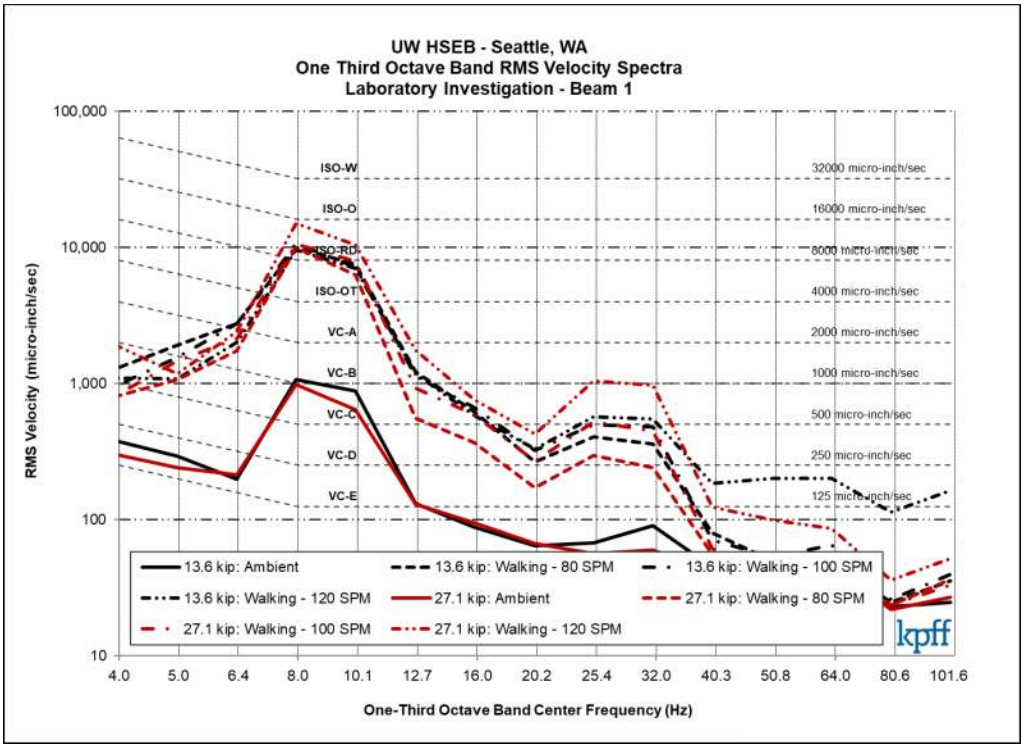

Figure 11: Beam 1 Vibration Response

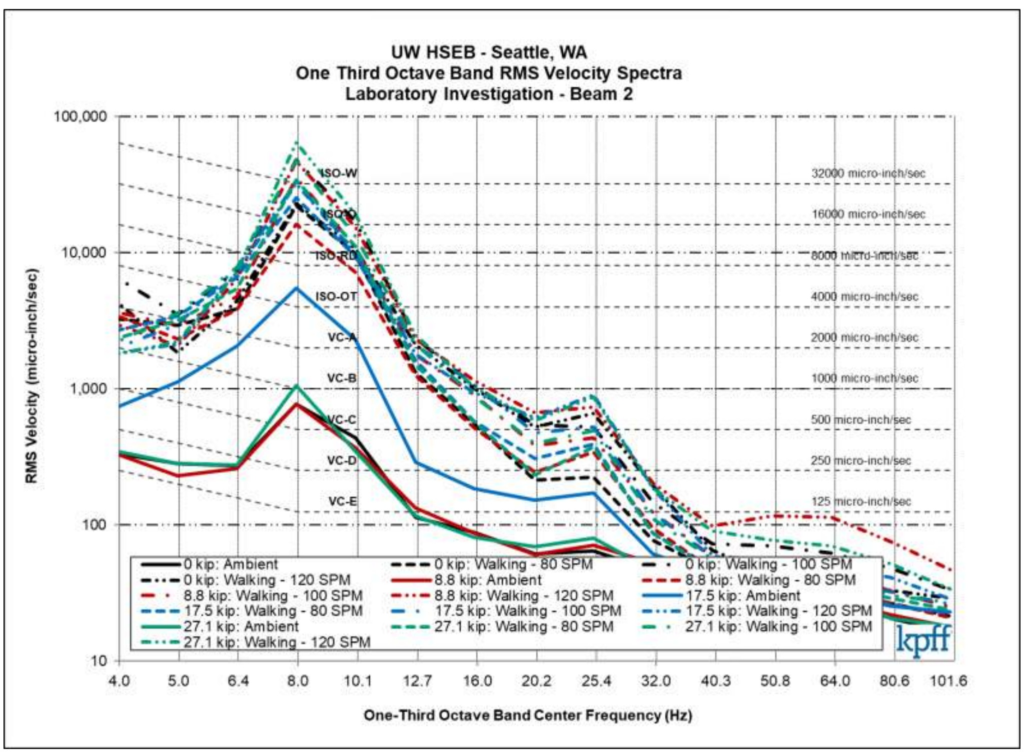

Figure 12: Beam 2 Vibration Response

Measured Natural Frequencies

A summary of the measured first mode natural frequencies from both the panel tests and the beam tests is presented below in Table 5. These were derived from the frequency spectra of the acceleration data recorded during the impulse load testing of each specimen. Plots of the frequency spectra from the impulse load tests are included in Appendix B for reference.

The measured natural frequencies of the CLT panels with and without concrete topping are compared with calculated natural frequencies in the section below titled "Frequency Modeling Using the Design Guide."

Table 5: Specimen First Mode Frequencies

Specimen & Test	Peak 1 (Hz)
3-Ply Bare Panel	17.7
5-Ply Bare Panel	23.3
7-Ply Bare Panel	28.8
3-Ply 3in. Conc. Topping	18.8
3-Ply 3in. Conc. Topping with Mesh	20.6
Beam 1: 13.6 Kip	8.8
Beam 1: 27.1 Kip	8.7
Beam 2: 0 Kip	8.7
Beam 2: 8.8 Kip	8.5
Beam 2: 17.5 Kip	8.5
Beam 2: 27.1 Kip	8.5

FREQUENCY MODELING USING THE DESIGN GUIDE

CLT Panel Section Properties for Analysis

An important objective of the testing and analysis phases of this project was to validate the modeling parameters described in the Design Guide for the flexural stiffness of CLT panels. Because CLT panels are composed of an odd number of timber laminations, the flexural properties of a panel are different in the two principal directions, that is, for out-of-plane flexure the panels have orthogonal properties.

Flexural stiffness is governed by the product of Young's modulus and the moment of inertia, or EI. The effective E of wood for bending that causes flexural stresses parallel to the wood grain may be an order of magnitude greater than for bending that causes flexural stresses perpendicular to the wood grain. Therefore, the most common approach to quantifying EI for CLT panels is to derive transformed sections based on the ratio of the modulus for bending parallel to and perpendicular to grain. Thus, there will be a higher value for EI associated with out-of-plane bending in the "strong direction" of the panel than the value for EI corresponding to bending in the "weak direction."

Methods for calculating the orthogonal flexural properties of CLT panels for out-of-plane bending are discussed in Section 3.3.3 of the Design Guide. In addition to considering different EI values for the two principal directions of the panel, it may be necessary to consider the contributions of shear strains to out-of-plane stiffness and deflections. Because the laminations in CLT perpendicular to the span direction have a low shear modulus, the shear deformations of CLT are higher relative to other common structural materials. Methods for including shear distortions in deflection calculations are also described in the Design Guide. It is suggested that for a given project, representative trial calculations should be run with and without inclusion of shear distortions to assess the importance of considering shear distortions in final design calculations.

A detailed example of the calculation of effective CLT section properties for finite element analysis (FEA) of a CLT panel are shown in Appendix E. These calculations also illustrate the process for computing effective composite section properties of a CLT panel with a concrete topping, and the process for computing in-plane stiffness properties for analysis and design of floor diaphragms that form part of a lateral force-resisting system. Finally, the example illustrates how effective section properties can be summarized and organized for entry into FEA software.

Finite Element Analysis of CLT Panels

Using the methods described above, section properties for all of the tested CLT panels were computed, and a finite element model was developed for each panel. The plan dimensions of the panels were 11 feet in the span direction by 8 feet perpendicular to the span direction.

Each panel was meshed with shell elements measuring 3 by 3 inches in plan, and a modal analysis was performed to calculate the fundamental periods of the panels. Figure 13 illustrates the first four calculated mode shapes. It should be noted that these mode shapes do not match the familiar first four vibration modes of a simply supported beam. A beam is typically analyzed in two dimensions, whereas the analysis of a plate requires three dimensions.

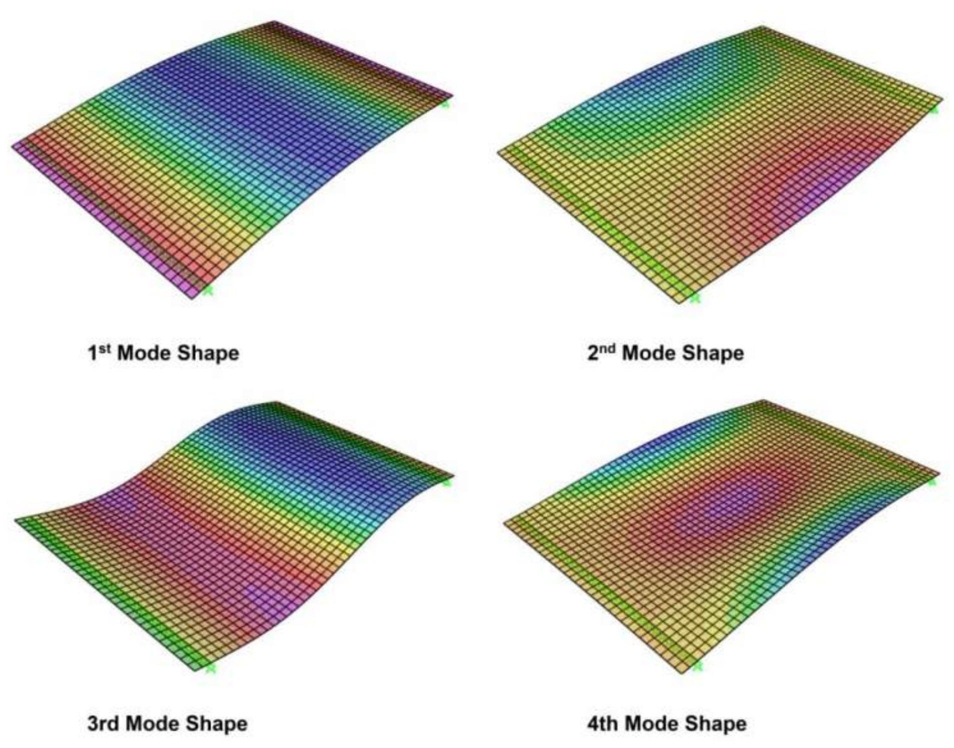

Figure 13: First Four Calculated Mode Shapes of CLT Panels

COMPARISON OF PANEL MEASUREMENTS AND PANEL MODELING

Table 6 below lists the measured fundamental frequencies and the calculated fundamental frequencies of the four types of CLT panels tested. The last column of the table indicates that in general good agreement was obtained between the measured and calculated frequencies.

The largest percentage difference is for the untopped 3-ply panel, for which the calculated frequency is 13.6% lower than the measured frequency. The reason for this difference is not known, although it has been the authors' observation when testing vibrations of floors in the field that if there is a discrepancy between measured and calculated floor frequencies, the measured frequencies are almost universally higher than the calculated frequencies. This is because field measurements include the effects of unrecognized factors that may stiffen a floor, such as the presence of non-structural elements, or material properties (e.g. concrete) that are higher than assumed. In the case of laboratory testing there are fewer uncontrolled variables, but a tendency towards measured frequencies being higher than calculated frequencies may still apply.

Not included in Table 6 is the measured and calculated frequencies for the 3-ply panel with topping that included expanded metal mesh stapled to the top surface of the CLT panel before casting the topping. The purpose of this mesh was to possibly improve the interaction between the CLT and the topping, thus increasing the composite stiffness of the CLT/concrete assembly. It appears that the initial stiffness of this specimen was higher than the specimen without the mesh, as reflected in the load-deflection plot of Figure 8, and in the higher natural frequency of the specimen before it was loaded: 20.6 Hz for the panel with mesh vs. 18.8 Hz for the panel without mesh. However, subsequent loading indicated that as the applied load increased, the CLT/concrete bond was susceptible to brittle fracture. While this is not a safety concern, further study of the interlock between the CLT and topping is required to achieve reliable composite stiffening.

Table 6: Comparison Measured Versus Modeled Natural Frequencies

Specimen	Measured 1st Mode (Hz.)	Modeled 1st Mode (Hz.)	Percent Difference
3-Ply	17.7	15.3	13.6%
5-Ply	23.3	23.4	0.4%
7-Ply	28.8	29.5	2.4%
3-Ply w/ 3 in. Conc Topping	18.8	18.5	1.6%

3. Field Measurements of Floor Vibrations

SUMMARY OF CONSTRUCTION STAGES

The vibration response of a floor in a building changes over the course of construction. That is, the measured floor vibrations in a structure due to footfall excitation will generally be greater during the initial phases of construction than after construction is complete. This is because as construction progresses elements are added to the structure that, in most cases, increase the stiffness of the floor, increase the vibrating mass of the floor, and increase the dynamic damping of the floor.

An important example for the HSEB project is the differences in vibration response between the stage at which only the steel beams and CLT panels have been installed, and the stage at which the 3-inch concrete topping slab has been placed. Because of the welded shear studs along the top flange of each steel beam, after the concrete slab is placed the slab and the steel beam act compositely, significantly increasing the flexural stiffness of the floor system. A limited degree of composite action may also exist between the CLT panels and the concrete topping, but unless a mechanical interlock has been intentionally created between the CLT and concrete, composite action will depend exclusively on chemical bond between the concrete and the CLT, which is not reliable or easily quantified.

Another factor that affects the vibration response of floors in nearly all buildings is the influence of non-structural elements such as partition walls, floor and ceiling finishes, mechanical and electrical systems, casework, furniture, etc. Depending on the quantity and configuration of the nonstructural elements associated with a particular floor, these elements can create a high level of dynamic damping, or even increase the stiffness of the floor, two factors that can greatly reduce both the amplitudes and durations of floor vibrations. An example of a non-structural element that could have a significant effect on floor vibrations in the HSEB is the non-structural partition walls, particularly in areas with numerous small rooms, such as in the Skills Lab area (see Figure 2). These partitions run from the top of the finished floor to the underside of the floor above, which creates a direct link between floor framing systems. This configuration of partition walls, which is common in health care and educational facilities, can provide significant additional stiffness and damping that reduces floor vibrations. (Note that this is not the same configuration of partition walls that is commonly found in commercial office buildings. Those partition walls often stop short of the underside of the floor above, at an elevation just above the suspended ceiling system). A photograph of a typical full-height partition wall on Level 2 of the HSEB is shown in Figure 14.

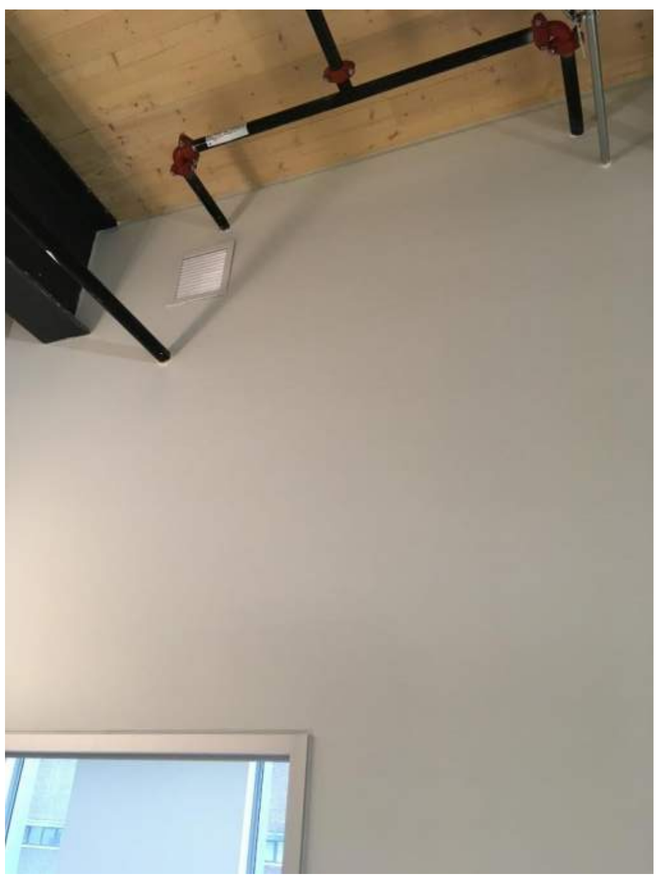

Figure 14: Nonstructural Partition Wall, Looking Up, Showing Contact Between Top of Wall and Structure

Given the considerations described above, three stages of construction were defined in this project to guide both laboratory testing and field measurements of floor vibrations in the HSEB over the course of construction:

1. “No Topping” stage: steel floor beams and CLT panels installed, but no topping slab
2. “Shell and Core” stage: concrete topping slab installed, but no non-structural interior components, such as partition walls and cabinets. Exterior cladding not yet installed.
3. “Substantial Completion” stage: Complete buildout of all non-structural interior elements, and exterior cladding installed. Timing is just prior to first occupancy.

Field measurements were taken at 11 locations on Level 2, as shown below in Figure 15. These locations were selected to capture a variety of conditions with different stiffness and damping properties. For example, locations 1 through 4 have similar structural conditions and different nonstructural partition walls. Additionally, location 9 primarily captures the vibration of a beam, while location 6 captures the combined vibration of two beams and the CLT spanning between those beams.

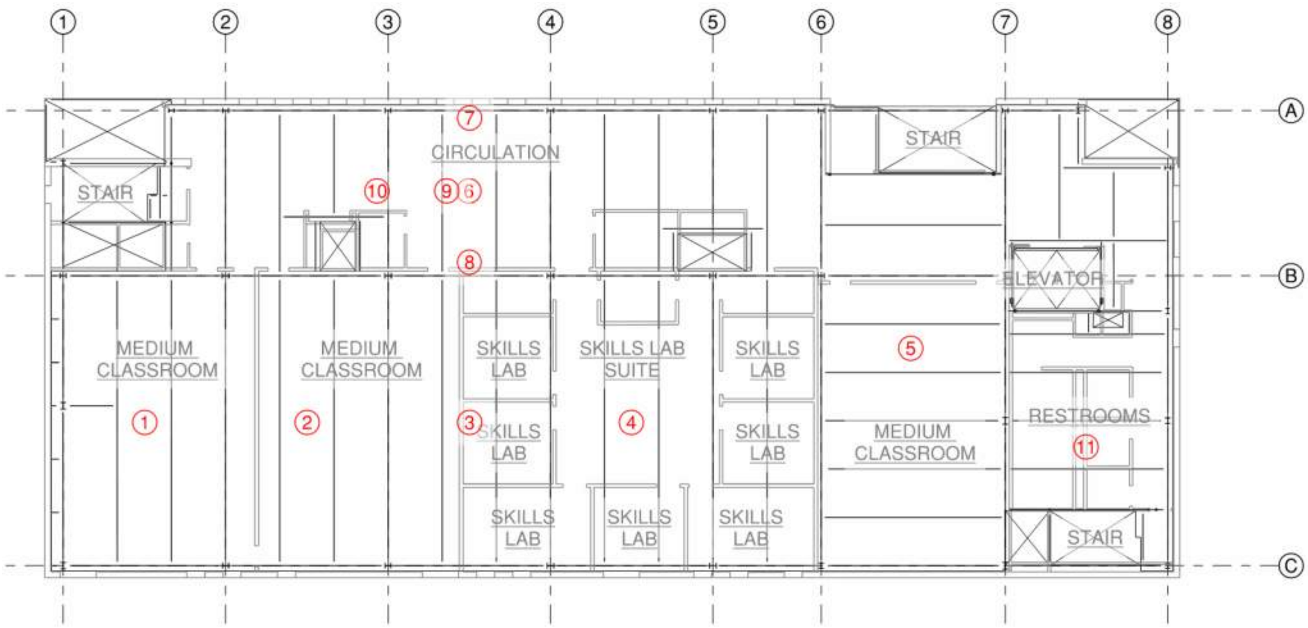

Figure 15: Level 2 Test Locations

MEASUREMENTS WITH AND WITHOUT CONCRETE SLAB

Peak accelerations were measured before and after the concrete topping slab was cast. These measurements were taken at all locations shown in Figure 15, except for location 10. Table 7 summarizes the results of the peak acceleration measurements. Four levels of excitation are included: ambient, 80 steps per minute (SPM), 100 SPM, and 120 SPM.

RMS velocities were also calculated for each condition. These results are plotted in Appendix C. The first 10 plots compare the different excitations and construction stages for each location. The final 6 plots compare all of the locations for each excitation and construction stage.

Table 7: No Topping Versus Shell and Core – Peak Acceleration (g)

Location	Construction Stage	Limit State	Excitation			
			Ambient	80 SPM	100 SPM	120 SPM
01	No Topping	Max	0.00622	0.04629	0.04499	0.07587
		Mean + 2σ	0.00350	0.01135	0.01324	0.02059
	Shell & Core	Max	0.00134	0.00542	0.00447	0.01126
		Mean + 2σ	0.00087	0.00237	0.00243	0.00537
02	No Topping	Max	0.00673	0.08015	0.05754	0.06320
		Mean + 2σ	0.00332	0.02483	0.01605	0.02193
	Shell & Core	Max	0.00131	0.01284	0.01534	0.00909
		Mean + 2σ	0.00075	0.00367	0.00409	0.00387
03	No Topping	Max	0.00614	0.04986	0.06954	0.06801
		Mean + 2σ	0.00330	0.01220	0.01880	0.02183
	Shell & Core	Max	0.00311	0.00602	0.00598	0.00816
		Mean + 2σ	0.00183	0.00219	0.00291	0.00475
04	No Topping	Max	0.00787	0.06457	0.08506	0.06908
		Mean + 2σ	0.00312	0.01349	0.01949	0.02115
	Shell & Core	Max	0.00446	0.00510	0.00579	0.00693
		Mean + 2σ	0.00173	0.00302	0.00278	0.00331
05	No Topping	Max	0.00609	0.06328	0.04010	0.06429
		Mean + 2σ	0.00250	0.01516	0.01530	0.02112
	Shell & Core	Max	-	-	-	-
		Mean + 2σ	-	-	-	-
06	No Topping	Max	0.00623	0.06703	0.05071	0.08938
		Mean + 2σ	0.00327	0.01438	0.01670	0.02985
	Shell & Core	Max	0.00347	0.00542	0.00880	0.01202
		Mean + 2σ	0.00167	0.00279	0.00456	0.00538
07	No Topping	Max	-	-	-	-
		Mean + 2σ	-	-	-	-
	Shell & Core	Max	0.00182	0.00201	0.00304	0.00806
		Mean + 2σ	0.00082	0.00100	0.00119	0.00174
08	No Topping	Max	-	-	-	-
		Mean + 2σ	-	-	-	-
	Shell & Core	Max	0.00156	0.00500	0.00824	0.00739
		Mean + 2σ	0.00075	0.00133	0.00188	0.00184
09	No Topping	Max	-	-	-	-
		Mean + 2σ	-	-	-	-
	Shell & Core	Max	0.00283	0.00421	0.00451	0.00628
		Mean + 2σ	0.00145	0.00225	0.00268	0.00373
11	No Topping	Max	0.00370	0.01313	0.02044	0.01857
		Mean + 2σ	0.00173	0.00568	0.00961	0.00827

A summary of the measured natural frequencies is presented below in Table 8. These were derived from the frequency spectra of the field measurements of acceleration at each location.

Table 8: No Topping Versus Shell and Core – Natural Frequencies

Location	Construction Phase	Peak 1 (Hz)	Peak 2 (Hz)	Peak 3 (Hz)
01	No Topping	6.4	25.3	31.5
	Shell & Core	6.0	89.7	-
02	No Topping	6.3	24.0	-
	Shell & Core	5.0	-	-
03	No Topping	4.5	23.5	-
	Shell & Core	5.6	-	-
04	No Topping	3.5	4.3	-
	Shell & Core	5.4	8.9	-
05	No Topping	7.2	14.9	33.2
	Shell & Core	-	-	-
06	No Topping	10.3	-	-
	Shell & Core	8.6	13.8	16.4
07	No Topping	20.0	33.9	-
	Shell & Core	18.2	25.2	35.9
08	No Topping	16.9	29.2	-
	Shell & Core	8.6	14.2	-
09	No Topping	9.4	12.2	15.9
	Shell & Core	8.5	13.3	-
10	No Topping	8.3	15.9	-
	Shell & Core	-	-	-
11	No Topping	12.6	16.8	21.6
	Shell & Core	-	-	-

MEASUREMENTS WITH AND WITHOUT BUILDING FINISHES

Peak accelerations were also measured before and after the building finishes were installed, also known as the stage of “Substantial Completion.” These measurements were taken at all locations shown in Figure 15. Table 9 summarizes the results of the peak acceleration measurements. Four levels of excitation are included: ambient, 80 steps per minute (SPM), 100 SPM, and 120 SPM.

Also, RMS velocities were calculated for each condition. These results are plotted in Appendix D. The first 11 plots compare the different excitations and construction stages for each location. The final 6 plots compare all of the locations for each excitation and construction stage.

Table 9: Shell and Core Versus Substantial Completion Peak Accelerations

Level	Construction Stage	Limit State	Excitation			
			Ambient	80 SPM	100 SPM	120 SPM
01	Shell & Core	Max	0.00134	0.00542	0.00447	0.01126
		Mean + 2σ	0.00087	0.00237	0.00243	0.00537
	Substantial Completion	Max	0.00399	0.00467	0.00558	0.00672
		Mean + 2σ	0.00202	0.00272	0.00303	0.00292
02	Shell & Core	Max	0.00131	0.01284	0.01534	0.00909
		Mean + 2σ	0.00075	0.00367	0.00409	0.00387
	Substantial Completion	Max	0.00206	0.00384	0.00448	0.05195
		Mean + 2σ	0.00117	0.00188	0.00241	0.00519
03	Shell & Core	Max	0.00311	0.00602	0.00598	0.00816
		Mean + 2σ	0.00183	0.00219	0.00291	0.00475
	Substantial Completion	Max	0.00085	0.00183	0.00231	0.00296
		Mean + 2σ	0.00048	0.00066	0.00078	0.00096
04	Shell & Core	Max	0.00446	0.00510	0.00579	0.00693
		Mean + 2σ	0.00173	0.00302	0.00278	0.00331
	Substantial Completion	Max	0.00099	0.00274	0.00262	0.00375
		Mean + 2σ	0.00059	0.00103	0.00145	0.00220
05	Shell & Core	Max	-	-	-	-
		Mean + 2σ	-	-	-	-
	Substantial Completion	Max	0.00222	0.00485	0.00538	0.00884
		Mean + 2σ	0.00097	0.00255	0.00292	0.00501
06	Shell & Core	Max	0.00347	0.00542	0.00880	0.01202
		Mean + 2σ	0.00167	0.00279	0.00456	0.00538
	Substantial Completion	Max	0.00219	0.00387	0.00647	0.00663
		Mean + 2σ	0.00118	0.00181	0.00334	0.00361
07	Shell & Core	Max	0.00182	0.00201	0.00304	0.00806
		Mean + 2σ	0.00082	0.00100	0.00119	0.00174
	Substantial Completion	Max	0.00147	0.00200	0.00334	0.00326
		Mean + 2σ	0.00075	0.00069	0.00085	0.00099
08	Shell & Core	Max	0.00156	0.00500	0.00824	0.00739
		Mean + 2σ	0.00075	0.00133	0.00188	0.00184
	Substantial Completion	Max	0.00164	0.00512	0.00576	0.00837
		Mean + 2σ	0.00088	0.00142	0.00157	0.00230
09	Shell & Core	Max	0.00283	0.00421	0.00451	0.00628
		Mean + 2σ	0.00145	0.00225	0.00268	0.00373
	Substantial Completion	Max	0.00205	0.00289	0.00302	0.00474
		Mean + 2σ	0.00105	0.00112	0.00149	0.00150
10	Shell & Core	Max	-	-	-	-
		Mean + 2σ	-	-	-	-
	Substantial Completion	Max	0.00166	0.00248	0.00309	0.00395
		Mean + 2σ	0.00085	0.00120	0.00158	0.00219
11	Shell & Core	Max	-	-	-	-
		Mean + 2σ	-	-	-	-
	Substantial Completion	Max	0.00082	0.00218	0.00245	0.00276
		Mean + 2σ	0.00049	0.00072	0.00070	0.00075

A summary of the measured natural frequencies is presented below in Table 10. These were derived from the frequency spectra of the field measurements of acceleration at each location.

Table 10: Shell and Core Versus Substantial Completion – Natural Frequencies

Location	Construction Phase	Peak 1 (Hz)	Peak 2 (Hz)	Peak 3 (Hz)
01	Shell & Core	6.0	89.7	-
	Substantial Completion	5.9	-	-
02	Shell & Core	5.0	-	-
	Substantial Completion	9.5	23.2	-
03	Shell & Core	5.6	-	-
	Substantial Completion	7.6	14.2	28.5
04	Shell & Core	5.4	8.9	-
	Substantial Completion	6.0	9.0	12.4
05	Shell & Core	-	-	-
	Substantial Completion	7.9	11.3	36.9
06	Shell & Core	8.6	13.8	16.4
	Substantial Completion	9.2	12.5	-
07	Shell & Core	18.2	25.2	35.9
	Substantial Completion	19.0	-	-
08	Shell & Core	8.6	14.2	-
	Substantial Completion	9.1	81.8	-
09	Shell & Core	8.5	13.3	-
	Substantial Completion	12.6	16.3	
10	Shell & Core	-	-	-
	Substantial Completion	9.2	13.0	-
11	Shell & Core	-	-	-
	Substantial Completion	9.2	14.8	23.1

VIBRATION MODELING USING DESIGN GUIDE

Model Calibration

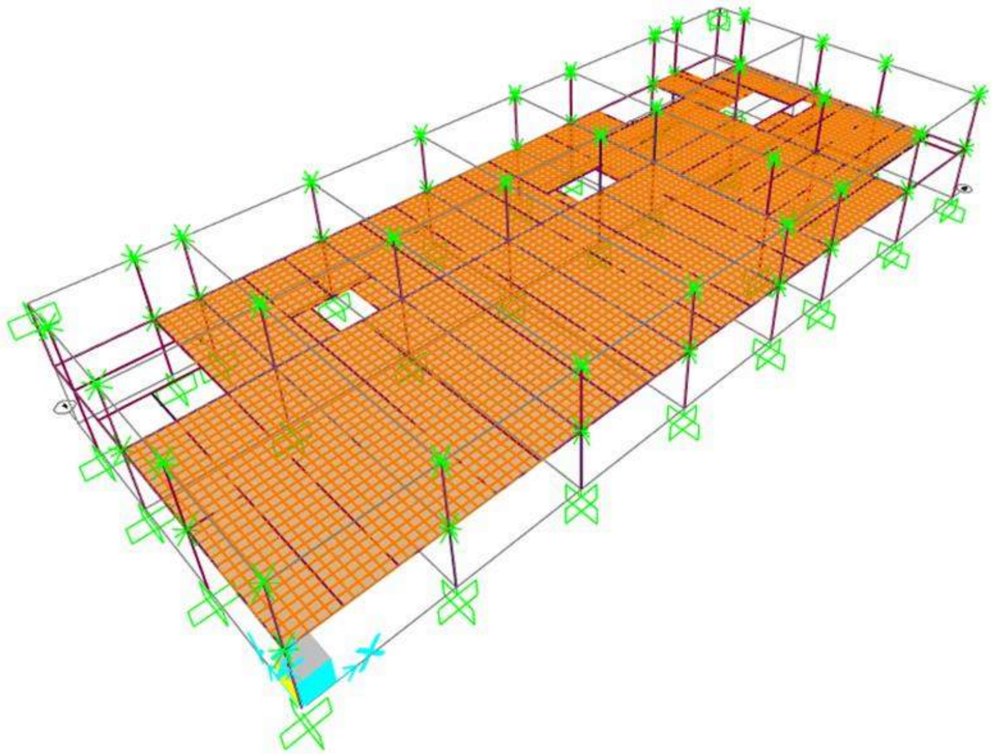

Figure 16: Level 2 Floor Vibration Model in SAP2000

The Level 2 floor plate was modeled in SAP2000 for construction stages 2 and 3: Shell and Core, and Substantial Completion. In each model, the concrete topping and CLT were assumed to be fully composite with the steel beams (achieved through welded headed studs). This composite action is modeled explicitly within the program by providing shell offsets per section 5.6 of the Design Guide. An illustration of the Level 2 floor plate model is shown in Figure 16, and an illustration showing the offsets of CLT shell elements with respect to the steel floor framing is shown in Figure 17.

Because there was no positive mechanical connection between the CLT panels and the concrete topping slab, composite action could only be developed through chemical bond between the CLT and concrete. This bond is neither reliable nor easily quantifiable, so only a low level of composite action was expected between the CLT panels and the concrete topping. The degree of composite action is defined in the Design Guide by the "partial composite action factor" γ (gamma), which varies between 0.0 and 1.0. A value of γ = 0.0 represents no composite action between the CLT and the topping slab. That is, the total flexural stiffness of the slab and CLT assembly is simply the sum of the flexural stiffness of the slab and the flexural stiffness of the CLT (after transforming the concrete material to wood using the modular ratio $n = E_{concrete}/E_{wood}$). A value of γ = 1.0 represents full composite action between the CLT and the topping slab. That is, the total flexural stiffness of the assembly is calculated from the combined, fully composite, slab and CLT sections (again, after transforming the concrete material to wood).

Values of γ for various composite assemblies are suggest in Table 3-6 of the Design Guide. For "Concrete topping cast directly on mass timber floor with no connection" the suggested range of γ is 0.05 to 0.15. It is also noted that "Values are based on limited testing field observations," and "Engineering judgment should be exercised when selecting the appropriate γ for a specific design scenario." For the HSEB project, the design team had the unusual advantage of data from full-scale flexural tests on composite floor panels and beams, and vibration tests of the completed floor assembly. Based on these tests, it was clear that composite action between the concrete topping slab and CLT panels was minimal, and analysis of the test data indicated partial composite action should be represented by a value of γ = 0.01. Appendix E contains an example of calculations that include the γ factor when computing partial composite section properties.

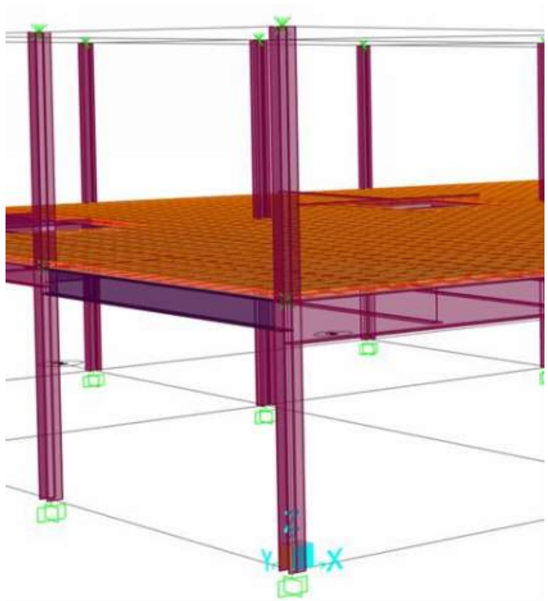

Figure 17: Modeled Floor System Build-Up

For the "Shell and Core" phase of construction the following modeling assumptions were made:

- Light damping, in the range of 1% to 2%, according to Design Guide Table 3-2, for the "Shell and Core" conditions where the concrete topping is installed, but without furnishings or non-structural partitions
- Concrete topping f'c = 7 ksi, according to the 28-day compressive strength report provided by the contractor (vibration testing was conducted at day 20)
- Young's modulus of concrete, E, was increased by a factor of 1.35 to account for modular increase at low-strains and modular increase under dynamic strain rates, per Design Guide section 3.3.5
- Partial composite action factor γ was taken as 0.01 for the concrete slab and CLT assembly, as explained above
- Full composite action was considered between the concrete topping and the steel framing. This composite action was achieved in construction using welded headed studs along the top flanges of steel beams.
- The self-weight and mass of steel framing members was modeled.
- The weight and the mass of the CLT (9 psf) and 3" concrete topping (36 psf) were modeled as additional spread loads over the shell elements. No superimposed dead load or live load contribution was considered in this model because of the intermediate stage of construction.
- See Appendix E for example calculations showing how the SAP shell element property modification factors were computed.

The fundamental vibration frequencies determined through field tests at select locations were compared with the dominant fundamental frequencies obtained through modal analysis with the model. To determine the dominant fundamental frequencies at a particular location in the model, the computed mode shapes were examined to identify modes with activity concentrated in the framing bay, or bays, of interest.

Generally, there was good agreement between the measured and modeled frequencies. In the long-span bays (in the lower left region of the plan view, see locations 1, 2, 3, and 4 in Figure 18), the measured fundamental frequencies of the bays fall in the 5 to 6 Hz range (see Table 8). This agrees with the analytical results, where modes 1 through 4 and 6 have frequencies between 4.9 and 6.5 Hz. Figure 18 below shows that these modes exhibit primary activity in the area of the four long-span bays. The measured frequencies in a short span bay (Locations 6, 8 and 9 in Figure 15; note that Location 7 was on a very stiff spandrel beam) were in the range of 8.5 to 8.6 Hz for the first frequency, and 13.3 to 14.2 Hz for the second frequency (see Table 8). This is in good agreement with the analytical frequencies in Figure 18, with the first activity in this bay occurring at mode 15 of the floor plate at 8.7 Hz, and subsequent activity at modes 22 and 24 at 11.5 and 12.0 Hz. Note that modes from the analytical model with primary activity in areas that were not measured are not discussed in this report because there is no field data to compare with the analysis results.

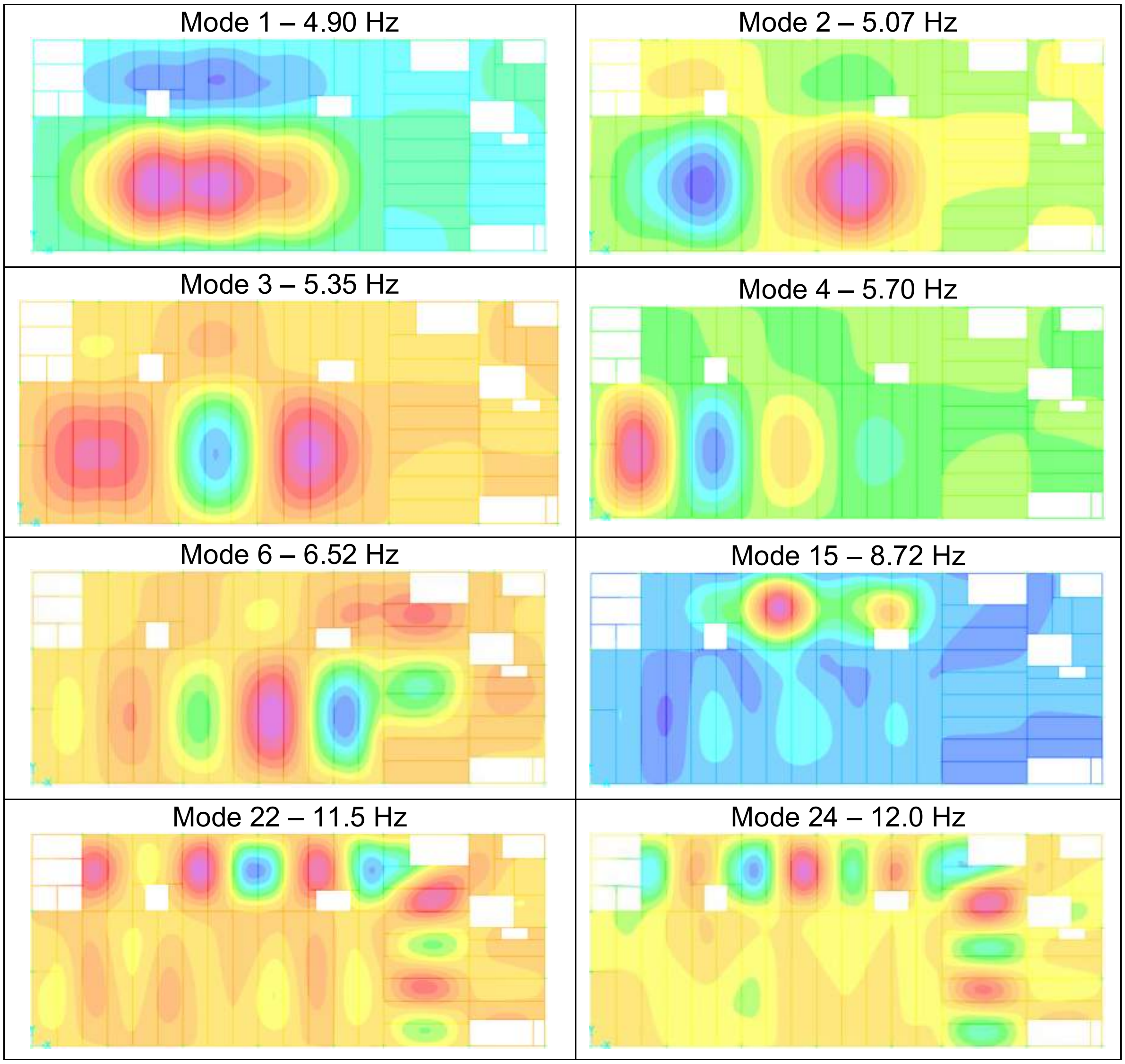

Figure 18: Modal Analysis Summary for Level 2 Floor Framing

COMPARISON OF MEASUREMENTS AND MODELING

A form of modal superposition analysis was employed in this study to analytically predict the vibration response of the floor to walking excitation. A general discussion of modal superposition methods may be found in section 4.3 of the Design Guide. The particular form of modal superposition analysis used in this study is described in detail in reference CCIP-16 and is referred to in this report as the "CCIP method." This method first requires development of a finite element model of the floor framing, or section of floor framing, that is of interest. This FEA model is used to perform a modal analysis of the modeled floor, and the results of the modal analysis are then provided as input to separate software for post-processing and execution of the modal superposition analysis. Some commercial FEA software packages perform both the modal analysis and execution of the modal superposition analysis within the framework of the software. In this study the preliminary modal analysis was performed using SAP2000, and then post-processing of the modal data, using the CCIP method, was carried out with separate proprietary software.

Footfall-induced vibration response of floors can be broadly described as falling into two categories: resonant response and impulsive response. According to section 4.3 of the Design Guide, a resonant response analysis should be considered if the first mode frequency of the floor is less than about 4 times the walking speed plus 2 Hz. For example, if the first natural frequency of a floor is 5 Hz, and the walking pace is 1.5 steps per second (1.5 Hz) then 4x1.5 + 2 = 8 Hz > 5 Hz, so resonant response is likely. Impulsive response occurs when natural frequency of the floor is greater than about 4 times the frequency of the walking pace. For example, for a walking pace of 1.5 steps per second and a floor natural frequency of 10 Hz, impulsive response would be likely.

In the case of the HSEB vibration analysis, the focus was on resonant response analysis. The first mode of the floor plate is 4.9 Hz, and the walking speeds considered range from 75 steps per minute (SPM) to just over 120 SPM, or 1.25 Hz to 2.1 Hz. For the HSEB floor, four times the walking frequency plus 2 Hz has a range of 7 to 10.4 Hz. Since the first mode of the floor, 4.9 Hz, is below this range, a resonant response analysis was performed.

An example of the peak accelerations calculated with the resonant response analysis is shown in Figure 19. These results reflect the maximum values of accelerations computed for any walking speed in the analysis, ranging from 75 to 126 steps per minute. This is referred to as the “enveloped” response.

The analytical results in Figure 19 are compared to the measured peak accelerations obtained from the floor vibration tests at the HSEB in Table 11. Results are shown for the four “long-span” bays in Figure 19 (locations 1, 2, 3, and 4) and for the “short-span” bay (location 6). Field vibration measurements were made at walking speeds of 80, 100, and 120 SPM, and the measured maximum acceleration values are reported in the third column of Table 11.

As discussed earlier in the section “Structural Vibration Criteria,” it is helpful to report peak accelerations from a field test of footfall-induced vibrations as the average of the data plus some multiple of the standard deviation of the data. This prevents fitting model results to outlying peaks that are not representative of the maximum accelerations generally observed in the overall test record. The designation of the number of standard deviations above the mean that defines the overall maximum for the record is somewhat dependent on the nature of the data (for example, if the data appear to represent a stationary process or an episodic process), and the duration of the record. An examination of all of the vibration data obtained in field tests at the HSEB indicated that the maximum accelerations could be characterized consistently by a multiplier of two times the standard deviation. These are the experimental values reported in Table 11.

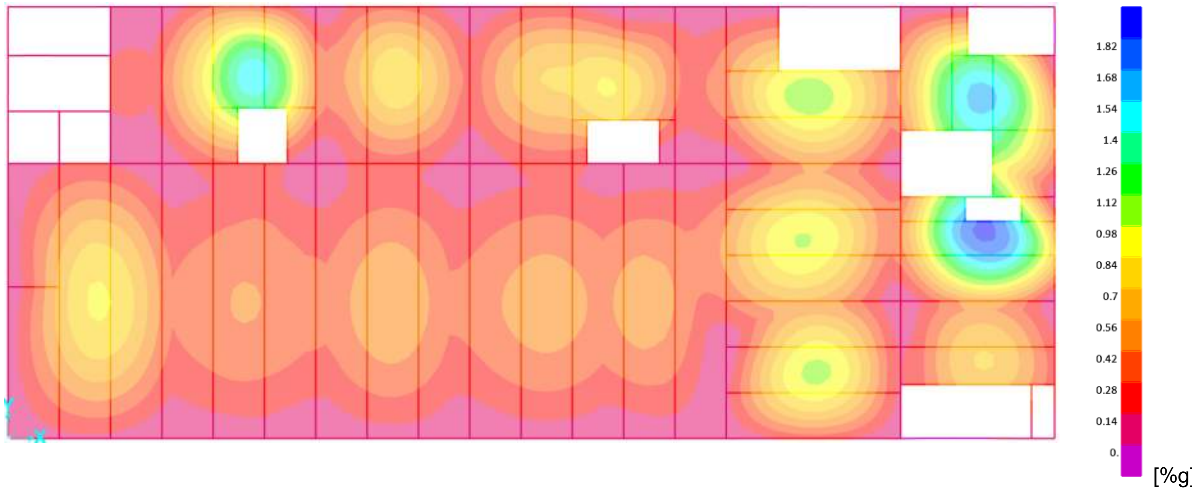

Figure 19: Enveloped Resonant Response Peak Accelerations from Modal Superposition Analysis, 2% Damping

Table 11: Measured Versus Modeled Acceleration Response

Location	Walking Speed (SPM)	2σ Acceleration (%g)	ξ = 1% Model Acceleration (%g)	ξ = 2% Model Acceleration (%g)
1	80	0.27	0.24	0.21
	100	0.30	0.19	0.18
	120	0.29	0.29	0.30
	75-126		1.7	0.86
2	80	0.19	0.30	0.17
	100	0.24	0.54	0.33
	120	0.52	0.18	0.17
	75-126		0.84	0.44
3	80	0.07	0.70	0.37
	100	0.08	0.37	0.25
	120	0.10	0.16	0.16
	75-126		1.0	0.53
4	80	0.10	0.43	0.25
	100	0.15	0.68	0.46
	120	0.22	0.15	0.15
	75-126		0.87	0.49
6	80	0.18	0.13	0.06
	100	0.33	0.13	0.13
	120	0.36	0.82	0.81
	75-126		1.6	0.82

The data from Table 11 are shown graphically below in Figure 20. It can be seen that the analysis results obtained for a damping value of 1% greatly exceed the values measured in the field, and that a damping value of 2% results in analytical predictions that are less conservative, but still about double the measured accelerations (the one exception is Location 2). The calculated accelerations are nearest the measured accelerations at a walking speed of 120 SPM (comparing the yellow bars to the green bars). This is consistent with the fact that the maximum walking speed in the analysis (126 SPM) was about the same as the maximum walking speed in the tests (120 SPM). Nonetheless, using a value of 2% damping in the analysis produces analytical results that are in most cases overly conservative compared to the measured accelerations. The Design Guide recommends "light damping" of 1% to 2% for this analysis. Clearly, for the HSEB analysis model, a higher value of damping would be needed to produce less conservative predictions of peak acceleration. Based on the trends observed in Figure 20, a damping value of 2.5% to 3% would yield results closer to the measured values..

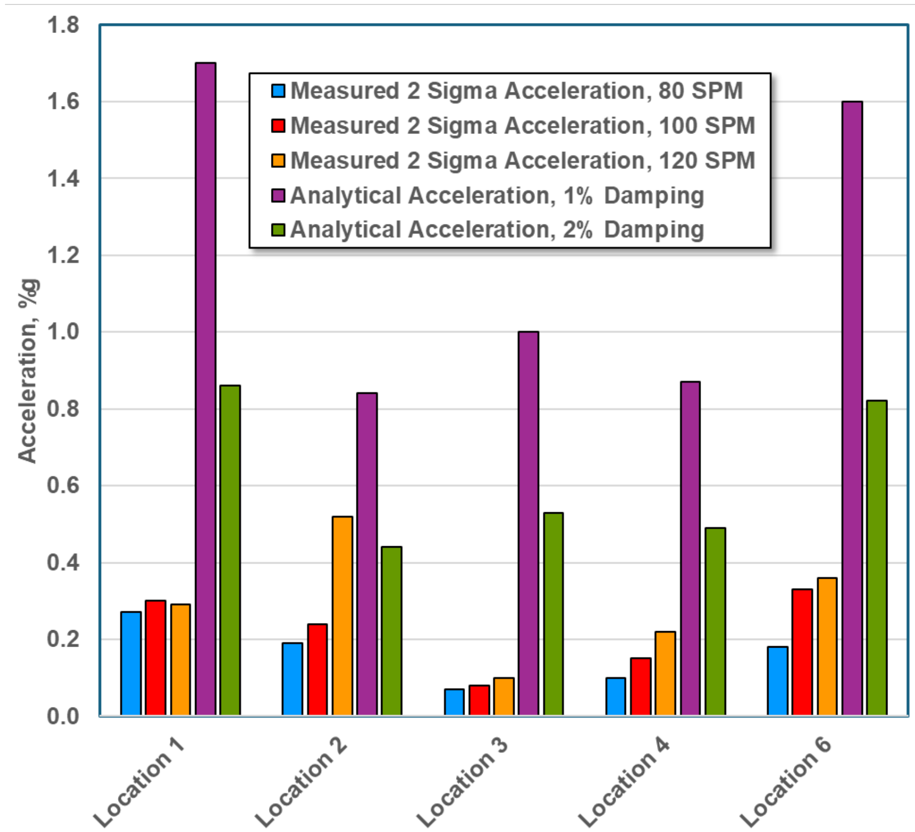

Figure 20: Measured Versus Modeled Acceleration Response

Appendices C and D contain one-third octave band spectra of measured of RMS velocity for all measurement locations and all walking speeds. As described earlier in the section Structural Vibration Criteria, these plots, along with ISO and VC vibration thresholds, are the de facto standard for rating the vibration performance of floors for sensitive equipment.

One of the primary objectives of this study is to evaluate the analytical modeling methods recommended in the Design Guide by comparing the results of the analysis with measured floor vibration data from the HSEB. Table 12 shows the measured RMS velocity in micro-inches per second (mips) at five measurement locations, for walking speeds of 80, 100, and 120 SPM at each location. Also shown in Table 12 are the analytical predictions of RMS velocity for structural damping values of 1% and 2%. It can be seen that the analytical predictions are in most cases greater than the measured values, but that the results for 2% damping are closer to the measured values than for 1% damping. As with the analytical predications of acceleration presented above, the Design Guide recommendation of 1% to 2% for this analysis appears to be too low. Improved predictions of RMS velocity might be obtained with a damping value of 2.5% to 3%.

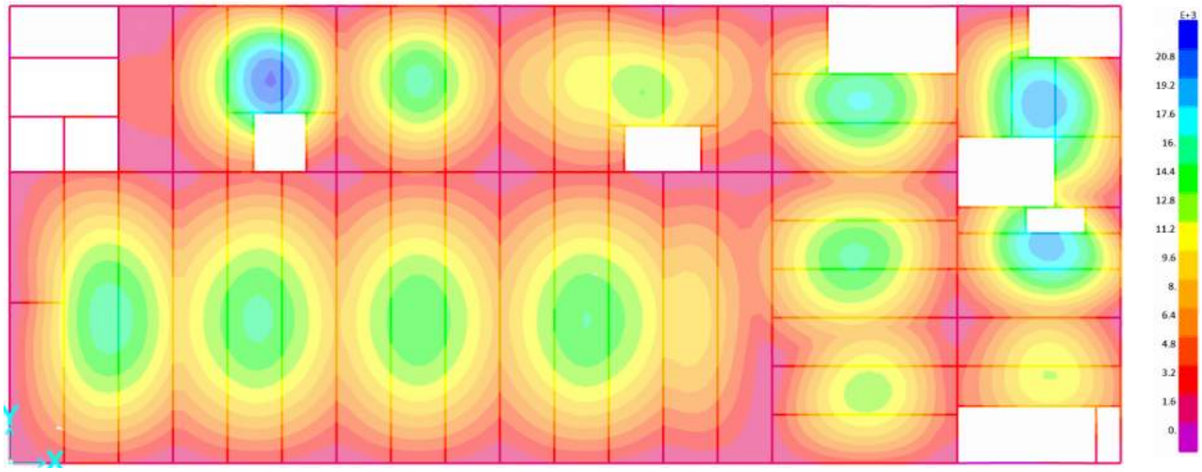

Figure 21: Example RMS Velocity Contour Plot Derived from the Modal Superposition Method

Table 12: Measured Versus Modeled RMS Velocity

Location	Walking Speed (SPM)	Measured RMS Velocity (mips)	ξ = 1% Model RMS Velocity (mips)	ξ = 2% Model RMS Velocity (mips)
1	80	6,000	11,000	10,400
	100	7,300	16,900	15,500
	120	23,000	22,400	20,800
2	80	9,400	10,800	10,000
	100	12,000	15,900	15,800
	120	13,600	21,600	20,300
3	80	6,400	10,600	9,700
	100	13,000	15,500	14,400
	120	16,000	20,900	19,500
4	80	20,200	11,000	10,000
	100	12,400	15,600	14,500
	120	7,000	20,800	19,500
6	80	7,000	10,900	9,800
	100	11,000	16,700	15,000
	120	15,800	23,000	21,100

4. References

CCIP-016 (2007), Willford, M.R., Young, P., *CCIP-016 – A Design Guide for Footfall Induced Vibration of Structures*, The Concrete Centre, London

CSI (2022), "SAP2000 Integrated Software for Structural Analysis and Design," Computers and Structures Inc., Berkeley, California

Design Guide (2021), *U.S. Mass Timber Floor Vibration Design Guide*, First Edition, WoodWorks – Wood Products Council, Washington, D.C.

PRG 320 (2019), *Standard for Performance-Rated Cross-Laminated Timber*, ANSI/APA PRG 320-2019, published by APA – The Engineered Wood Association, Tacoma, WA, 2020

Appendix A

Structural Research Laboratory Testing Report

This page intentionally left blank.

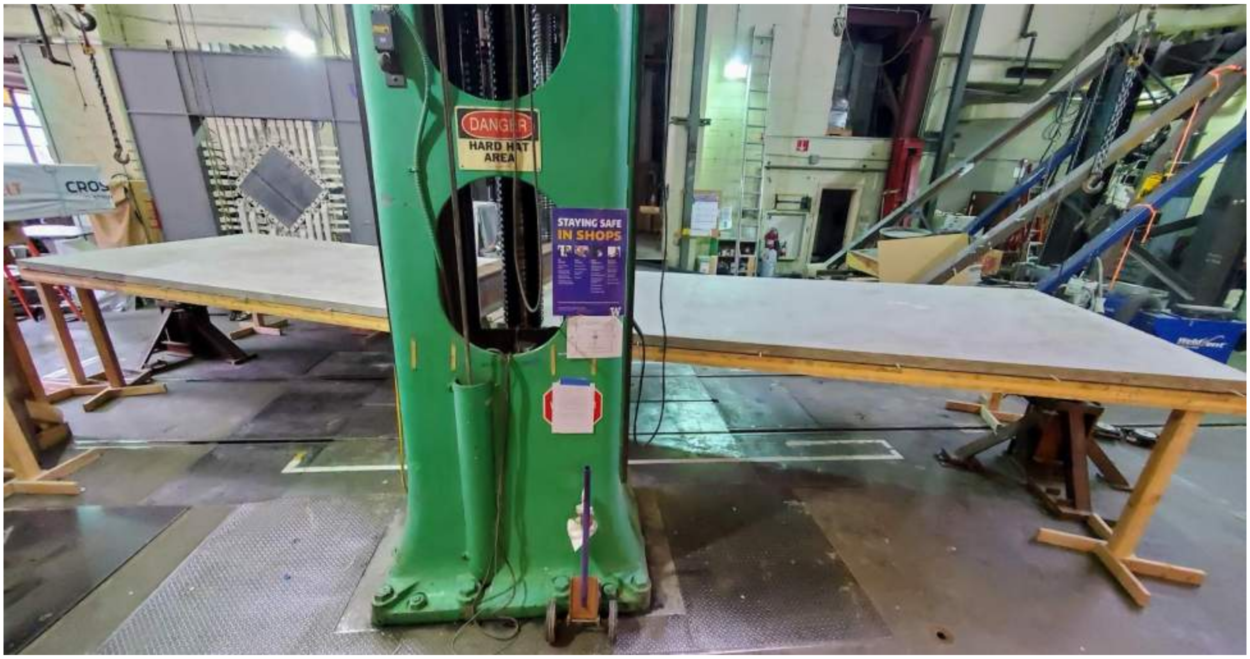

Structural Research Laboratory Commercial Testing Report

CLIENT: Jacob McCann, SE
KPFF Consulting Engineers

TEST INFORMATION:

Testing Dates: May 14, 2020, June 11, 2020, June 29, 2020 – July 2, 2020
Performed By: Vince Chaijaroen, Structural Research Lab Manager
Directed By: Jeffrey Berman Ph.D., Professor, SRL Director
Witnessed By: Jacob McCann, SE, Principal, KPFF
Andy Taylor, PhD, SE, FACI, Technical Director, KPFF
Addie Lederman, EIT, Design Engineer, KPFF
Jessica Westermeyer, PE, Associate, KPFF

Introduction:

The University of Washington (UW) Structural Research Laboratory (SRL) was contracted to conduct bending testing of a composite beam system designed by KPFF Consulting Engineers and bending testing of cross-laminated (CLT) timber panels. The tests were conducted on May 14, 2020, June 11, 2020, and June 29, 2020 through July 2, 2020 using the 2.4 million pound Universal Testing Machine (UTM) in the SLR and was witnessed by Jacob McCann, Andy Taylor, Addie Lederman, and Jessica Westermeyer of KPFF. Vibration testing was also performed on the constructed specimens by KPFF engineers but those tests are outside the scope of this report.

Test Specimen:

The beam test specimens were a steel beam composite with a concrete topping slab and CLT decking. The appendix contains drawings for the beam specimens. Figure A.1 shows a 3D rendering of the composite beam. The panel specimens are listed in Table A1. Each panel was 8’-0” x 12’-0” with the strong axis in the long dimension.

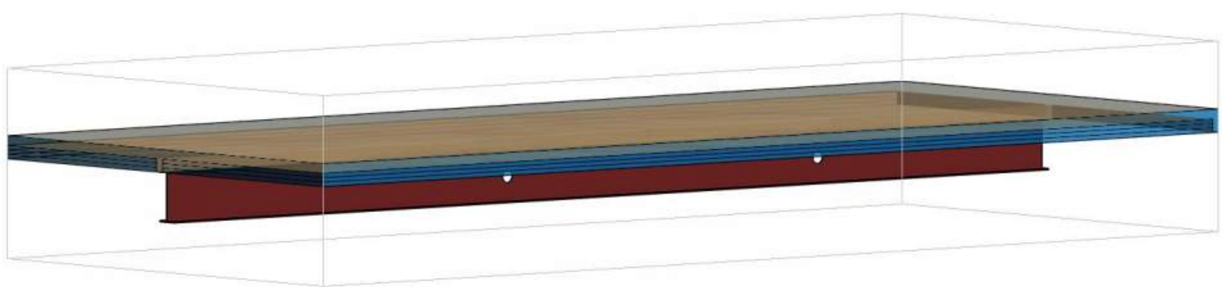

Figure A.1: Composite Beam Rendering

Table A1: CLT Panel Experiments

Specimen	CLT Layup
3-Ply bare panel	V2M1.1-105V
5-Ply bare panel	V2M1.1-175V
7-Ply bare panel	V2M1.1-245V
3-Ply panel with 3” concrete topping	V2M1.1-105V
3-Ply panel with 3” concrete topping over expanded sheet metal mesh	V2M1.1-105V

Test Setup, Instrumentation and Loading:

The composite beam was constructed under the SRL’s UTM cross head and supported on steel stands with a rocker. Three-point bending was applied using a loading beam to spread the load from the UTM platen over the width of the specimen. The specimen is shown in Figure A.2, additional details are provided in the appendix. The cross sectional view shows the 1" diam. diagonal struts fabricated from electrical conduit that were used to shore the CLT deck and concrete topping to the steel beam to ensure the concrete deck cured composite with the steel beam. The CLT decking was installed per the detail in Figure A.3 provided by KPFF, and a rebar mat of #4 @ 16" OC each way was provided at mid-depth of the 3" concrete topping slab per the structural drawings. To prevent a bearing failure of the CLT on the ¾" lag bolts, 3/8" threaded rods were installed transverse the to the beam span to tie the two sides of the deck together. This better simulates the demands on the lag bolts in the in situ conditions where the CLT would span to an adjacent parallel steel beam.

The panel tests were supported on a pin and a roller 6" from each end for an 11'-0" span. An example of the test setup is shown in Figure A.4.

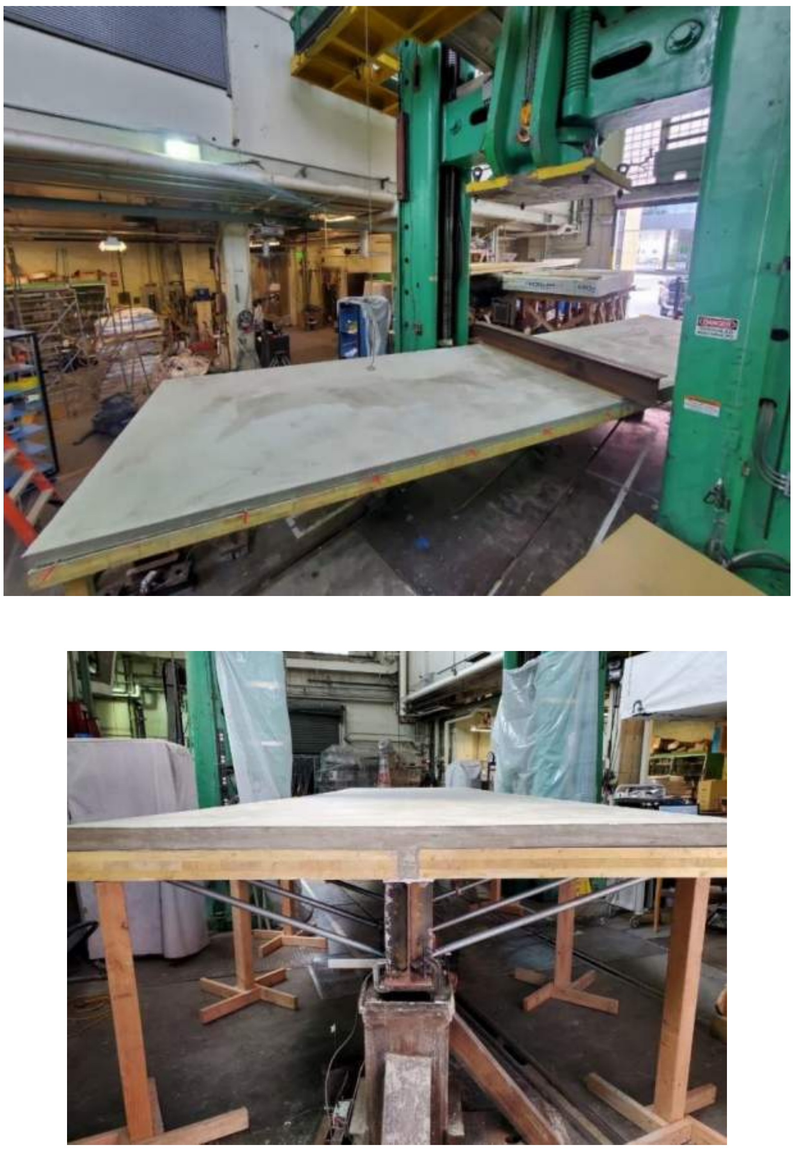

Figure A.2: Composite Beam Construction

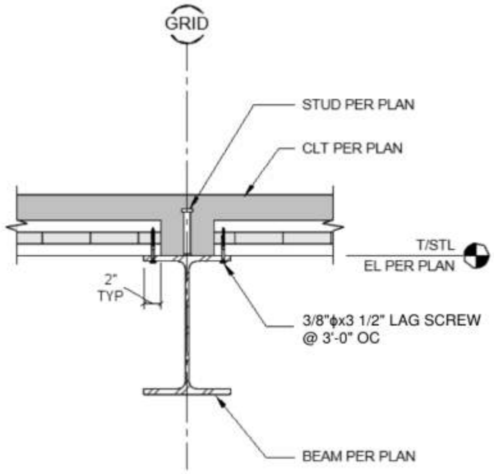

Figure A.3: Typical Composite Beam Section

Figure A.4: 3-Ply Panel Bending Test

Instrumentation for the beam tests included the UTM's internal load cell and internal linearly variable displacement transducer (LVDT). The load cell is calibrated to NIST standards annually and the most recent calibration certificate is provided in the appendix. The LVDT measures the displacement of the UTM cross head. For the beam tests, a set of strain, vertical displacement, and horizontal slip measurements were also made. The vertical displacement measurements were made using calibrated string potentiometers mounted to the bottom flange of the beam. The slip measurements were made by casting a steel rod into the concrete topping through a hole in the CLT alongside the beam flange. A Duncan pot was mounted to the underside of the beam top flange, and attached to a bracket that was attached to the rod coming down from the concrete. The beam instrumentation plan is shown in Figure A.5. Note that the outermost strain gage plans were only used in the second beam specimen, and there was only one slip measurement at each end on the first specimen.

Three-point bending was applied to increments of the total superimposed design load and vibration measurements were made. Then a loading protocol from IBC §1709.3 was followed. The loading protocols for each beam are as follows:

<u>Composite Beam 1:</u>

1) Load to 0.5 x factored superimposed design load = 13.6 kips
2) Unload completely
3) Vibration measurements suite
4) Load to 1.0 x factored superimposed design load = 27.1 kips
5) Unload completely
6) Vibration measurements suite
7) Document slab cracking extents

IBC Protocol starts:

8) Load to 2.0 x factored superimposed design load = 54.3 kips
9) Hold load for 24 hours
10) Unload completely
11) Check that beam recovers a minimum of 75% of the maximum deflection
12) Load to minimum 2.5 x factored superimposed design load = 67.9 kips

IBC Protocol ends

13) Load to failure = 72.3 kips

After the first test, it was decided that it was permitted to load to the unfactored (service level) superimposed design load per the IBC, and the loading procedure was changed to the following:

<u>Composite Beam 2:</u>

1) Load to 0.5 x service superimposed design load = 8.8 kips
2) Unload completely

3)	Vibration measurements suite
4)	Load to 1.0 x service superimposed design load = 17.5 kips
5)	Unload completely
6)	Vibration measurements suite
7)	Load to 1.0 x factored superimposed design load = 27.1 kips
8)	Vibration measurements suite
9)	Document slab cracking extents

IBC Protocol starts:

10)	Load to 2.0 x unfactored superimposed design load = 35.1 kips
11)	Hold load for 24 hours
12)	Unload completely
13)	Check that beam recovers a minimum of 75% of the maximum deflection
14)	Load to minimum 2.5 x unfactored superimposed design load = 43.9 kips

IBC Protocol ends

15)	Load to failure = 59.5 kips

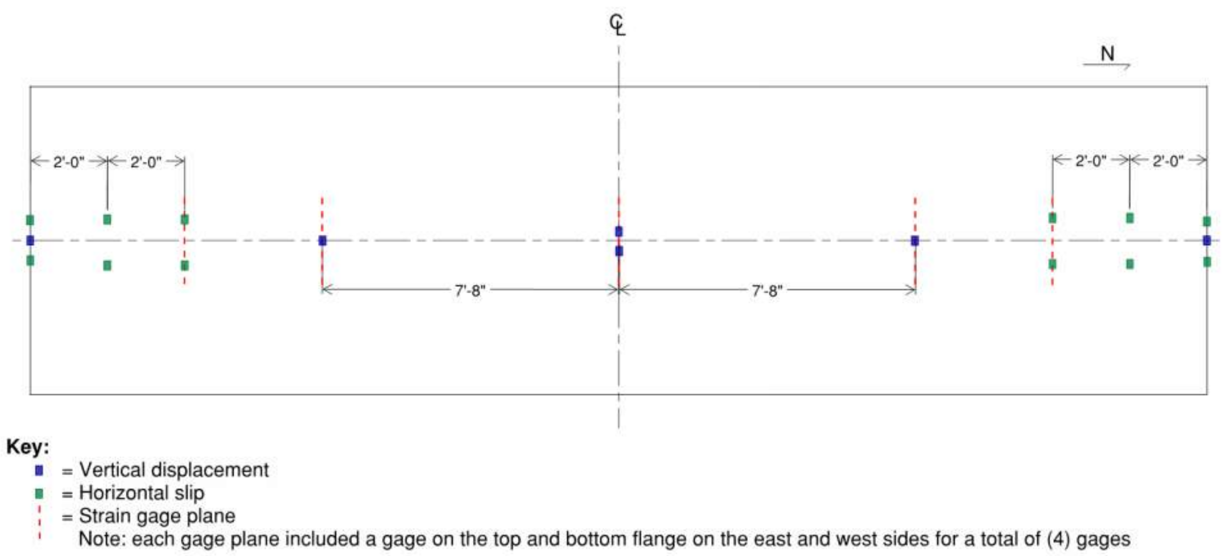

Figure A.5: Composite Beam Test Instrumentation

Instrumentation for the panel tests also included the UTM's internal load cell and LVDT. In addition, the panel tests included a set of vertical displacement measurements. The instrumentation plan for the panel tests is shown in Figure A.6.

Three point bending was applied quasi-statically to the panels. Each panel was loaded to failure. All of the panels failed via tension rupture of the bottom laminate except for the 7-ply panel. The 7-ply panel failed in rolling shear.

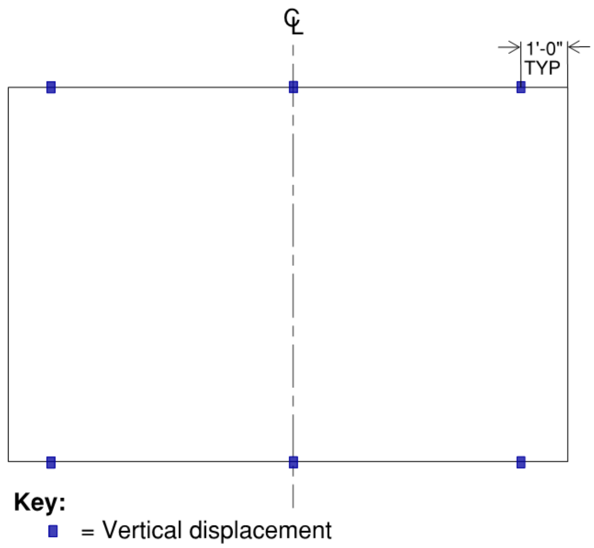

Figure A.6: Panel Test Instrumentation

Test Results:

The first composite beam reached a maximum of 72.3 kips, and the second beam reached a maximum of 59.5 kips. Both beams held the load in the first step of the IBC protocol for 24 hours without substantial creep. The first beam did not recover 75% of the maximum imposed deformation because the long duration load was 2.0 times the factored superimposed dead load. However, the load-displacement curve shows that if the beam had unloaded elastically from 35.1 kips (2.0 times the unfactored superimposed dead load), the beam would have recovered the required amount. The second beam, which was loaded to 35.1 kips for 24 hours, recovered exactly 75% of the maximum displacement. And, both beams reached 2.5 times the superimposed design load before failure. The load-displacement curves from the centerline displacement measurements are shown in Figure A.7.

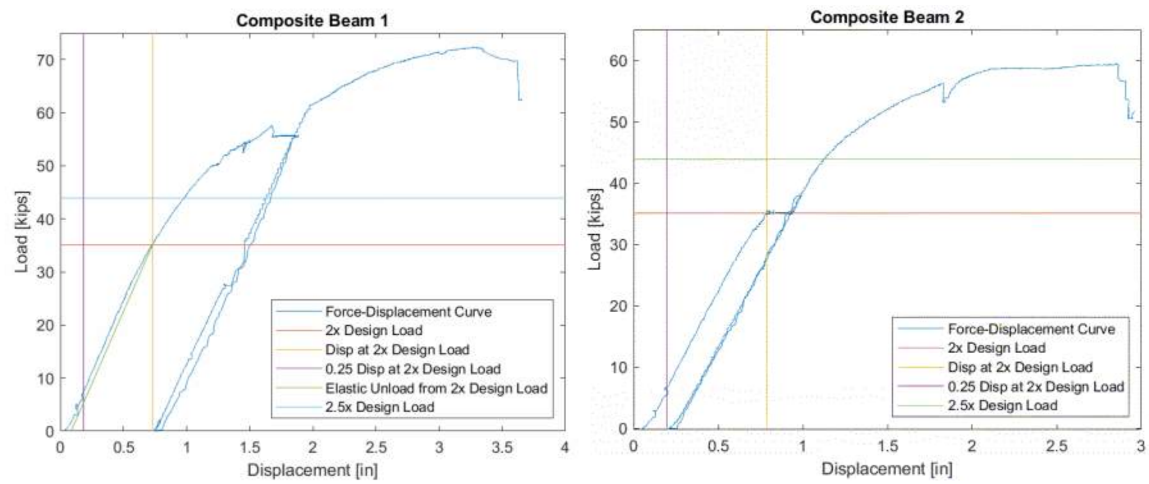

Figure A.7: Composite Beam Force-Displacement Curves

The force-displacement curves from the panel tests are shown in Figure A.8.

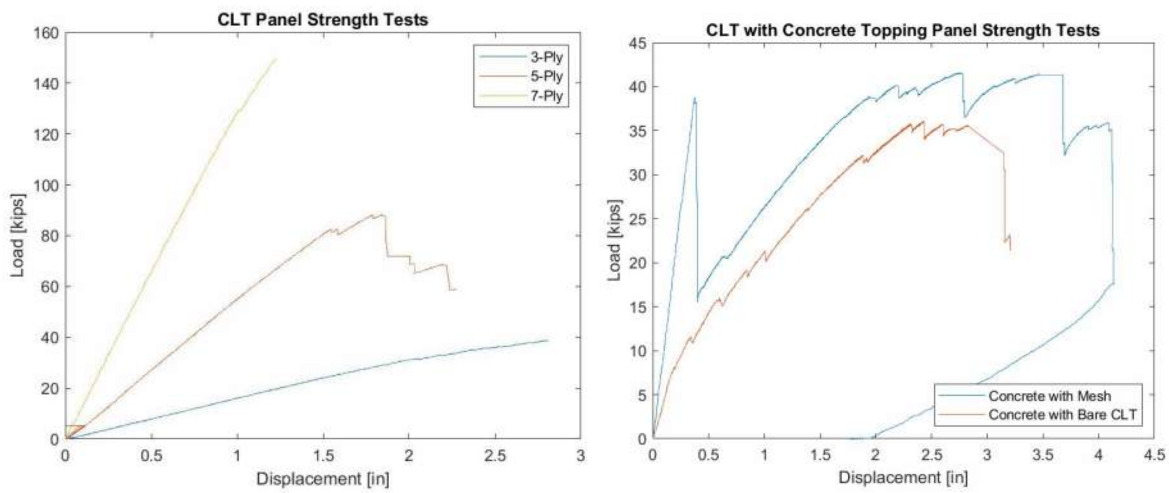

Figure A.8: Panel Test Force-Displacement Curves

<u>Laboratory Disclaimer Statement:</u>

The UW Structural Research Laboratory (UWSRL) provides commercial testing services. Unless otherwise specified in the contract, these services are limited to testing and data collection. The results are valid at the time the test occurs on the specific specimens tested.

The agreement is between the two parties, which include the UWSRL and the client requesting the testing services ("Client"). The UWSRL and Client agree that the relationship between the parties established by this Agreement does not constitute a partnership, joint venture, agency, or contract of employment of any kind between them and that nothing herein shall be interpreted as establishing any form of exclusive relationship between the parties. The client shall release, hold harmless and indemnify the University of Washington, its Regents, officers, agents, employees and students from any and all claims, damages, costs (including reasonable attorney fees) and liabilities arising out of the testing. Neither party shall have any liability of any kind to the other Party for any indirect damages, including, but not limited to, lost profits, lost revenues, or loss of use.

Verification of Results:

The SRL Director, Professor Jeffrey Berman, and the SRL Manager Vince Chaijaroen, have reviewed the test results and verify their correctness.

Prof. Jeffrey Berman
Thomas and Marilyn Neilson Associate Professor
SRL Director
Department of Civil and Environmental Engineering
University of Washington
jwberman@uw.edu

Appendix

UTM Calibration Certificate

National Standards

ANAB ACCREDITED ISO/IEC 17025 ANSI/NCSL Z540-1 ilac-MRA Certificate #L2271

NATIONAL STANDARDS TESTING LABORATORY

P.O. Box 5808
15753 Crabbs Branch Way
Rockville, Maryland 20855

301-590-0097
1-877-CAL-FORCE
www.forcelab.com

Testing Laboratory

Lab No. SJT.01/M10237 Trans Letter 3-26-19 Order No. Credit Card

Certificate of Verification

In accordance with ASTM Standard Practices E 4-16

Baldwin Testing Machine No. 224842-A

Calibration Location
University of Washington
201 More Hall
Seattle, WA 98195

Baldwin Model 2,400,000 LBF Test Machine Serial Number 224842-A was verified in accordance with ASTM Standard E 4-16, "Standard Practices for Force Verification of Testing Machines". This standard has been approved for use by agencies of the Department of Defense. The following range was verified in accordance with E 4-16 within ± 1% on May 30, 2019 and complies with ISO/IEC 17025:20052005 and ANSI/NCSL Z540-1:1994 (R2002).

Range 1: 2,400,000 lbf range from 20,000 lbf minimum to 2,400,000 lbf maximum.

Elastic Calibration Devices Used In This Verification

Cell ID	Serial Number	Calibration Date	Recall Date	Device Manufacturer	Operating Mode	Class "A" Lower Limit	Class "A" Upper Limit
K	**110410**	**9/26/18**	**9/26/20**	**Strainsense Company**	**Compression**	**20,000 lbf**	**1,000,000 lbf**
L	**110411**	**9/26/18**	**9/26/20**	**Strainsense Company**	**Compression**	**20,000 lbf**	**1,000,000 lbf**
M	**51016 (Br.B)**	**9/26/18**	**9/26/20**	**BLH**	**Compression**	**20,000 lbf**	**1,000,000 lbf**
N	**110711**	**9/26/18**	**9/26/20**	**Strainsense Company**	**Compression**	**20,000 lbf**	**1,000,000 lbf**

The elastic calibration devices were calibrated to ASTM Specification E 74 by National Standards Testing Laboratory and are traceable to the National Institute of Standards and Technology. The calibrations of these devices comply with ISO/IEC 17025:2005, ANSI/NCSL Z540-1:1994 (R2002), and 10CFR Part 21.

The results of the verification are given in the attached Verification Report. Per Section 16 of E 4-16 it is recommended that the testing machine be reverified within 1 year. This certificate and report shall not be reproduced except in full without the written approval of NSTL.

NOTE: This Certificate of Verification and Verification Report is a statement of the performance of the test machine as operating on the date of verification. National Standards Testing Laboratory accepts no liability for any loss or damage resulting in any way from the use by the customer (purchaser), his agents and assigns, or any other user of any testing machine verified by NSTL, nor from the use by anyone (including but not limited to the above parties) of the verification certificate, report, data, and/or analysis provided by NSTL.

A. Vincent Gredone III
Director

Attachments: verification report

Page 1 of 2

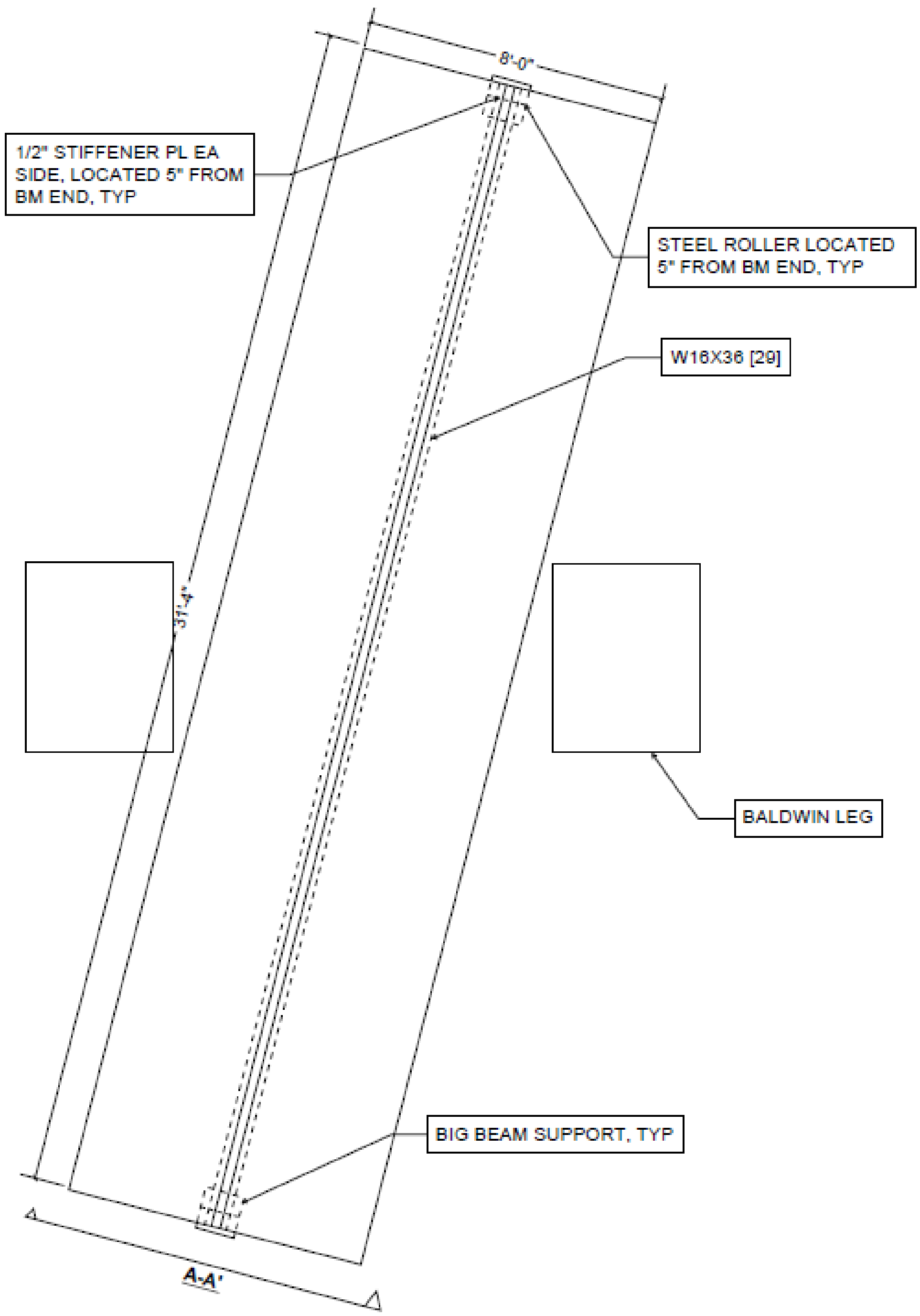

Schematic of Composite Beam Test Setup

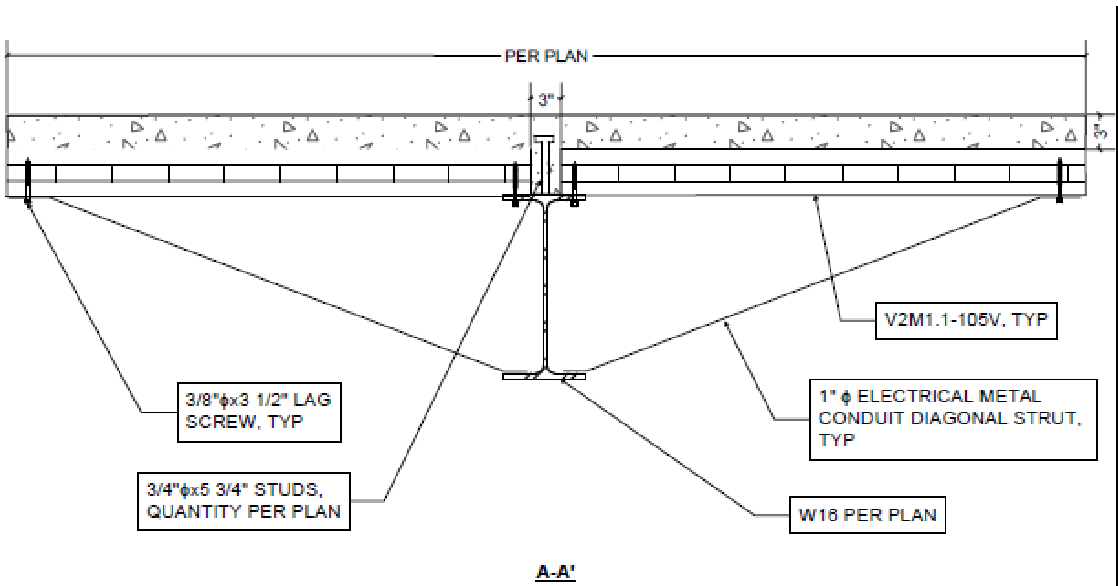

NOTES:

1. BEAM SUPPORTS NOT SHOWN FOR CLARITY
2. CAL PORTLAND CONCRETE MIX 63169, f'_c = 5 KSI

Schematic of Composite Beam Cross-Section

Appendix B

Plots of Frequency Spectra from Laboratory Impulse Testing

This page intentionally left blank.

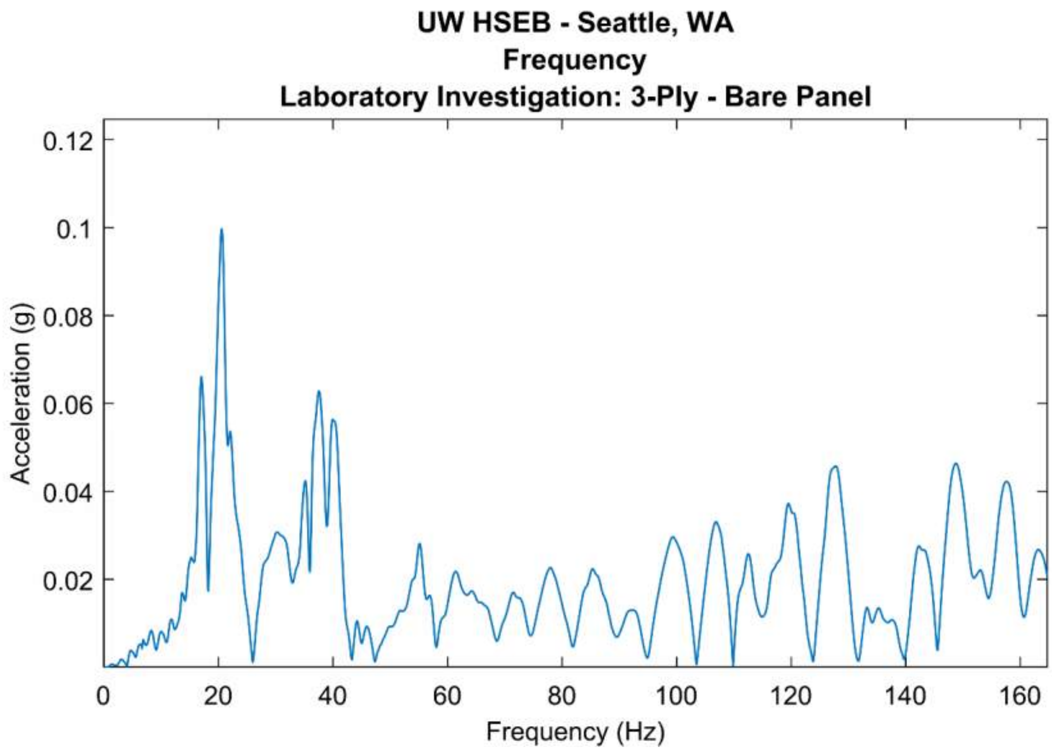

Figure B1: 3-Ply Bare Panel - Natural Frequencies

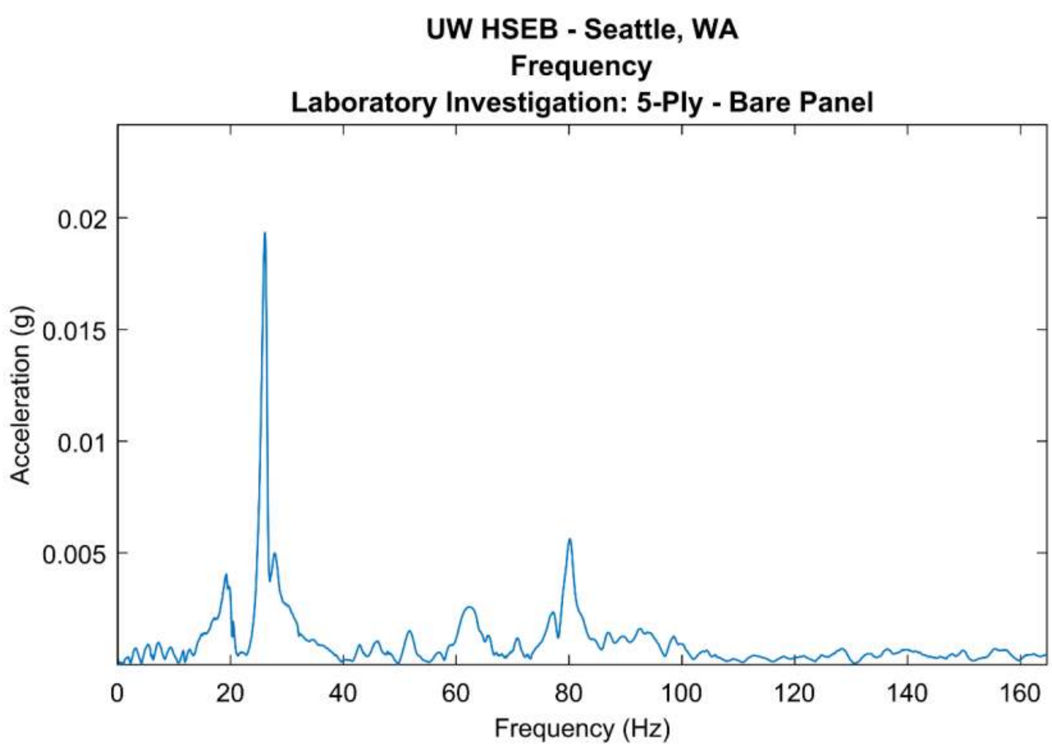

Figure B2: 5-Ply Bare Panel - Natural Frequencies

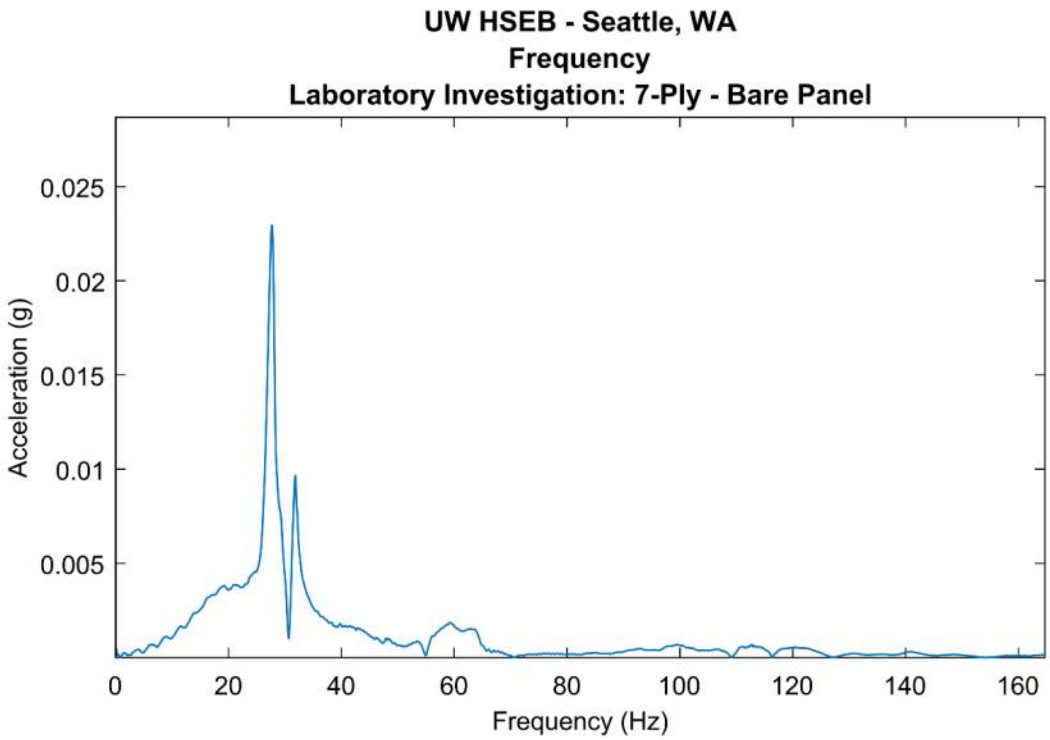

Figure B3: 7-Ply Bare Panel - Natural Frequencies

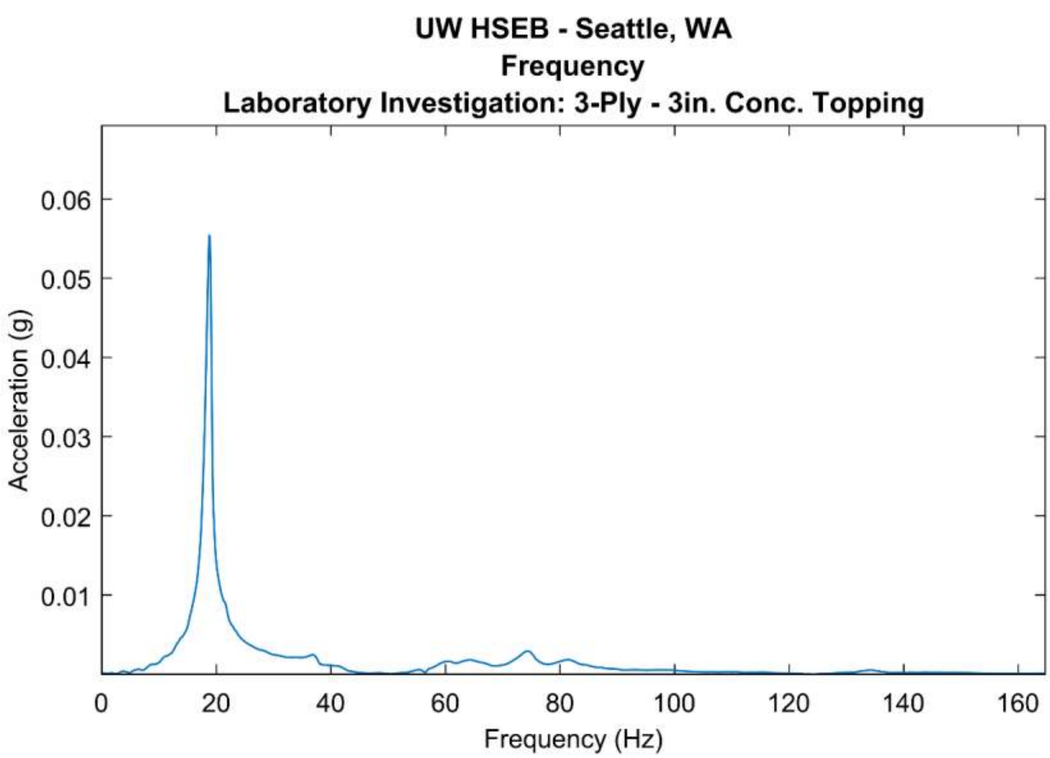

Figure B4: 3-Ply Panel with Conc. Topping - Natural Frequencies

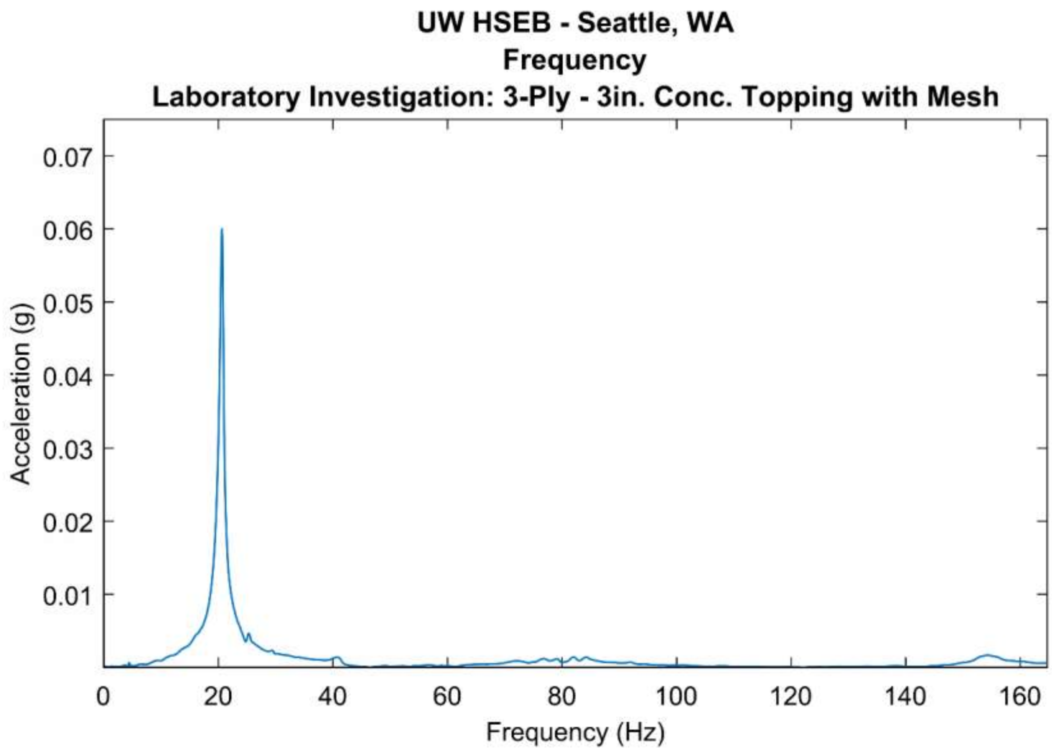

Figure B5: 3-Ply Panel with Conc Topping & Mesh - Natural Frequencies

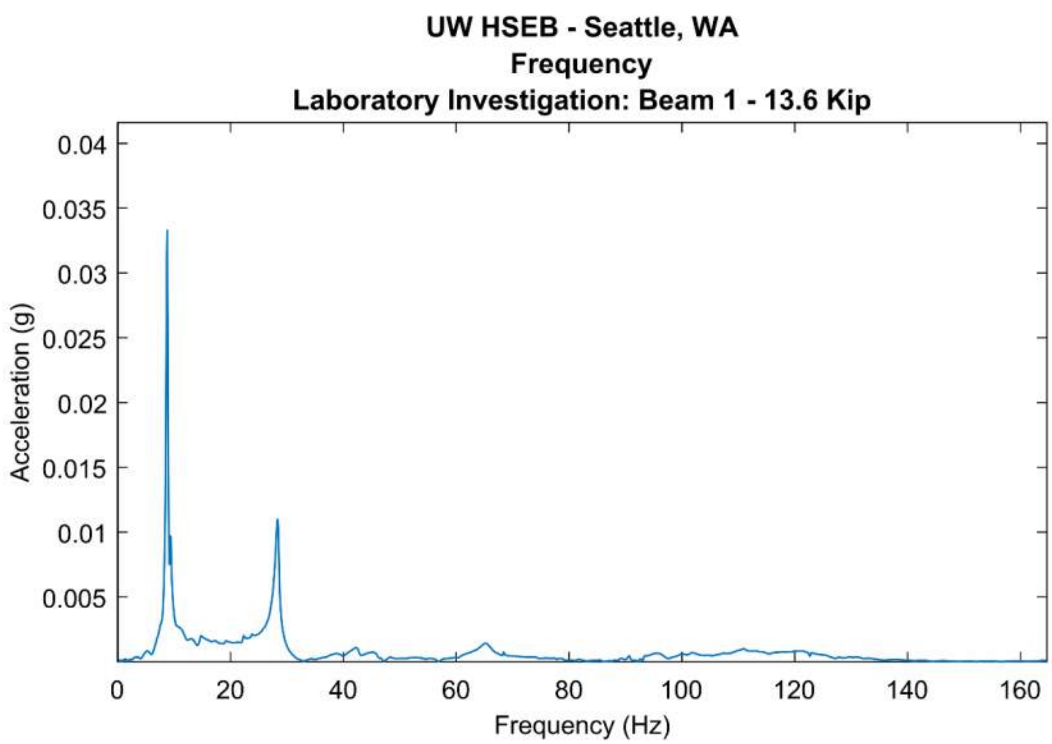

Figure B6: Beam 1 Post 13.6 Kip Load - Natural Frequencies

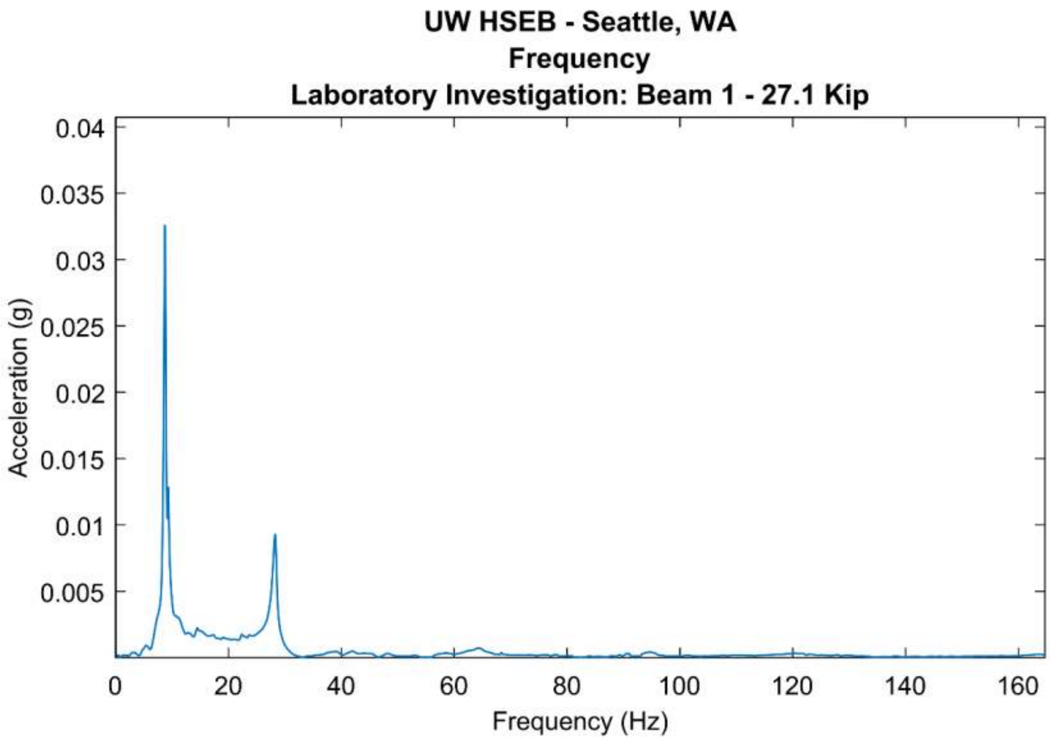

Figure B7: Beam 1 Post 27.1 Kip Load - Natural Frequencies

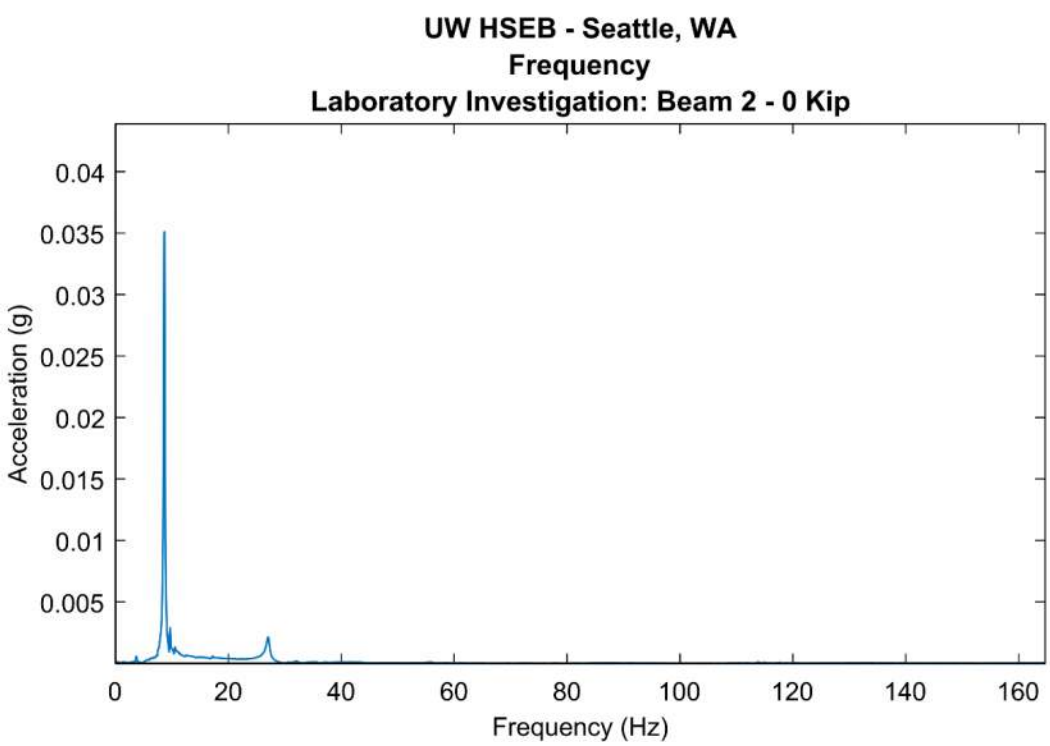

Figure B8: Beam 2 Unloaded - Natural Frequencies

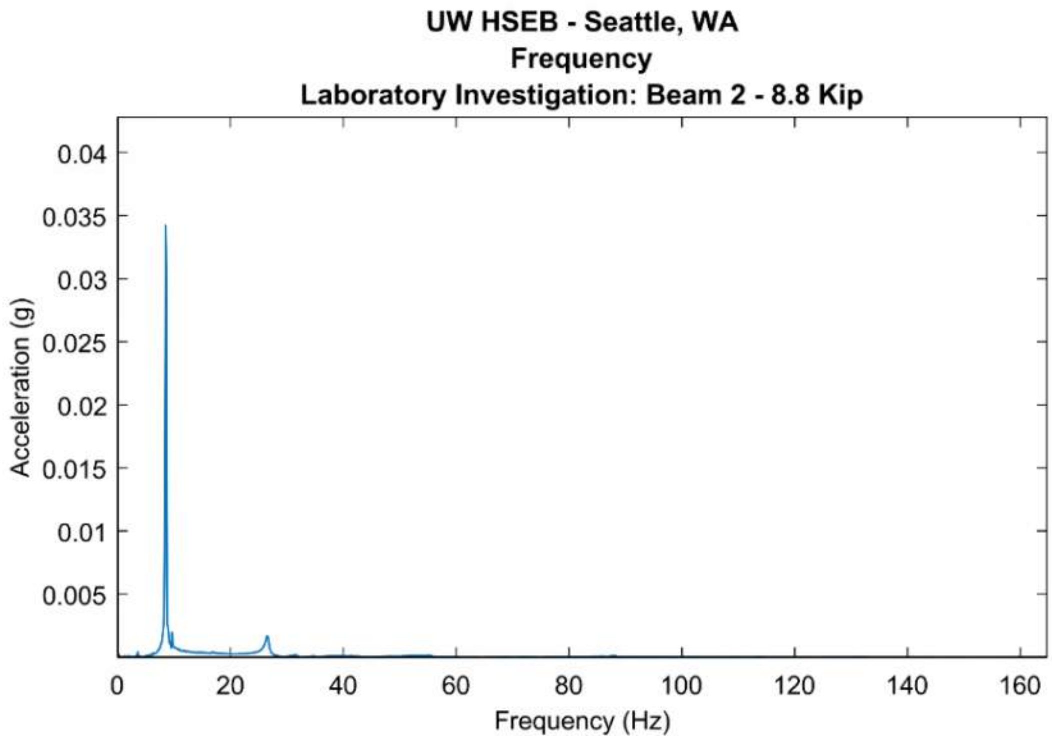

Figure B9: Beam 2 Post 17.5 Kip Load - Natural Frequencies

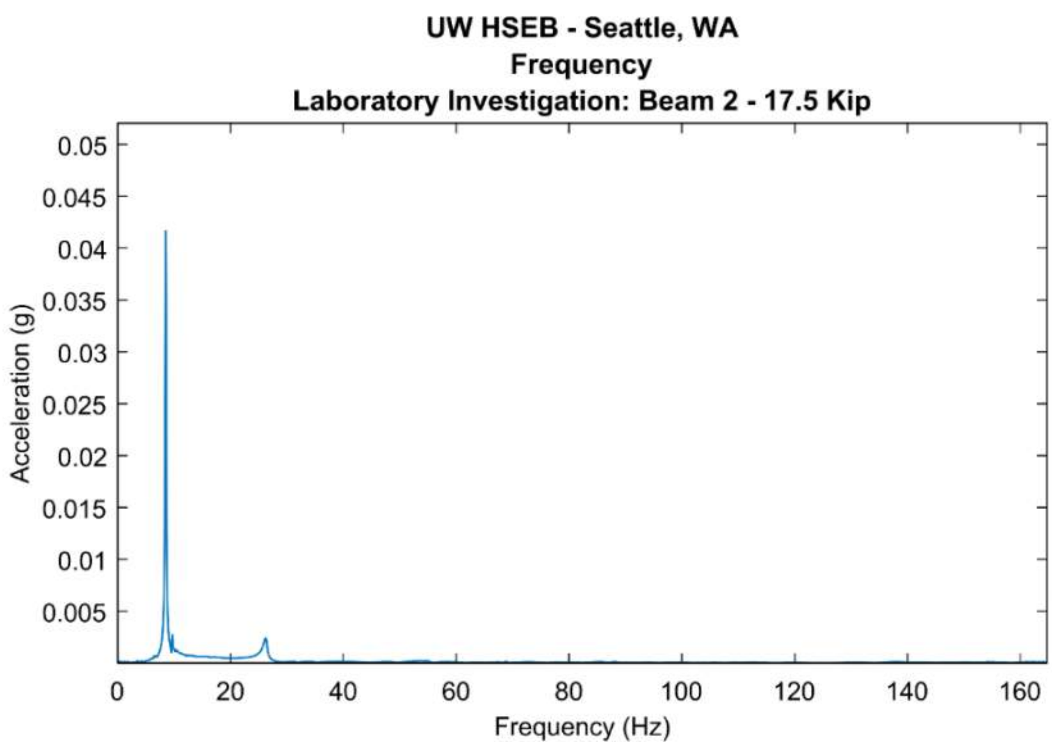

Figure B10: Beam 2 Post 17.5 Kip Load - Natural Frequencies

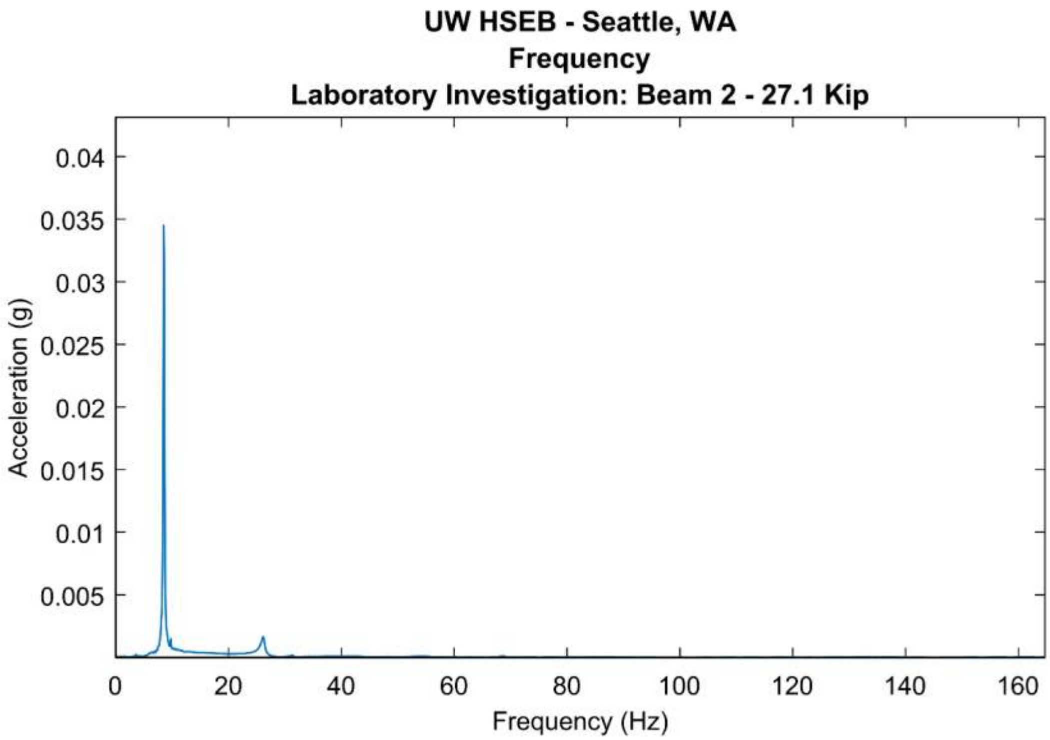

Figure B11: Beam 2 Post 27.1 Kip Load - Natural Frequencies

Appendix C

Vibration Plots for Field Testing with and without Concrete Slab

This page intentionally left blank.

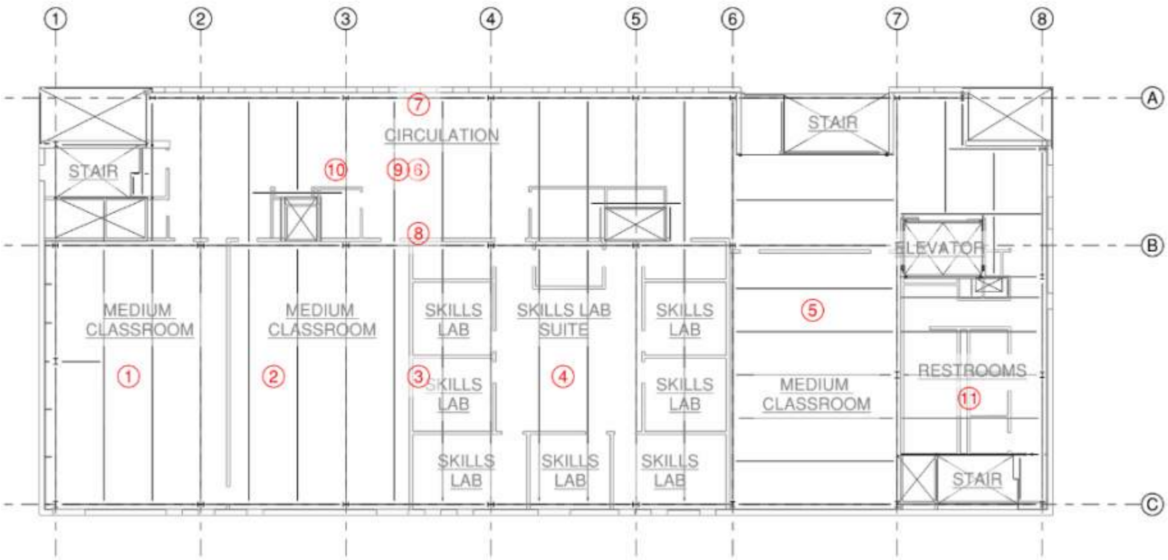

Figure C1: Level 2 Test Locations

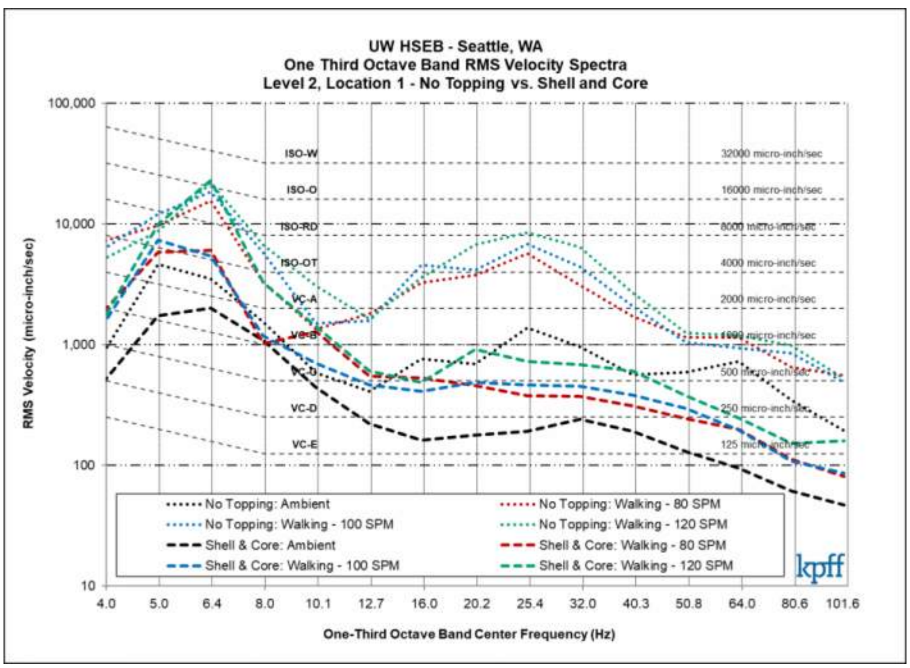

Figure C2: Vibration Response at Location 1, No Topping vs. Shell & Core

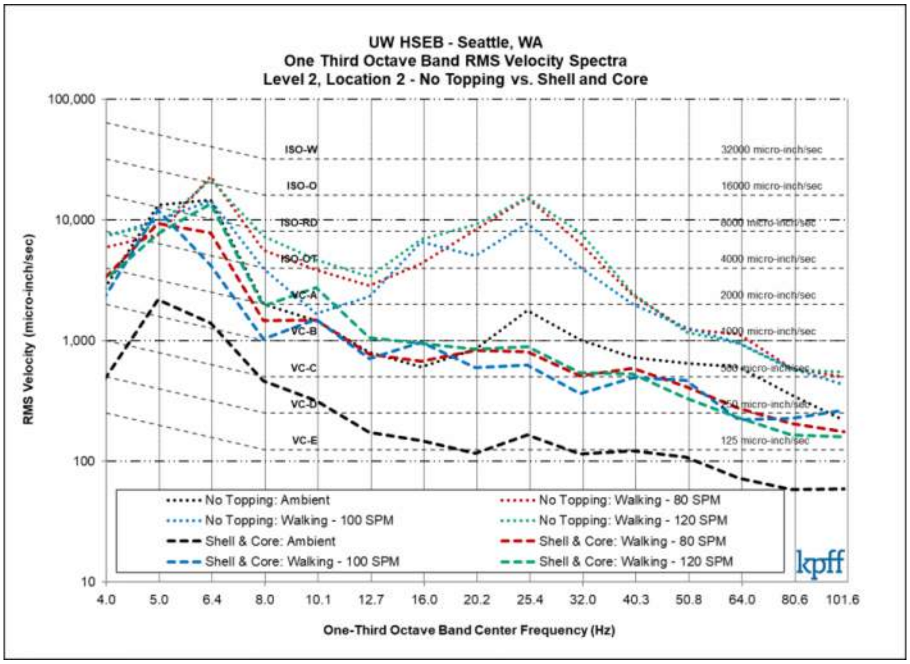

Figure C3: Vibration Response at Location 2, No Topping vs. Shell & Core

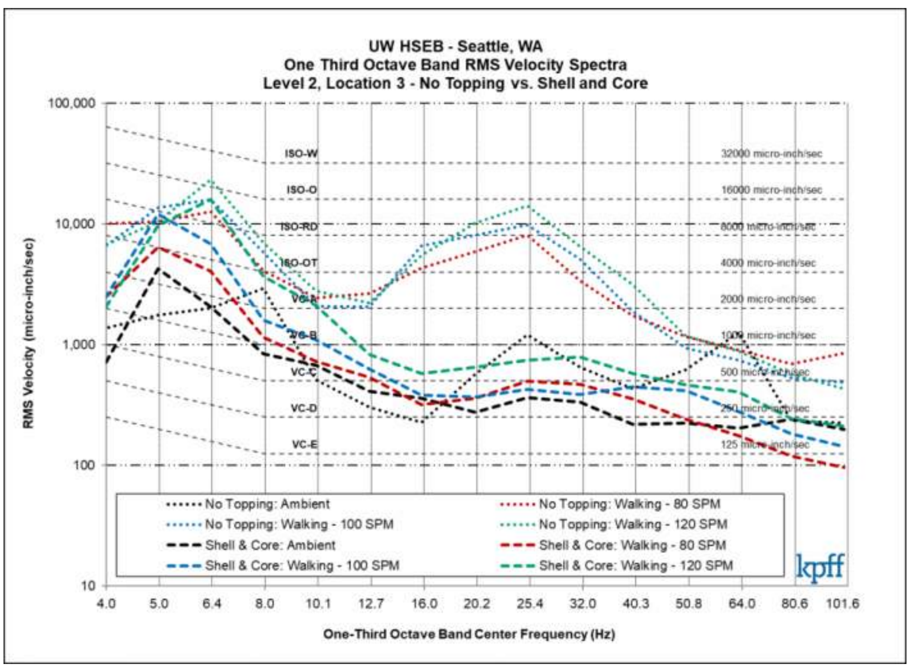

Figure C4: Vibration Response at Location 3, No Topping vs. Shell & Core

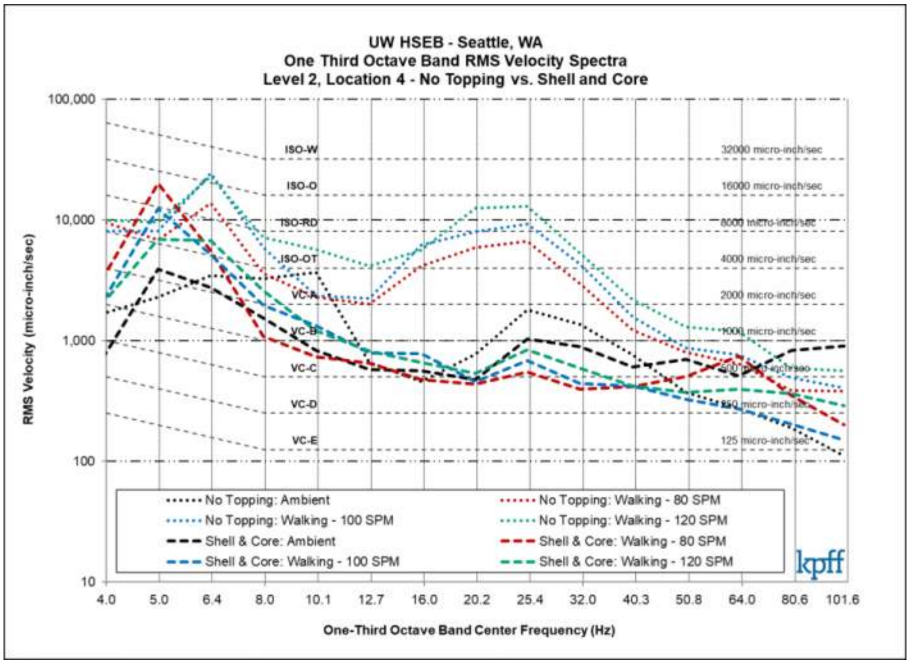

Figure C5: Vibration Response at Location 4, No Topping vs. Shell & Core

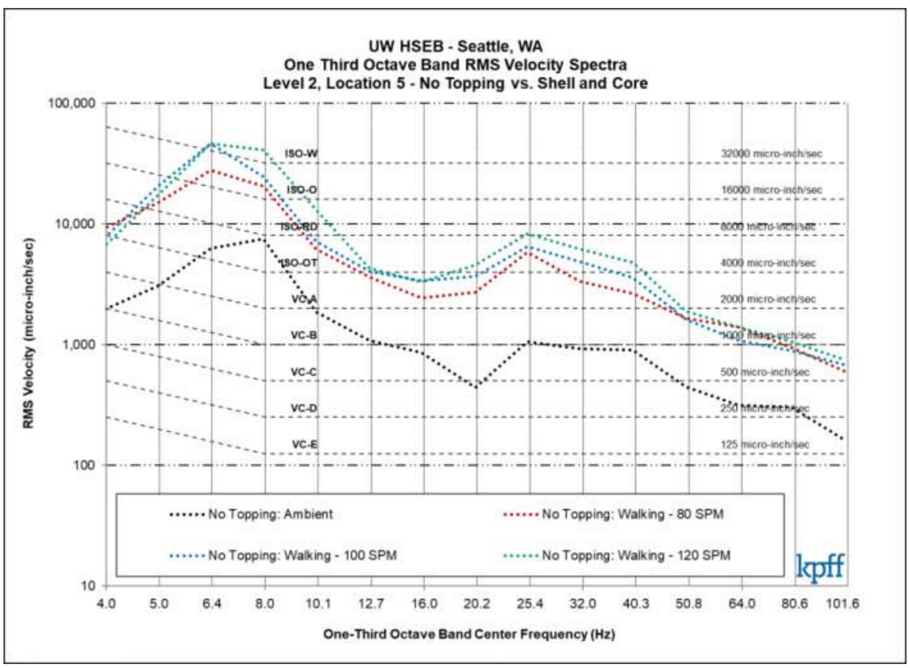

Figure C6: Vibration Response at Location 5, No Topping vs. Shell & Core

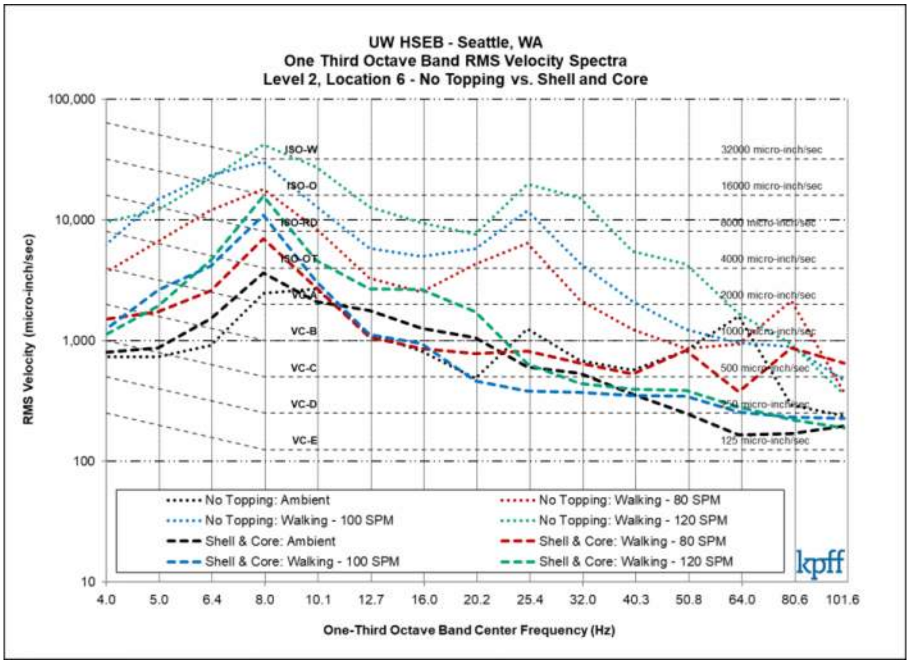

Figure C7: Vibration Response at Location 6, No Topping vs. Shell & Core

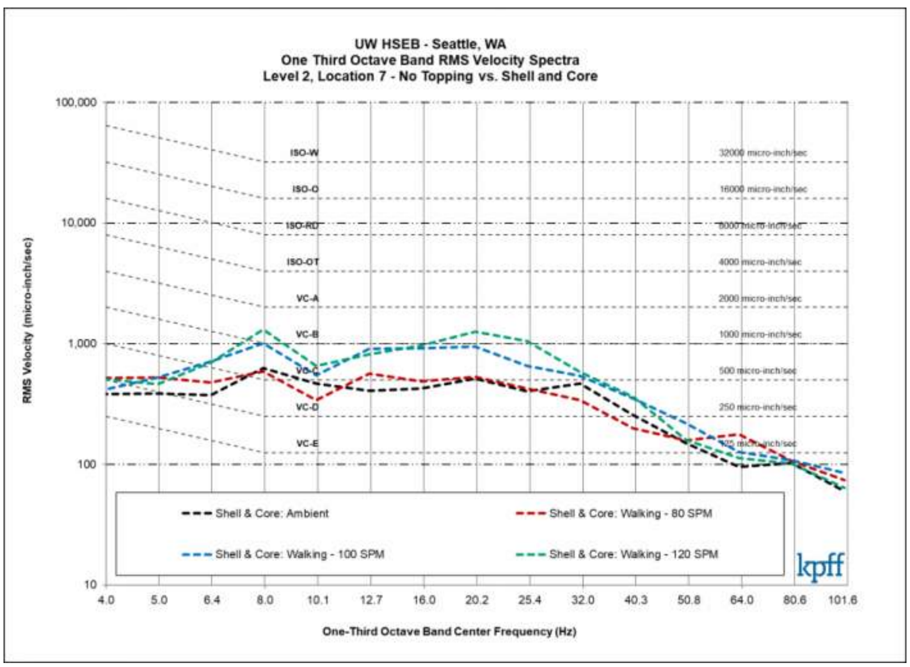

Figure C8: Vibration Response at Location 7, No Topping vs. Shell & Core

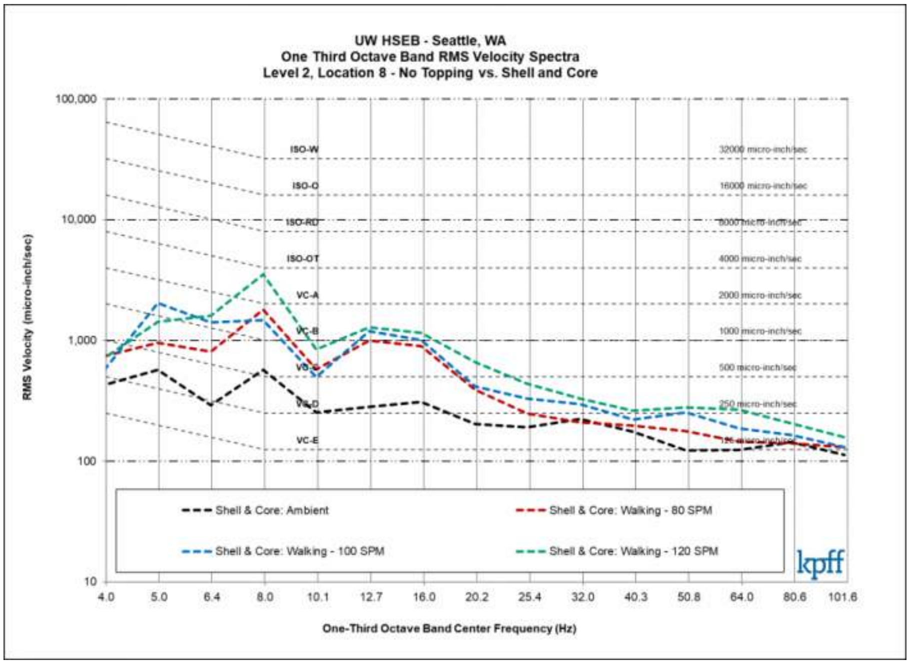

Figure C9: Vibration Response at Location 8, No Topping vs. Shell & Core

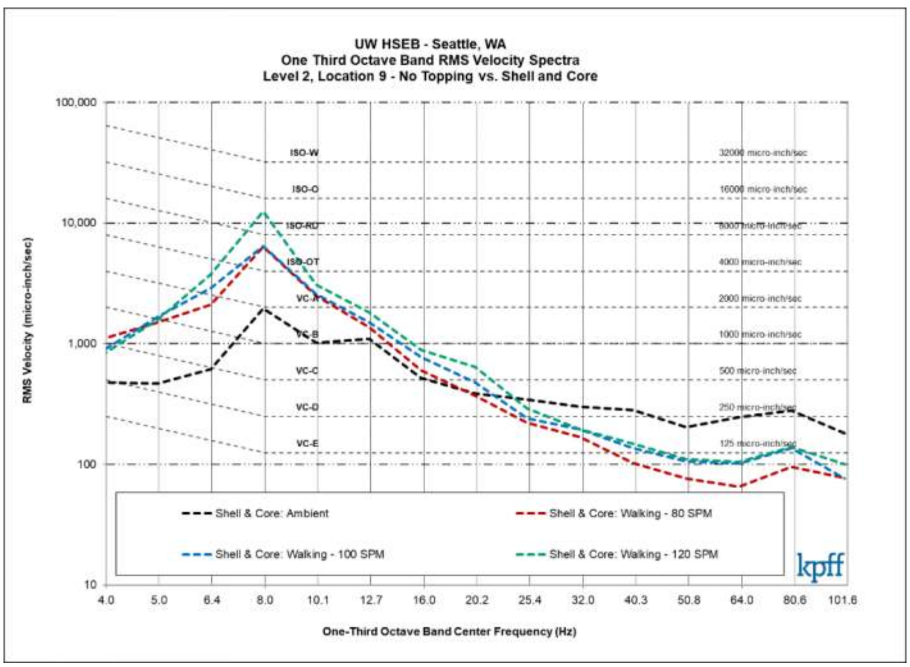

Figure C10: Vibration Response at Location 9, No Topping vs. Shell & Core

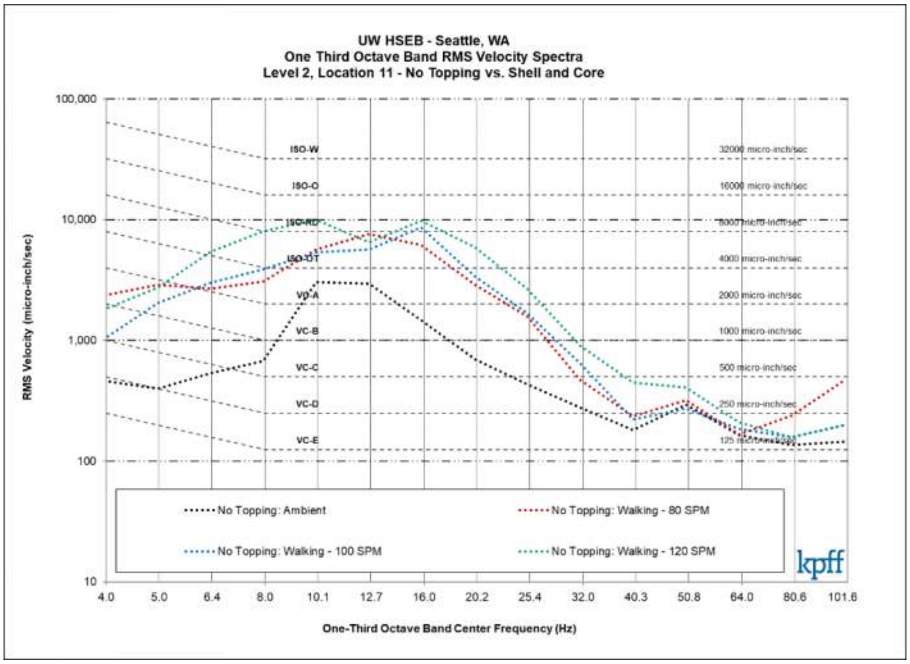

Figure C11: Vibration Response at Location 11, No Topping vs. Shell & Core

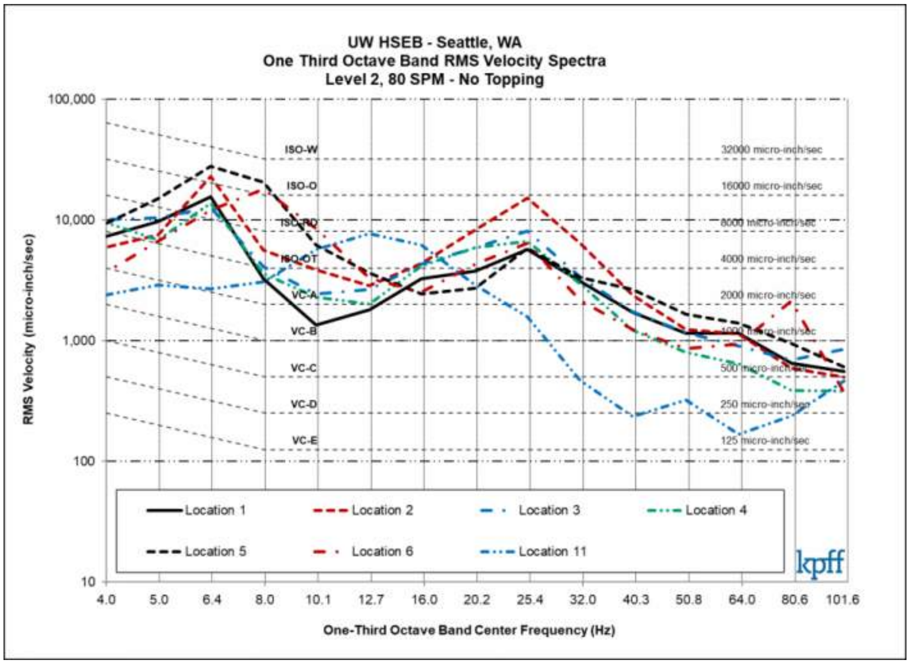

Figure C12: Vibration Response at 80 SPM, No Topping

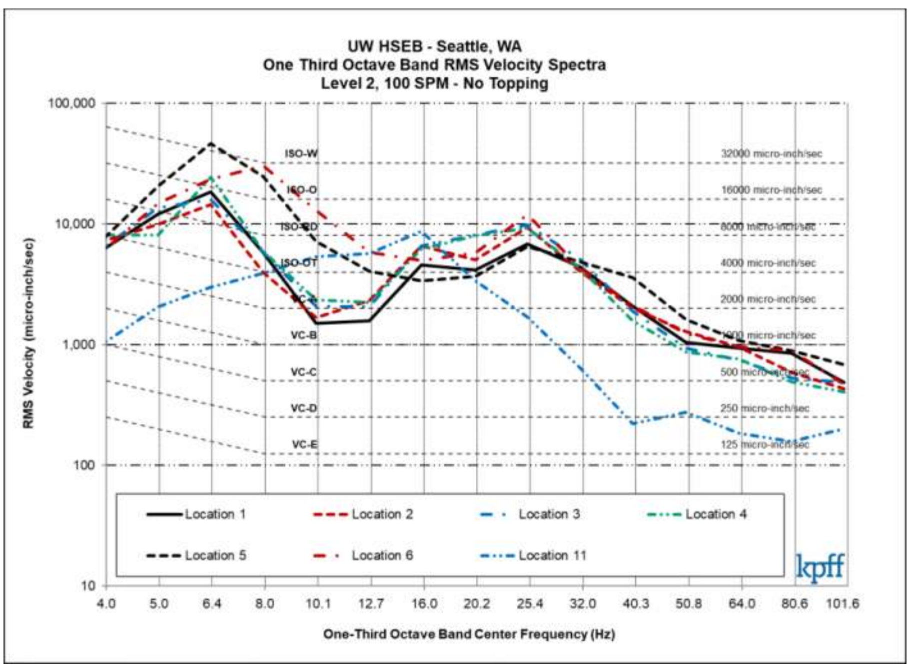

Figure C13: Vibration Response at 100 SPM, No Topping

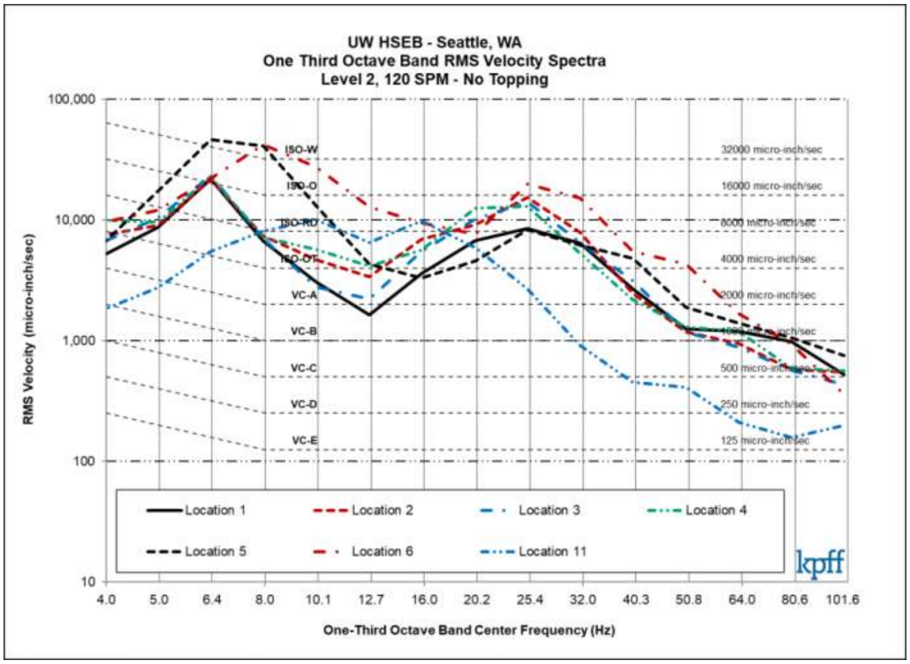

Figure C14: Vibration Response at 120 SPM, No Topping

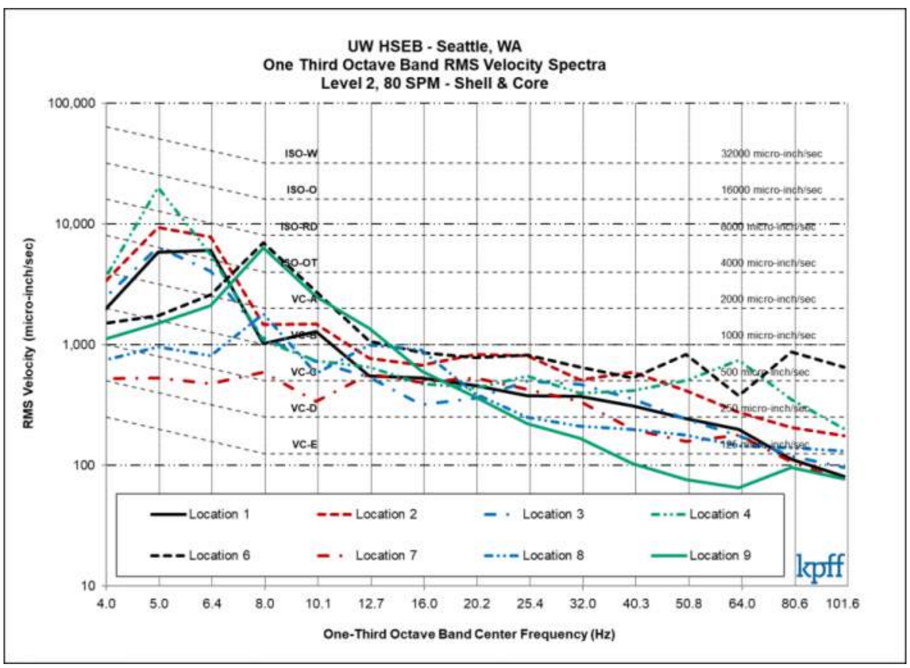

Figure C15: Vibration Response at 80 SPM, Shell & Core

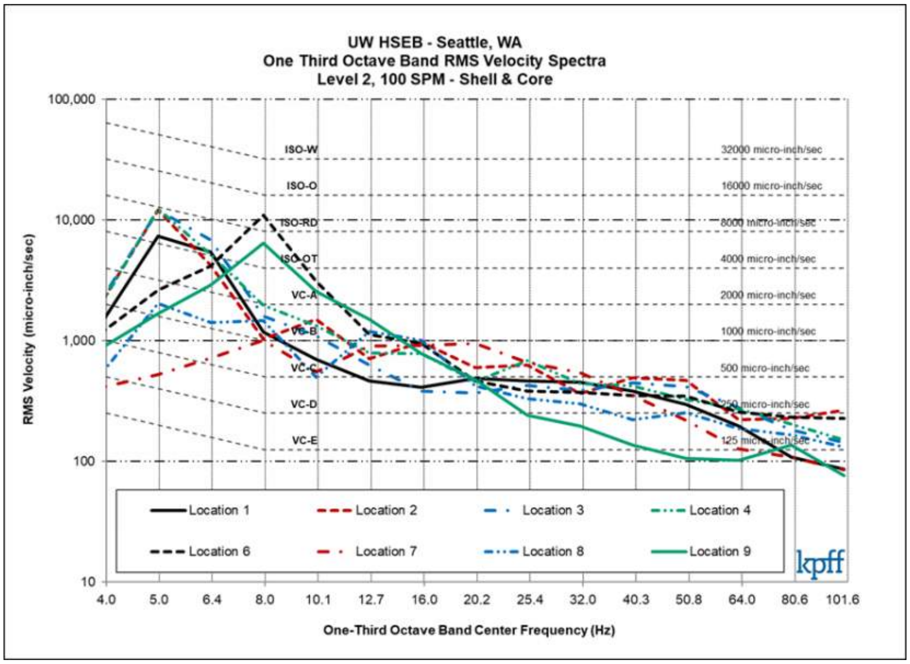

Figure C16: Vibration Response at 100 SPM, Shell & Core

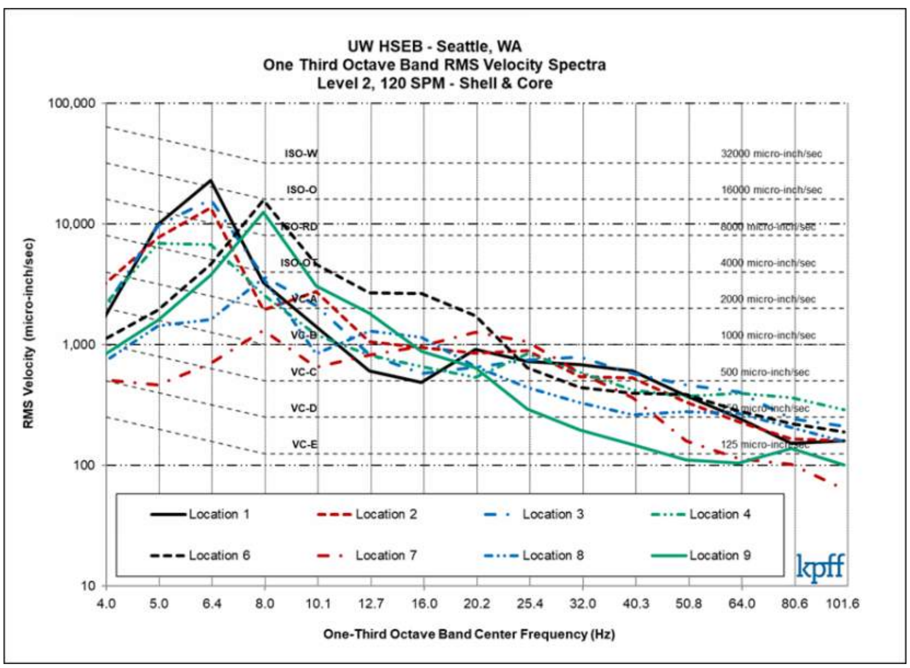

Figure C17: Vibration Response at 120 SPM, Shell & Core

This page intentionally left blank.

Appendix D

Vibration Plots for Field Testing with and without Building Finishes

This page intentionally left blank.

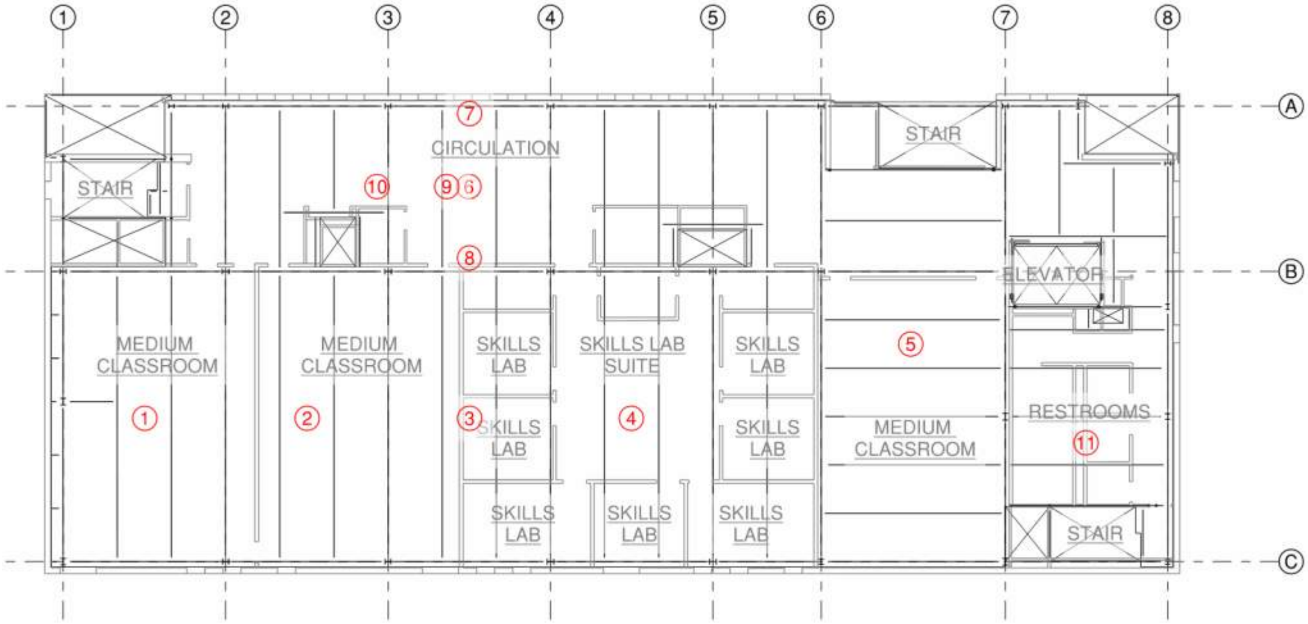

Figure D1: Level 2 Test Locations

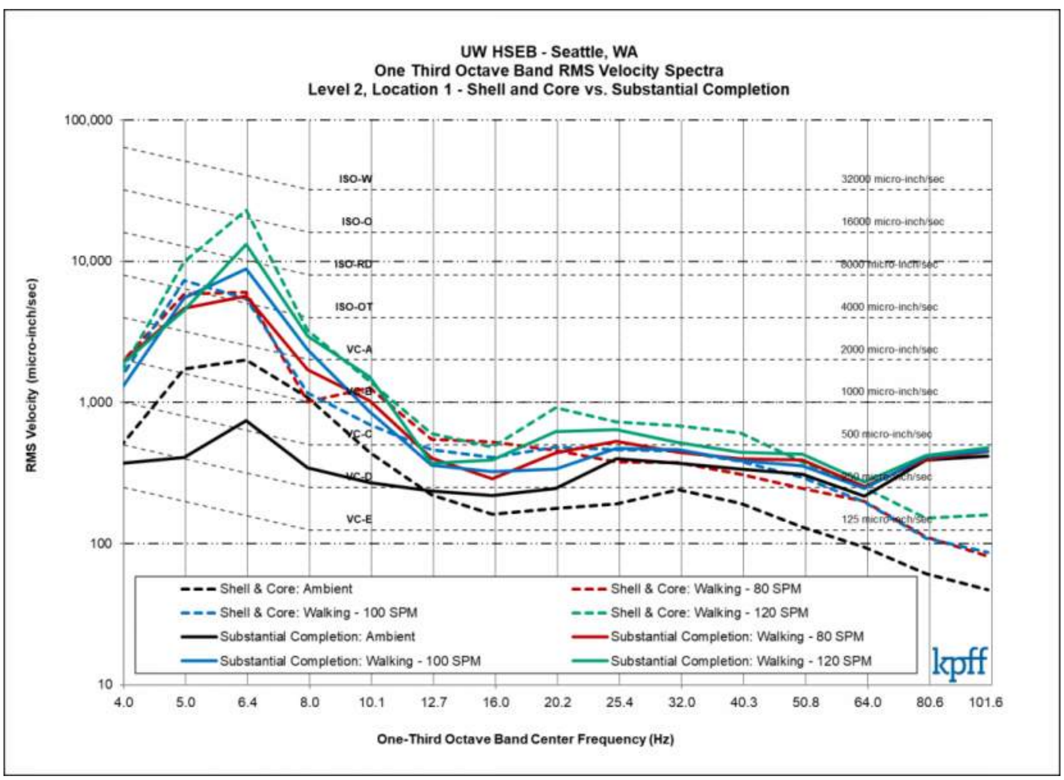

Figure D2: Vibration Response at Location 1, Shell & Core vs. Substantial Completion

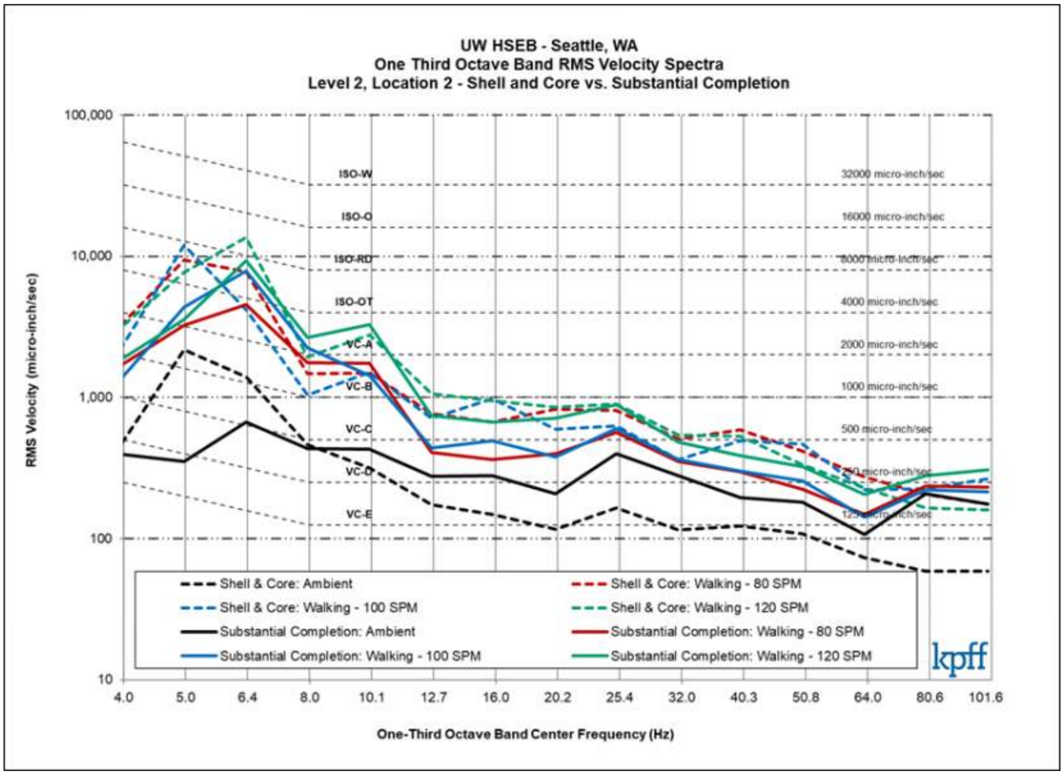

Figure D3: Vibration Response at Location 2, Shell & Core vs. Substantial Completion

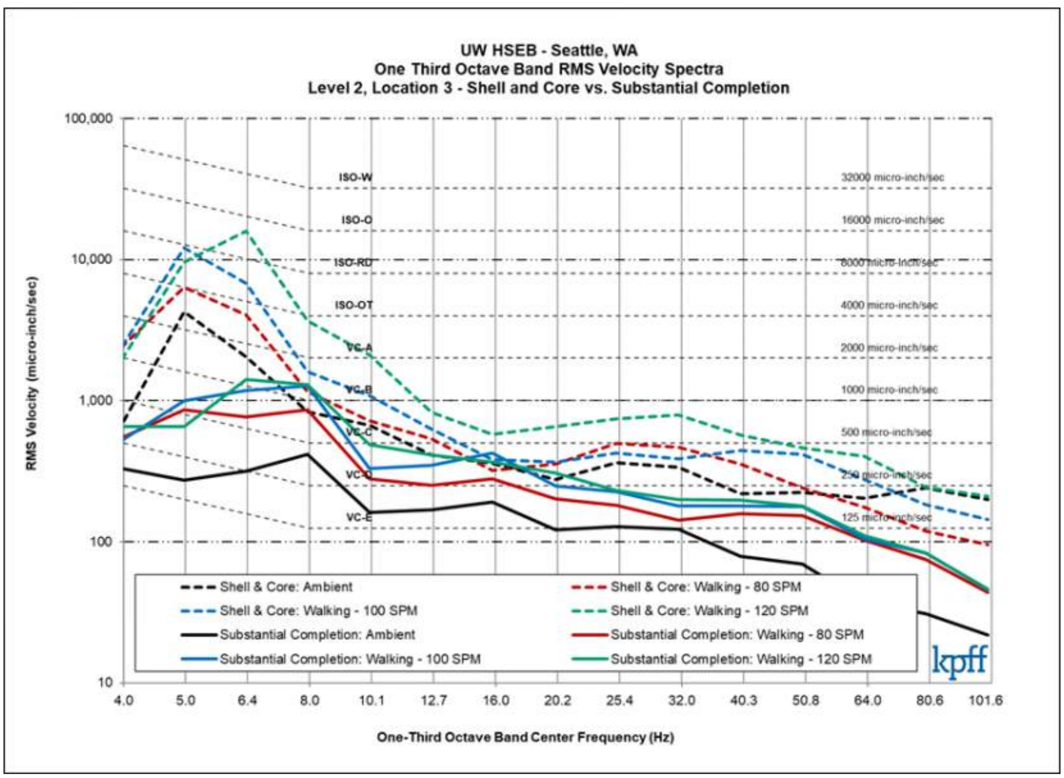

Figure D4: Vibration Response at Location 3, Shell & Core vs. Substantial Completion

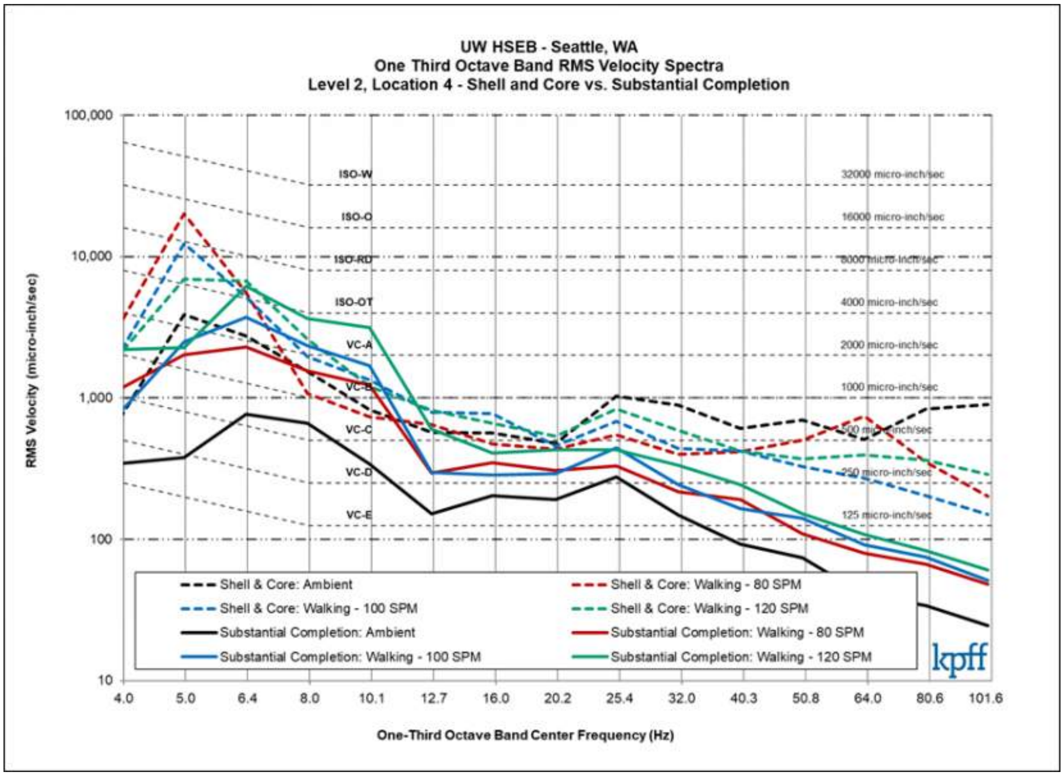

Figure D5: Vibration Response at Location 4, Shell & Core vs. Substantial Completion

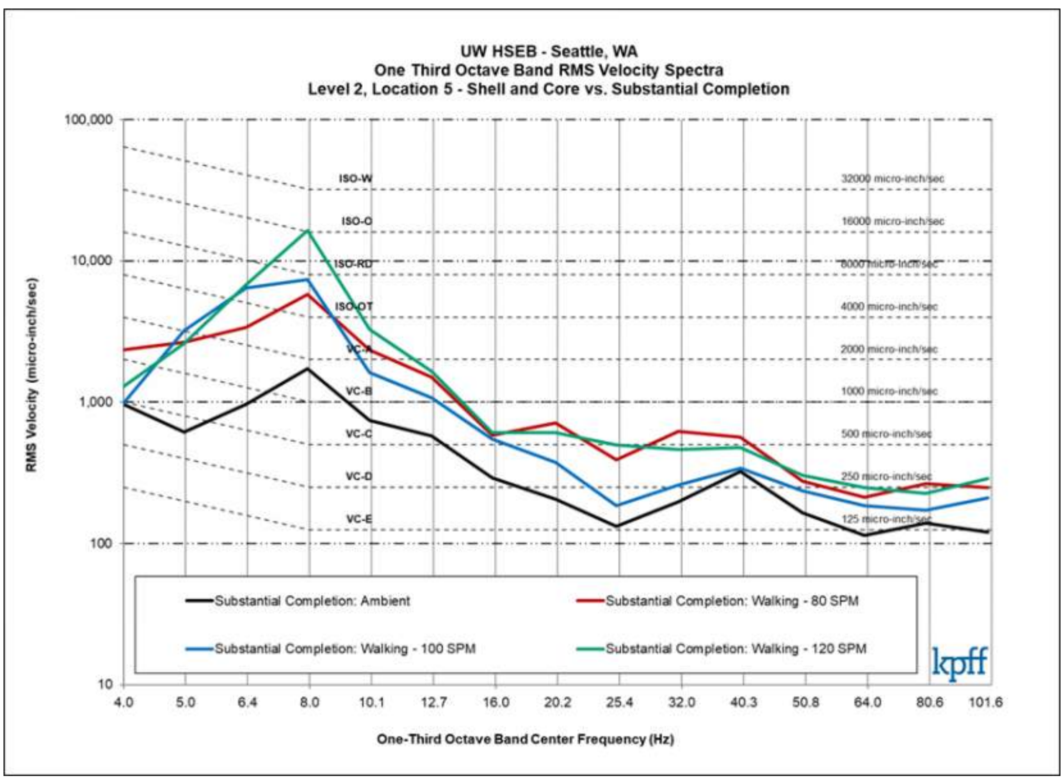

Figure D6: Vibration Response at Location 5, Shell & Core vs. Substantial Completion

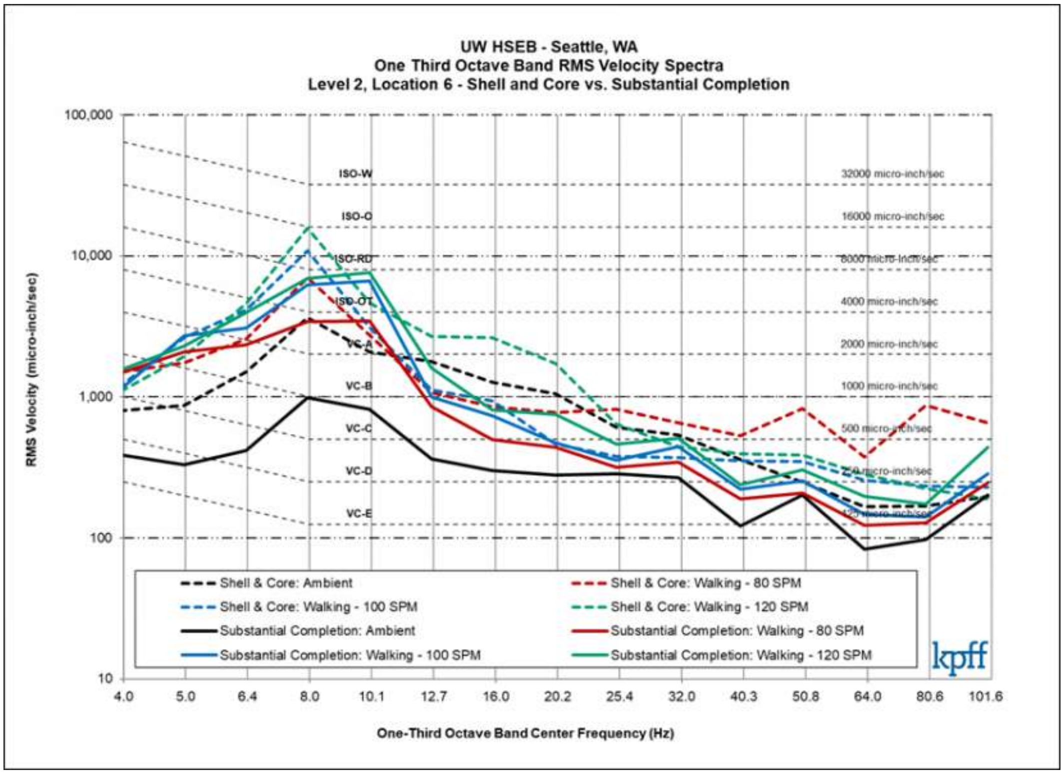

Figure D7: Vibration Response at Location 6, Shell & Core vs. Substantial Completion

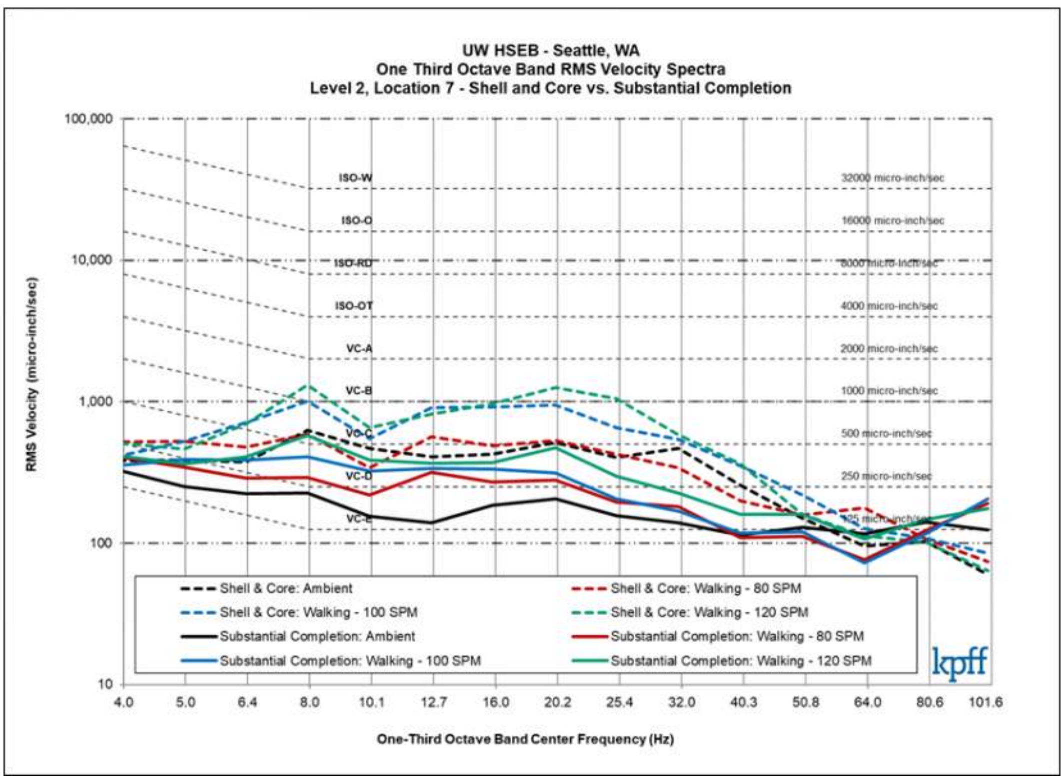

Figure D8: Vibration Response at Location 7, Shell & Core vs. Substantial Completion

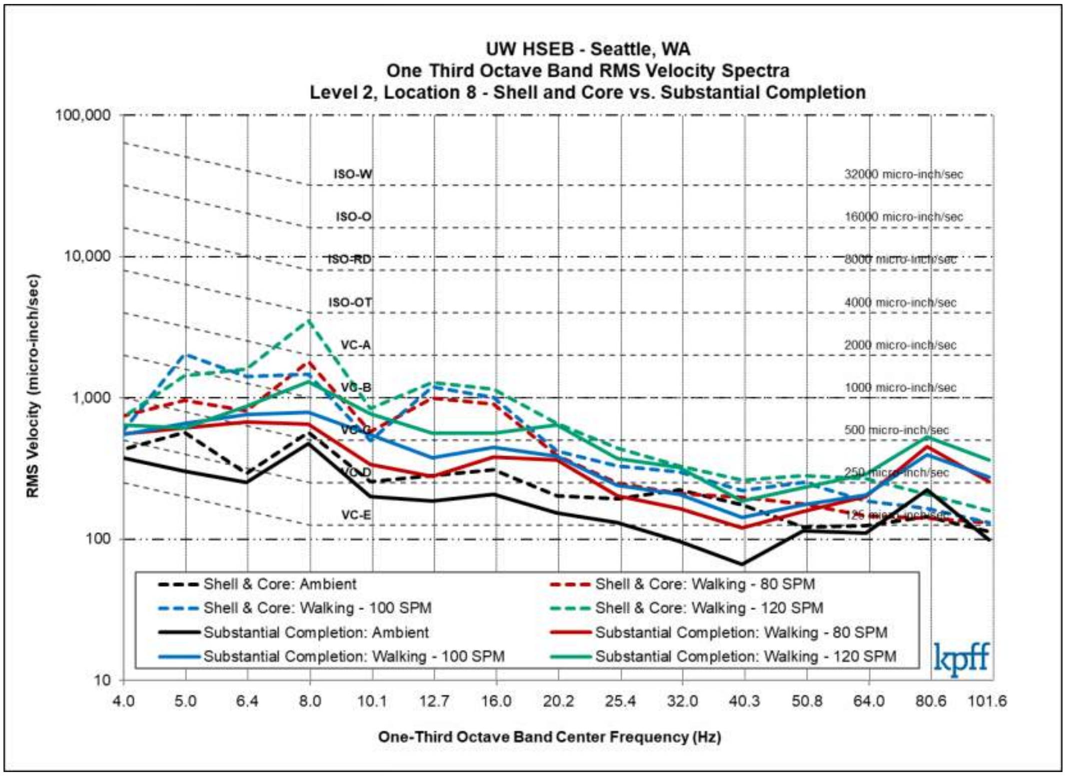

Figure D9: Vibration Response at Location 8, Shell & Core vs. Substantial Completion

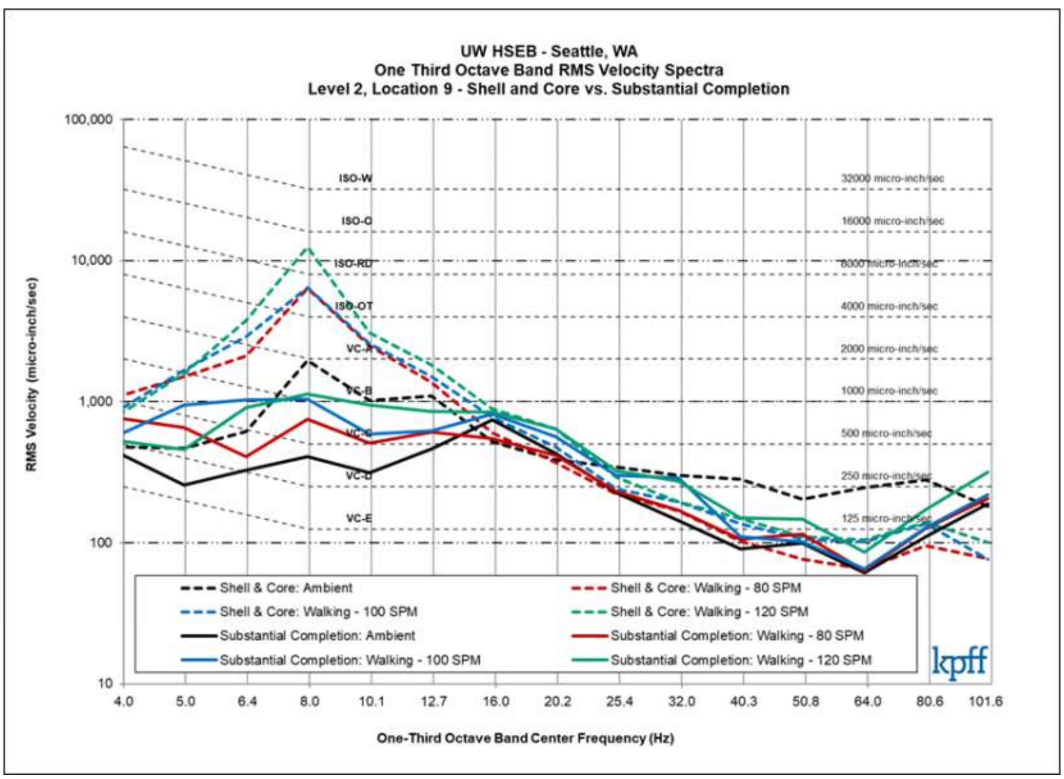

Figure D10: Vibration Response at Location 9, Shell & Core vs. Substantial Completion

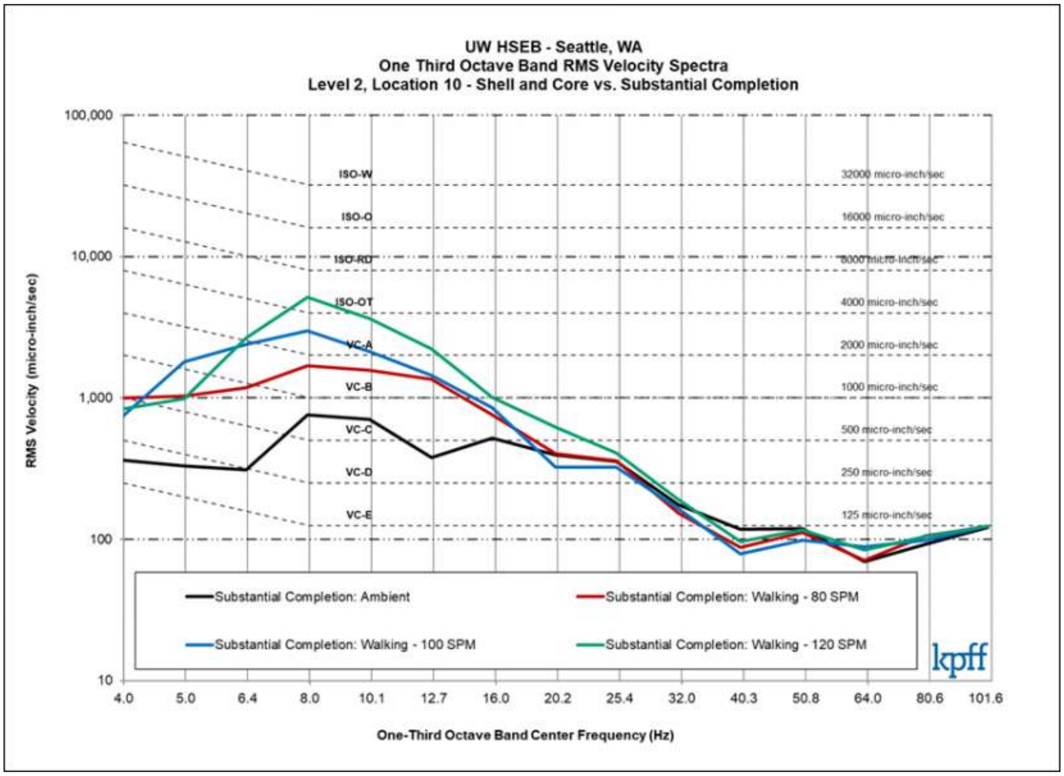

Figure D11: Vibration Response at Location 10, Shell & Core vs. Substantial Completion

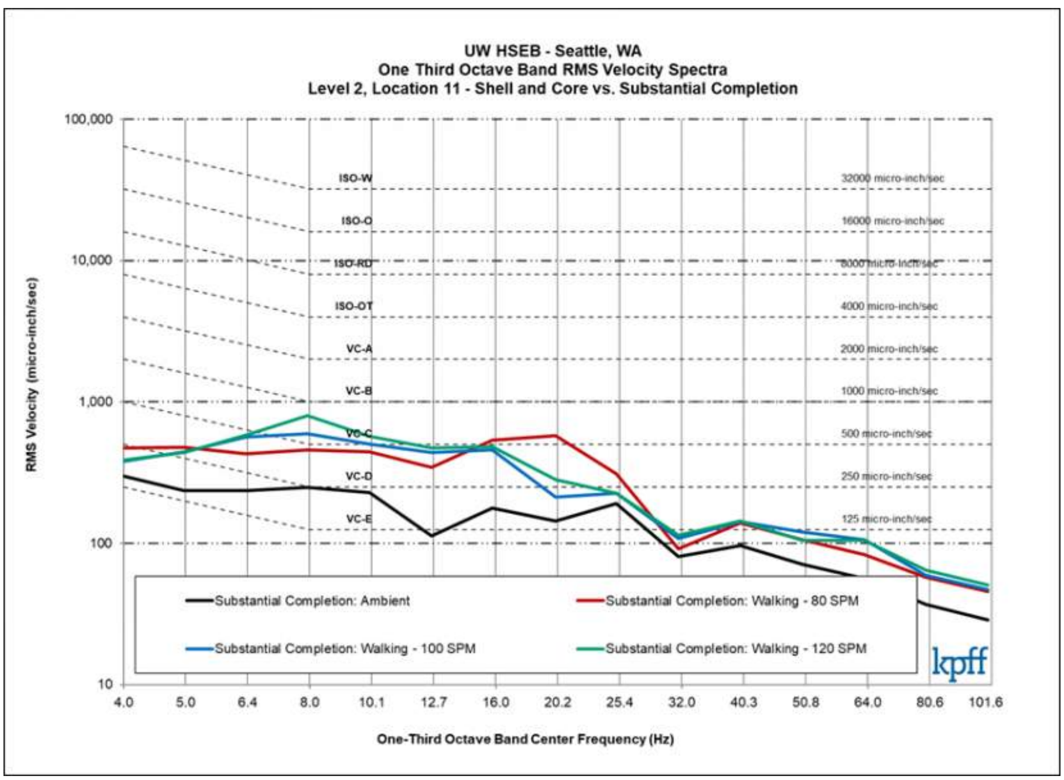

Figure D12: Vibration Response at Location 11, Shell & Core vs. Substantial Completion

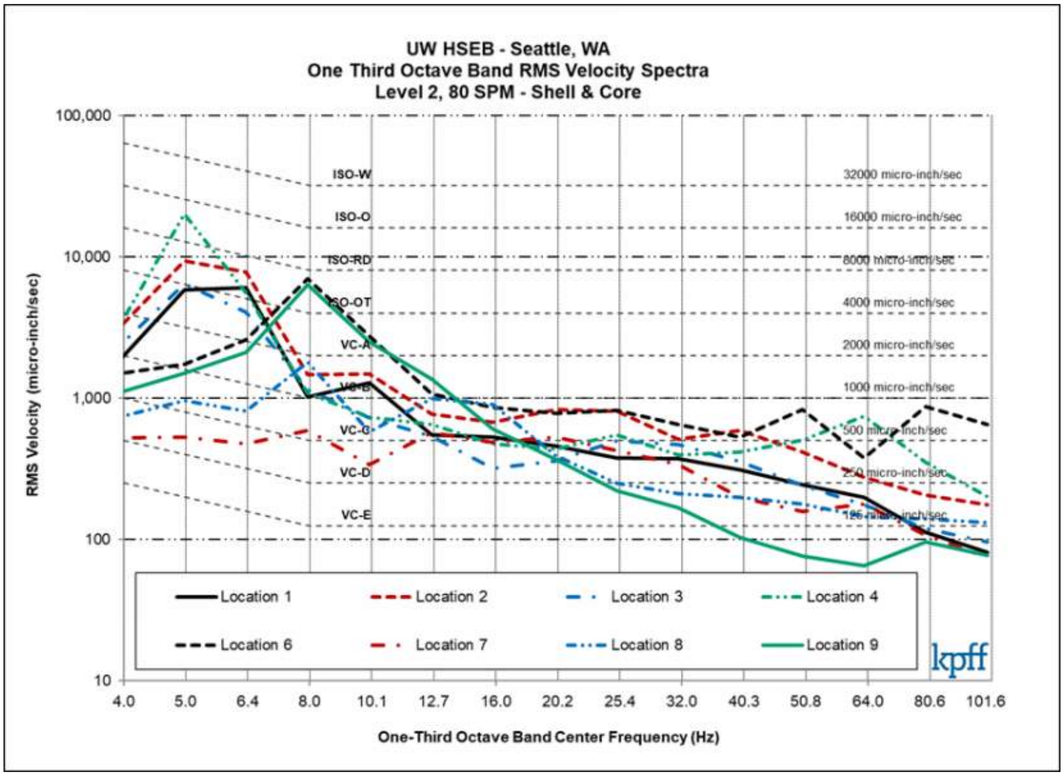

Figure D13: Vibration Response at 80 SPM, Shell & Core

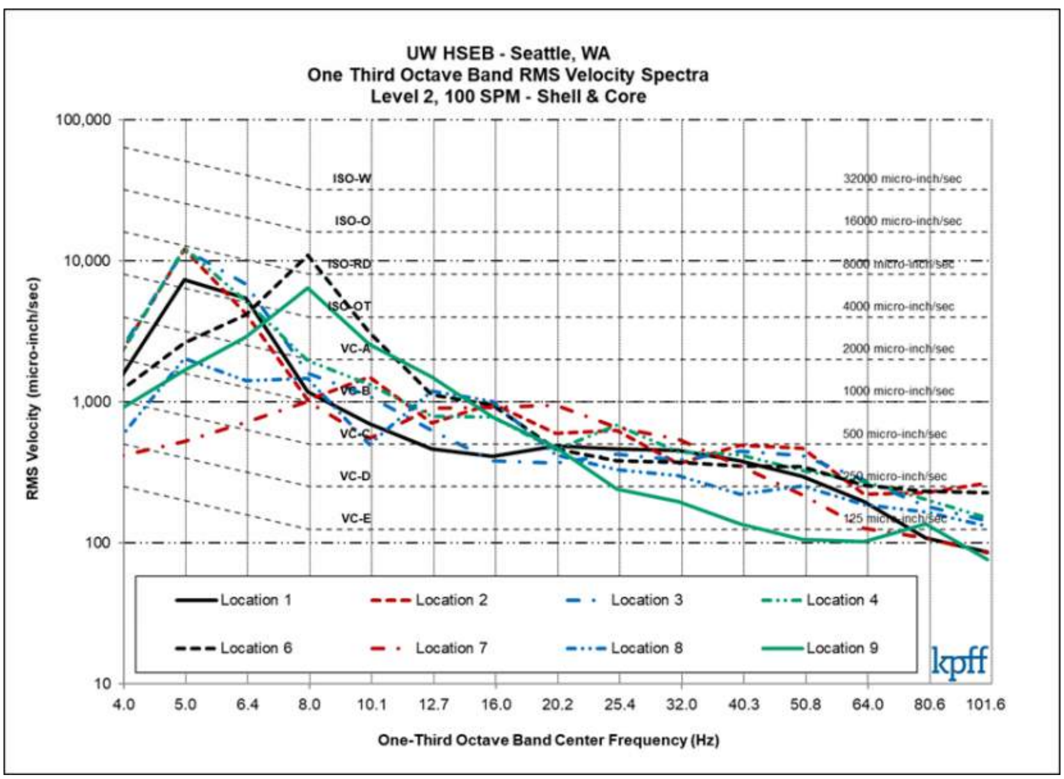

Figure D14: Vibration Response at 100 SPM, Shell & Core

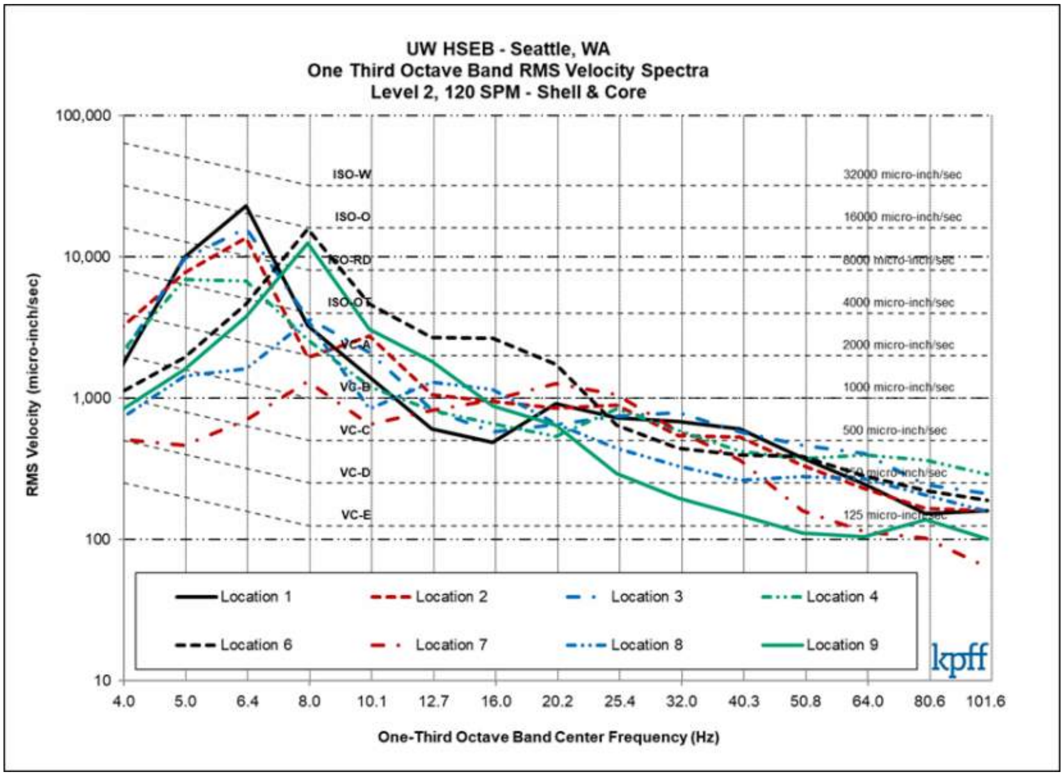

Figure D15: Vibration Response at 120 SPM, Shell & Core

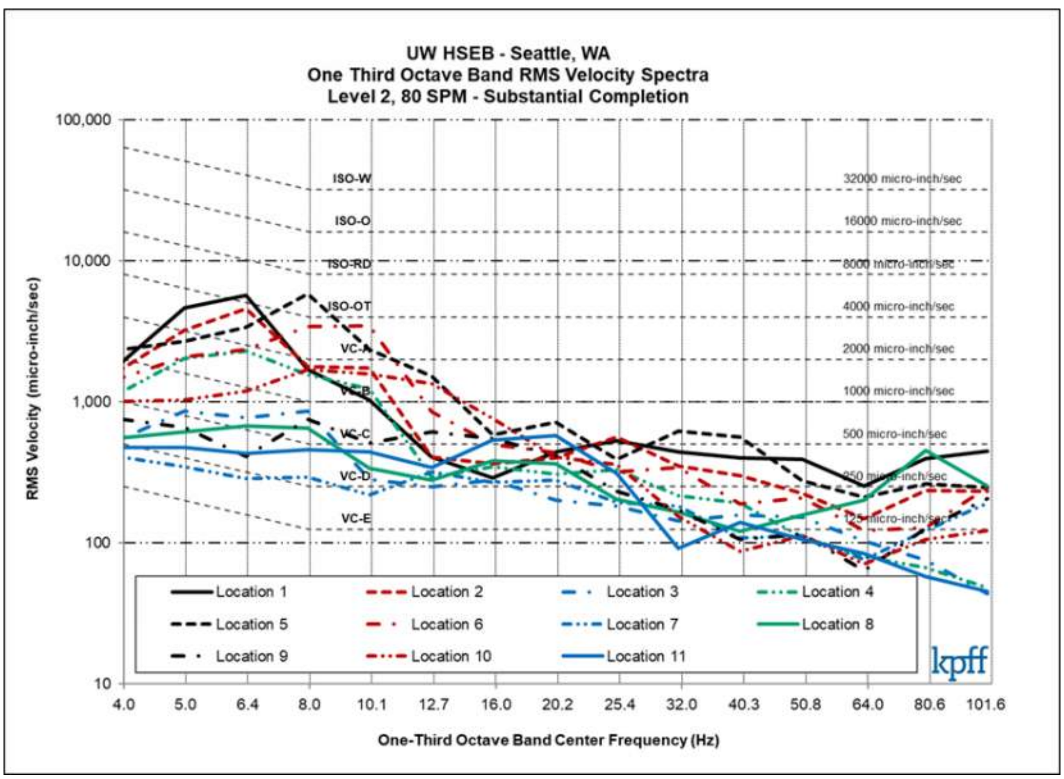

Figure D16: Vibration Response at 80 SPM, Substantial Completion

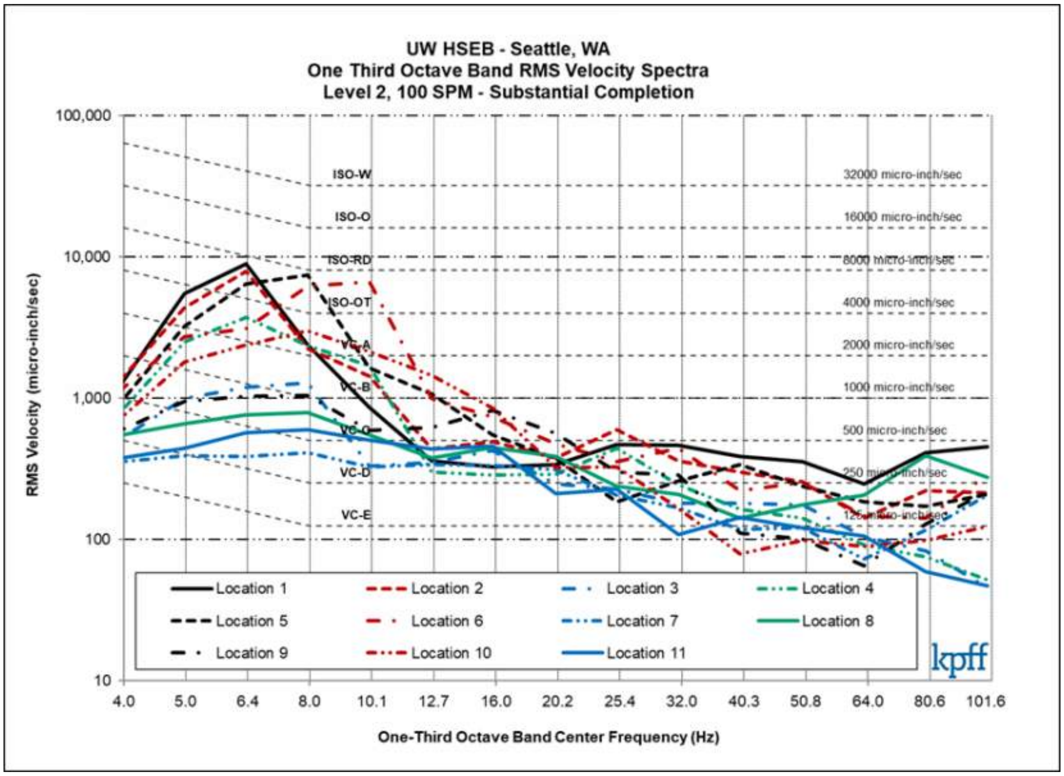

Figure D17: Vibration Response at 100 SPM, Substantial Completion

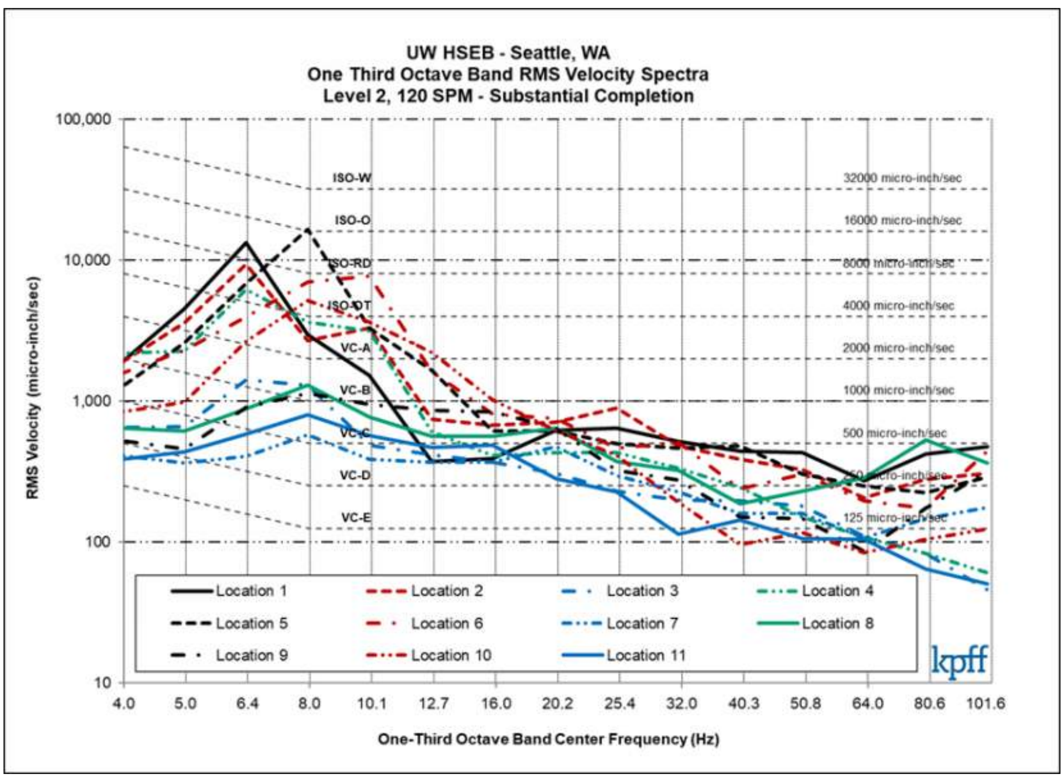

Figure D18: Vibration Response at 120 SPM, Substantial Completion

This page intentionally left blank.

Appendix E

Example Calculations for Orthogonal CLT Section Properties

kpff		Project:	UW HSEB
		Job Number:	1900047
		Date:	2-May-24
1601 5th Avenue, Suite 1600		Location:	Seattle, WA
Seattle, WA 98101 206.622.5822	HSEB Phase II Floor Plate Section Properties	By:	AWT

Finite Element Shell Element Section Property Derivation

MATERIAL DEFINITIONS

CLT Parameters

Layer 1 thickness	$t_{l,1}$	1.38	in	
Layer 2 thickness	$t_{l,2}$	1.38	in	
Layer 3 thickness	$t_{l,3}$	1.38	in	
Total CLT thickness	t_{CLT}	4.14	in	
CLT Grade		V2M1.1-105V		
Unit weight		9.0	psf	Dry weight

Primary Spanning Direction

CLT Modulus	E_0	1400	ksi

Secondary Spanning Direction

CLT Modulus	E_{90}	1400	ksi

Concrete Parameters

Concrete thickness	t_c	3	in
Concrete strength	f'_c	7	ksi
Static conc modulus	$E_{c,S}$	4769	ksi
Concrete shear modulus	G_c	1908	ksi
Dynamic E increase	E*factor	1.35	
Dynamic conc modulus	$E_{c,D}$	6438	ksi
Composite Action	γ	0.010	gamma
Effective conc modulus	$\gamma E_{c,D}$	64	ksi
Unit weight		145	pcf

Note: All calculations assume a 1' strip width.

Strip width	b	12	in
Weak axis E reduction	E/factor	30	Note: Scales the ply modulus to its orthogonal direction modulus.
E to G reduction	E/factor	16	Note: Scales the ply modulus to its shear shear modulus.
Weak axis G reduction	G/factor	10	Note: Scales the ply shear modulus to its orthogonal direction strength.

	Primary Spanning Layers			Secondary Spanning Layers		
Primary Span E	$E_{0,1}$	1400	ksi	$E_{90,1}$	47	ksi
Secondary Span E	$E_{0,2}$	47	ksi	$E_{90,2}$	1400	ksi
Primary Span $G_{13,23}$	$G_{0,1}$	87.5	ksi	$G_{90,1}$	8.75	ksi
Secondary Span G	$G_{0,2}$	8.75	ksi	$G_{90,2}$	87.5	ksi
In Plane Shear Modulus	$G_{0,12}$	87.5	ksi	$G_{90,12}$	87.5	ksi

BARE CLT SECTION PROPERTIES

Diaphragm Action Section Properties

In-Plane Axial Stiffness - Primary Direction

	E_{eff} [ksi]	A [in^2]	EA_{eff} [kips]	
Layer 1	1400	16.6	23184	
Layer 2	47	16.6	773	
Layer 3	1400	16.6	23184	
Total		$EA_{eff,11}$	47141	kips/ft width

In-Plane Axial Stiffness - Secondary Direction

	E_{eff} [ksi]	A [in^2]	EA_{eff} [kips]	
Layer 1	47	16.6	773	
Layer 2	1400	16.6	23184	
Layer 3	47	16.6	773	
Total		$EA_{eff,22}$	24730	kips/ft width

In Plane Shear Stiffness

CLT Contribution GA_{eff} 4347 kips/ft width

Out of Plane Section Properties

Out of Plane Bending - Primary Direction

	E [ksi]	y [in]	t [in]	$E_1bt^3/12$ [ksi]	$E_1A(y\text{-}y\_bar)^2$ [ksi]	Layer Sum [ksi]	
Layer 1	1400	0.69	1.38	3679	44152	47831	
Layer 2	47	2.07	1.38	123	0	123	
Layer 3	1400	3.45	1.38	3679	44152	47831	
Total					$EI_{eff,11}$	95784	k-in^2

Out of Plane Bending - Secondary Direction

	E [ksi]	y [in]	t [in]	$E_1bt^3/12$ [ksi]	$E_1A(y\text{-}y\_bar)^2$ [ksi]	Layer Sum [ksi]	
Layer 1	0	0.00	0	0	0	0	
Layer 2	1400	2.07	1.38	3679	0	3679	
Layer 3	0	0.00	0	0	0	0	
Total					$EI_{eff,22}$	3679	k-in^2

Out of Plane Shear Stiffness - Primary Direction

	G [ksi]	t [in]	t/Gb	t/Gb factor	factor* t/Gb	
Layer 1	87.5	1.38	0.00131	0.5	0.00066	
Layer 2	8.75	1.38	0.01314	1	0.01314	
Layer 3	87.5	1.38	0.00131	0.5	0.00066	
Totals		4.14			0.01446	
$a = \sum t-(t_1+t_n)/2$		2.76		$GA_{eff,13}$	527	klf

Out of Plane Shear Stiffness - Secondary Direction

	G	t	t/Gb	t/Gb factor	factor* t/Gb	
	[ksi]	[in]				
Layer 1	8.75	1.38	0.01314	0.5	0.00657	
Layer 2	87.5	1.38	0.00131	1	0.00131	
Layer 3	8.75	1.38	0.01314	0.5	0.00657	
Totals		4.14			0.01446	
$a = \sum t-(t_1+t_n)/2$		2.76		$GA_{eff,23}$	527	klf

CLT WITH CONCRETE TOPPING SECTION PROPERTIES

Diaphragm Action Section Properties

In-Plane Axial Stiffness - Primary Direction

	E_{eff}	A	EA_{eff}	
	[ksi]	[in^2]	[kips]	
Layer 1	1400	16.6	23184	
Layer 2	47	16.6	772.8	
Layer 3	1400	16.6	23184	
Concrete	64	36.0	2318	
Total		$EA_{eff,11}$	49459	kips

In-Plane Axial Stiffness - Secondary Direction

	E_{eff}	A	EA_{eff}	
	[ksi]	[in^2]	[kips]	
Layer 1	47	16.6	772.8	
Layer 2	1400	16.6	23184	
Layer 3	47	16.6	772.8	
Concrete	64	36.0	2318	
Total		$EA_{eff,22}$	27047	kips

In-Plane Shear Stiffness

CLT Contribution	4347	kips/ft width
Concrete Contribution	68673	kips/ft width
Total	73020	kips/ft width

Out of Plane Section Properties

Determine primary direction composite centroid

Note: b term for concrete layer includes γ, y is measured from the bottom of the CLT.

E_1 1400 ksi

Layer	E	n	b	t	A	y	Ay
			[in]	[in]	[in^2]	[in]	[in^3]
Layer 1	1400	1.0	12	1.38	16.6	0.69	11.4
Layer 2	47	0.033	0.400	1.38	0.6	2.07	1.1
Layer 3	1400	1.0	12	1.38	16.6	3.45	57.1
Concrete	6438	4.6	0.55	3	1.7	5.64	9.3
Total					35		79

y_bar, primary direction 2.24 in

Out of Plane Bending via parallel axis theorem - Primary Direction

	y	t	$E_1bt^3/12$	$E_1A(y-y\_bar)^2$	Layer Sum	
	[in]	[in]	[ksi]	[ksi]	[ksi]	
Layer 1	0.69	1.38	3679	55505	59185	
Layer 2	2.07	1.38	123	22	144	
Layer 3	3.45	1.38	3679	34096	37775	
Concrete	5.64	3	173829	26835	200664	
Total				$EI_{eff,11}$	297768	k-in^2

Determine secondary direction composite centroid

E_1	1400 ksi						
	E	n	b	t	A	y	Ay
Layer			[in]	[in]	[in^2]	[in]	[in^3]
Layer 1	0	0.0000	0	0.00	0.00	0.00	0.0
Layer 2	1400	1.0000	12	1.38	16.56	2.07	34.3
Layer 3	47	0.0333	0.4	1.38	0.55	3.45	1.9
Concrete	6438	4.5986	0.6	3.00	1.66	5.64	9
Total					18.8		46
ᵧ_bar, secondary direction	2.43	in					

Out of Plane Bending via parallel axis theorem - Secondary Direction

	y	t	$E_1bt^3/12$	$E_1A(y-y\_bar)^2$	Layer Sum	
	[in]	[in]	[ksi]	[ksi]	[ksi]	
Layer 1	0.00	0.00	0	0	0	
Layer 2	2.07	1.38	3679	2930	6609	
Layer 3	0.00	0.00	0	4546	4546	
Concrete	5.64	3	173829	0	173829	
Total				$EI_{eff,22}$	184984	k-in^2

Out of Plane Shear Stiffness - Primary Direction

CLT Contribution	527	kips
Concrete Contribution	68673	kips
$GA_{eff,13}$	69200	kips

Out of Plane Shear Stiffness - Secondary Direction

CLT Contribution	527	kips
Concrete Contribution	68673	kips
$GA_{eff,23}$	69200	kips

SUMMARY AND SAP2000 SECTION DEFINITIONS

Effective Section Properties

CLT with Concrete Topping

In-plane axial	$EA_{eff,11}$=	49,459	kips/ft width
	$EA_{eff,22}$=	27,047	kips/ft width
In-plane shear	GA_{eff}=	73,020	kips/ft width
Out of plane bending	$EI_{eff,11}$=	297,768	kip-in^2/ft width

SAP2000 Property Definitions

Define a dummy material for the shell section:

Material	CLT V2M1.1-105V	
Unit weight	0.0	pcf
E	1400	ksi
Assumed v	0	
G	700	ksi
Element total thickness	4.14	in

Dummy Section Properties

In-plane axial	EA_{11}=	69,552	kips/ft width
	EA_{22}=	69,552	kips/ft width
In-plane shear	GA=	34,776	kips/ft width
Out of plane bending	EI_{11}=	99,341	kip-in^2/ft width
	EI_{22}=	99,341	kip-in^2/ft width
Out of plane shear	GA_{13}=	34,776	kips/ft width
	GA_{23}=	34,776	kips/ft width

<u>Property Modifiers - with Concrete</u>

In-plane axial	f_{11}	0.71	
	f_{22}	0.39	
In-plane shear	f_{12}	2.10	
Out of plane bending	m_{11}	3.00	
	m_{22}	1.86	
	m_{12}	1.99	
Out of plane shear	v_{13}	1.99	
	v_{23}	1.99	
Element Offset		2.33	in

Floor Masses

CLT	9	psf
Concrete	36	psf
SDL+LL Contribution	0	psf
g	32.2	ft/s^2

	[psf]	[$p_m$sf]
Lower bound superimposed load	45	1.41